



**Gold Nanoparticle-Chitosan Hydrogel  
mediated wound healing and delivery of 5-  
Fluorouracil to cancer cells *in vitro***

**By**  
**Varshan Gounden**  
**219006317**

Submitted in fulfilment of the academic requirements for the degree of  
Master of Science in the School of Life Sciences, University of  
KwaZulu-Natal, Durban

**Supervisor:** Prof M. Singh

Signed: \_\_\_\_\_

Date: 15 January 2025

## Abstract

Cancer is a severe disease, devastating lives worldwide. Despite the numerous benefits of anticancer medication, their efficacy is compromised by insufficient selectivity and rapid metabolic degradation. In response to the requirement for novel drugs with improved therapeutic efficacy, delivery systems are being developed to mitigate the adverse effects of chemotherapy. The management of chronic wounds is a significant yet often overlooked concern, vital for preserving the mental and physical welfare of patients and enhancing their overall quality of life. In recent years, the application of hydrogels has significantly mitigated deficiencies in drug delivery and wound healing due to their similarity to the extracellular matrix (ECM) and stimuli-responsive properties, which facilitate drug release from contracting polymer chains in response to changes in pH, light, and temperature. Chitosan (CS) is an ideal, natural, and biologically compatible polymer that has a structural resemblance to glycosaminoglycans in the ECM and contains  $\text{NH}_2$  and  $\text{OH}$  groups that are functionally significant for its pH sensitivity and conformation. Gold nanoparticles (AuNPs) serve as inert, non-toxic physical crosslinkers for the development of "reversible" hydrogels utilizing electrostatic attraction with the cationic CS. This study outlines the synthesis of a CS hydrogel, physically cross-linked with AuNPs, followed by the encapsulation of 5-FU. The physicochemical properties of the CS, CS-Au, and CS-Au-5-FU hydrogels were analysed, and the identification of distinctive peaks in Fourier transform infrared (FTIR) spectroscopy, along with a peak at 530 nm under UV-visible spectroscopy, confirmed their successful synthesis. Transmission electron microscopy (TEM) confirmed the production of spherical nanoparticles (NPs) with an average diameter of approximately 89.31 nm. Scanning electron microscopy (SEM) demonstrated a porous network surface morphology for the CS and CS-Au hydrogels, conducive for diffusion and functioning as a synthetic extracellular matrix. The zeta potentials recorded using dynamic light scattering (DLS) were  $+11.1 \pm 0.1$  mV and  $+15.87 \pm 1.18$  mV for the CS-Au and CS-Au-5-FU hydrogels, respectively, suggesting moderate stability of the NPs. CS can function as a steric stabilizer to enhance the overall stabilization of the NP. Rheological analyses revealed a non-Newtonian shear-thinning property, characterized by a progressive reduction in viscosity with an increasing shear rate, along with a thixotropic behavioural characteristic attributed to hydrogel recovery following shear stress. This indicated a suitability for injection *in vivo* and application on dynamic wound surfaces. A thermal stability test using thermogravimetric analysis (TGA) demonstrated enhanced stability for the CS-Au hydrogel

relative to the CS hydrogel due to physical crosslinking, as evidenced by a 21.21 °C increase in the endothermic peak. The pH sensitivity and reswelling of the CS-Au hydrogel were examined, revealing a significant pH-dependent uptake in water. At pH 4.5, the hydrogel achieved a higher equilibrium quicker than at pH 7.4 and pH 10.5. This can be attributed to an increased concentration of protonated hydroxyl and amino groups, in tandem with the relaxation of the polymer chains enabling water absorption. It was determined that the CS-Au hydrogel attained a favourable drug (5-FU) loading capacity of 77.71%. An *in vitro* lysozyme-mediated degradation study of the CS-Au and CS-Au-5-FU hydrogels demonstrated a natural, progressive degradation profile that facilitated cellular proliferation and removal from the body. The drug release studies conducted in simulated cancer and physiological microenvironments indicated a sustained, pH-dependent release with specificity for the acidic cancer microenvironment (pH 4.5 and 6.5). The *in vitro* 3-(4,5-dimethylthiazol-2-yl)-2,5-diphenyltetrazolium bromide (MTT) cytotoxicity assay was performed on three human cell lines: HEK293 (embryonic kidney), HeLa (cervical carcinoma), and MCF-7 (breast adenocarcinoma). The results demonstrated a notable specificity of the CS-Au-5-FU hydrogel for the cancer cells (HeLa and MCF-7) and a diminished cytotoxicity in the non-cancer cells (HEK293). Minimal cytotoxicity was observed at all hydrogel concentrations, with some proliferation noted at 20 µg/ml for the CS and CS-Au hydrogels in the HEK293 cells. This suggests suitability for wound healing applications. The scratch assay illustrated the complete closure of the wounds at low concentrations (15.63 and 31.25 µg/ml), confirming the capacity of the hydrogel to imitate the extracellular matrix (ECM). The positive findings from this study confirm the potential of these CS-Au hydrogels to function as smart *in vitro* delivery systems and scaffolds for wound healing, warranting additional optimizations and *in vivo* studies.

**Keywords:** Cancer, wound healing, hydrogel, chitosan, gold-nanoparticles, 5-fluorouracil, cytotoxicity.

## **Preface**

The experimental work described in this dissertation was carried out in the Discipline of Biochemistry, School of Life Sciences, University of KwaZulu-Natal, Durban under the supervision of Prof Moganavelli Singh.

These studies represent original work by the author and have not otherwise been submitted in any form for any degree or diploma to any tertiary institution. Where use has been made of the work of others it is duly acknowledged in the text.

## **Supervisors Declaration**

The research contained in this dissertation was completed by the candidate while based in the Discipline of Biochemistry, School of Life Sciences, of the College of Agriculture, Engineering and Science, University of KwaZulu-Natal, Westville Campus, South Africa. The research was financially supported by the National Research Foundation (NRF).

The contents of this work have not been submitted in any form to another university and except where the work of others is acknowledged in the text, the results reported are due to investigations by the candidate.

As the candidate's supervisor I approve this thesis for submission.

A solid black rectangular box redacting the signature of the supervisor.

Signed: Prof Moganavelli Singh

Date:

## **Declaration 2: Publications**

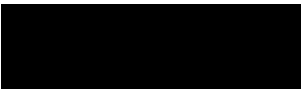
My role in the review paper is indicated. The \* indicates the corresponding author.

Gounden, V., & Singh, M\*. (2024). Hydrogels and Wound Healing: Current and Future Prospects. *Gels*, 10(1). <https://doi.org/10.3390/gels10010043>

## Declaration-Plagiarism

I, Varshan Gounden, declare that:

1. The research reported in this thesis, except where otherwise indicated, is my original research.
2. This thesis has not been submitted for any degree or examination at any other university.
3. This thesis does not contain other persons' data, pictures, graphs, or other information, unless specifically acknowledged as being sourced from other persons.
4. This thesis does not contain other persons' writing unless specifically acknowledged as being sourced from other researchers. Where other written sources have been quoted then:
  - a. their words have been re-written, but the general information attributed to them has been referenced.
  - b. where their exact words have been used, then their writing has been placed in italics and inside quotation marks and referenced.
5. This thesis does not contain text, graphics or tables copied and pasted from the Internet, unless specifically acknowledged, and the source being detailed in the thesis and in the References sections.

Signed: 

Date:

## **Acknowledgements**

*I wish to express my sincere gratitude and appreciation to the following people:*

- To Professor Singh, your guidance, patience and support has been invaluable throughout this entire process.
- To my family (Salven, Mogashree and Sayuri Gounden) for their encouragement and moral support.

## **Dedication**

*To my beloved aunt, the late Sheila Govender, who bravely fought stage IV pancreatic cancer.*

*Thank you for your everlasting belief in me and teaching me to never doubt myself.*

# TABLE OF CONTENTS

|                                  |       |
|----------------------------------|-------|
| ABSTRACT.....                    | II    |
| PREFACE.....                     | IV    |
| SUPERVISORS DECLARATION .....    | V     |
| DECLARATION 2: PUBLICATIONS..... | VI    |
| DECLARATION-PLAGIARISM .....     | VII   |
| ACKNOWLEDGEMENTS .....           | VIII  |
| DEDICATION .....                 | IX    |
| LIST OF FIGURES .....            | XIV   |
| LIST OF TABLES.....              | XVII  |
| LIST OF ABBREVIATIONS .....      | XVIII |

## CHAPTER 1: INTRODUCTION

|   |   |
|---|---|
| 1.1 BACKGROUND AND SIGNIFICANCE OF THE STUDY..... | 2 |
| 1.2 AIMS AND OBJECTIVES .....                     | 4 |
| 1.3 OUTLINE OF THESIS .....                       | 4 |
| 1.3 REFERENCES.....                               | 5 |

## CHAPTER 2: A LITERATURE REVIEW OF THE CS-AU HYDROGEL IN ANTI-CANCER DRUG DELIVERY

|  |    |
|--|----|
| 2.1 INTRODUCTION.....  | 8  |
| 2.2 CANCER.....  | 10 |
| 2.2.1. The Tumour Micro-environment .....  | 11 |
| 2.2.2 Conventional Cancer Therapy .....  | 12 |
| 2.3 5-FLUOROURACIL (5-FU) .....  | 13 |
| 2.3.1 Conventional drug delivery.....  | 15 |
| 2.3.2 An ideal drug delivery system.....   | 16 |
| 2.4 HYDROGELS FOR DRUG DELIVERY .....  | 16 |
| 2.4.1 Mechanisms of hydrogel drug release .....  | 17 |
| 2.4.2 Stimuli-responsive hydrogels for drug delivery .....   | 19 |
| 2.4.3 Targeted drug release mechanism of pH-responsive hydrogels in the tumour-<br>microenvironment (TME)..... | 20 |
| 2.4.4 Chitosan in hydrogels .....  | 21 |
| 2.4.5 Cross-linking of hydrogels.....  | 23 |

|  |    |
|--|----|
| 2.4.6 Chemically cross-linked hydrogels.....   | 24 |
| 2.4.7 Physically cross-linked hydrogels.....   | 25 |
| 2.5 NANOTECHNOLOGY AND NANOMEDICINE .....      | 26 |
| 2.5.1 Nanoparticle-crosslinked hydrogels.....  | 28 |
| 2.5.2 Metallic Nanoparticles .....             | 30 |
| 2.5.2 Gold Nanoparticles (AuNPs) .....         | 31 |
| 2.5.3 Gold nanoparticles in drug delivery..... | 32 |
| 2.6 PREVENTION OF OPSONIZATION .....           | 35 |
| 2.7 CELLULAR UPTAKE .....                      | 36 |
| 2.7.1 Intracellular trafficking .....          | 37 |
| 2.8 REFERENCES .....                           | 38 |

### **CHAPTER 3: A LITERATURE REVIEW OF THE CS-AU HYDROGEL AS A WOUND SCAFFOLD**

|   |    |
|---|----|
| 3.1 INTRODUCTION.....   | 51 |
| 3.2 THE SKIN.....   | 52 |
| 3.2.1 Wound Healing Phases.....                                 | 53 |
| 3.2.2 Acute and Chronic Wounds.....                             | 55 |
| 3.2.3 Socio-economic Impact of Chronic Wounds .....             | 57 |
| 3.3 CURRENT TREATMENT METHODS .....                             | 58 |
| 3.3.1 Dressings .....   | 58 |
| 3.3.2 Negative Pressure Therapy .....                           | 59 |
| 3.3.3 Surgery.....  | 59 |
| 3.3.4 Hyperbaric Oxygen Therapy .....                           | 59 |
| 3.4 IDEAL WOUND HEALING SYSTEM.....                             | 60 |
| 3.4.1 Hydrogels in wound-healing.....                           | 60 |
| 3.4.2 Hydrogels as a replicate extracellular matrix (ECM) ..... | 61 |
| 3.4.3 Hydrogels as a first aid for burn wounds .....            | 62 |
| 3.5 NATURAL AND SYNTHETIC HYDROGELS .....                       | 63 |
| 3.5.1 Synthetic Hydrogels.....                                  | 63 |
| 3.5.1.1 Polyethylene glycol (PEG).....                          | 64 |
| 3.5.1.2 Polyvinyl alcohol (PVA).....                            | 65 |
| 3.5.1.3 Polyvinylpyrrolidone (PVP).....                         | 65 |
| 3.5.2 Natural hydrogels.....                                    | 66 |
| 3.5.2.1 Gelatin.....  | 66 |
| 3.5.2.2 Hyaluronic acid.....                                    | 67 |
| 3.5.2.3 Alginate.....   | 68 |
| 3.5.2.4 Chitosan (CS).....                                      | 70 |
| 3.5.3 Advanced Hydrogels.....                                   | 71 |
| 3.5.3.1 Sprayable hydrogels .....                               | 71 |
| 3.5.3.2 “Smart” hydrogels.....                                  | 72 |
| 3.5.3.3 Nanogels .....  | 73 |

|   |    |
|---|----|
| 3.5.3.3.1 Gold nanoparticle hydrogels ..... | 74 |
| 3.6 REFERENCES.....                         | 75 |

## **CHAPTER 4: MATERIALS AND METHODS**

|   |    |
|---|----|
| 4.1 MATERIALS .....   | 89 |
| 4.2 METHODS .....   | 89 |
| 4.2.1 Synthesis of Chitosan-gold (CS-Au) Hydrogel .....             | 89 |
| 4.2.2 Characterization .....  | 89 |
| 4.2.2.1 <i>UV-visible (UV-vis) Spectroscopy</i> .....               | 89 |
| 4.2.2.2 <i>Fourier Transform Infrared (FTIR) Spectroscopy</i> ..... | 90 |
| 4.2.2.3 <i>Dynamic Light Scattering (DLS)</i> .....                 | 90 |
| 4.2.2.4 <i>Transmission Electron Microscopy (TEM)</i> .....         | 90 |
| 4.2.2.5 <i>Scanning Electron Microscopy (SEM)</i> .....             | 90 |
| 4.2.2.6 <i>Thermogravimetric Analysis (TGA)</i> .....               | 91 |
| 4.2.2.7 <i>Rheological studies</i> .....                            | 91 |
| 4.2.3 RESWELLING AND PH SENSITIVITY .....                           | 91 |
| 4.2.4 DRUG ENCAPSULATION.....                                       | 91 |
| 4.2.5 <i>IN VITRO</i> DEGRADATION.....                              | 92 |
| 4.2.6 DRUG RELEASE.....   | 92 |
| 4.2.6.2 <i>Drug release kinetics</i> .....                          | 93 |
| 4.2.7 CELL CULTURE AND MAINTENANCE.....                             | 93 |
| 4.2.8 <i>IN VITRO</i> CYTOTOXICITY .....                            | 93 |
| 4.2.9 SCRATCH ASSAY .....   | 94 |
| 4.2.10 STATISTICAL ANALYSIS .....                                   | 94 |

## **CHAPTER FIVE: RESULTS AND DISCUSSION**

|  |     |
|--|-----|
| 5.1 CHARACTERIZATION.....                                  | 96  |
| 5.1.1 UV-vis Spectroscopy.....                             | 96  |
| 5.1.2 Fourier Transform Infrared Spectroscopy (FTIR) ..... | 97  |
| 5.1.3 Dynamic Light Scattering (DLS).....                  | 98  |
| 5.1.4 Transmission Electron Microscopy (TEM) .....         | 99  |
| 5.1.5 Scanning Electron Microscopy (SEM) .....             | 100 |
| 5.1.6 Thermogravimetric Analysis (TGA).....                | 102 |
| 5.1.7 Rheological studies .....                            | 104 |
| 5.2 RE-SWELLING AND PH SENSITIVITY .....                   | 108 |
| 5.3 DRUG ENCAPSULATION .....                               | 109 |
| 5.4 <i>IN VITRO</i> DEGRADATION .....                      | 110 |
| 5.5.1 DRUG RELEASE .....                                   | 111 |
| 5.5.2 DRUG RELEASE KINETICS .....                          | 113 |
| 5.6 <i>IN VITRO</i> CYTOTOXICITY .....                     | 114 |
| 5.7 SCRATCH ASSAY .....                                    | 117 |

5.8 REFERENCES..... 123

**CHAPTER SIX: CONCLUSION AND FUTURE PERSPECTIVES**

6.1 CONCLUSION..... 130

6.2 FUTURE STUDIES..... 130

**APPENDIX A- PUBLISHED MANUSCRIPT.....132**

**APPENDIX B – TURNITIN REPORT .....133**

## List of Figures

**Figure 2.1:** The Hallmarks of Cancer

**Figure 2.2:** Primary (A) and Secondary (B) mechanisms of chemotherapy

**Figure 2.3:** Mechanism of action of 5-FU

**Figure 2.4:** Disadvantages of conventional drug delivery systems

**Figure 2.5:** Hydrogel administration routes

**Figure 2.6:** Mechanisms of drug release from a chitosan hydrogel

**Figure 2.7:** Stimuli-responsive drug release by "smart" hydrogels

**Figure 2.8:** Swelling of a cationic polymer hydrogel to facilitate drug release

**Figure 2.9:** Structure of chitin and chitosan

**Figure 2.10:** Single and multi-stimuli responsive application of chitosan hydrogels in cancer therapy

**Figure 2.11:** Physical, chemical, and double network hydrogel cross-linking

**Figure 2.12:** Synthesis of hydrogels using high-energy radiation

**Figure 2.13:** Favourable characteristics of nanoparticles for drug delivery

**Figure 2.14:** Combined advantages of a nanoparticle cross-linked hydrogel

**Figure 2.15:** Different methods to synthesize nanoparticle hydrogels

**Figure 2.16:** Types and therapeutic benefits of metal nanoparticles

**Figure 2.17:** The different shapes of gold nanoparticles that can be synthesized

**Figure 2.18:** Photothermal effect of gold nanoparticles

**Figure 2.19:** Attachment of drugs on AuNPs through covalent bonds

**Figure 2.20:** Gold nanoparticle formation and physical cross-linking of chitosan

**Figure 2.21:** Evasion of nanoparticle opsonization with polymers

**Figure 2.22:** The enhanced permeability and retention effect in cancer tissue

**Figure 2.23:** *In vivo* behaviour and fate of nanogels

**Figure 3.1:** The structure of the skin illustrating the three layers: epidermis, dermis, and hypodermis

**Figure 3.2:** The four phases of wound healing and their approximate duration for acute and chronic wounds

**Figure 3.3:** Illustration of the differences in acute and chronic wounds during wound healing

**Figure 3.4:** Properties required for an ideal wound healing system

**Figure 3.5:** Different types of cross-linking in hydrogels

**Figure 3.6:** Natural and synthetic polymers being used in hydrogel dressings

**Figure 3.7:** Sensors detected by "smart" hydrogels

**Figure 3.8:** (A) Nanoparticles embedded in a hydrogel. (B) Cross-linking between polymer particles

**Figure 5.1:** Images of the formulated (A) CS, and (B) CS-Au hydrogels

**Figure 5.2:** UV-vis spectroscopy of the CS-Au hydrogel after heating for 10 and 20 minutes

**Figure 5.3:** FTIR spectra of CS, AuNP, 5-FU, CS-Au, and CS-Au-5-FU

**Figure 5.4:** TEM images of the CS-Au hydrogel exhibiting a (A) spherical morphology and (B) a crosslinking matrix

**Figure 5.5:** SEM images depicting the structural morphology of the (A) CS and (B) CS-Au hydrogels

**Figure 5.6:** Thermogravimetric Analysis of the (A) CS and (B) CS-Au hydrogels

**Figure 5.7:** Flow curves depicting viscosity vs shear rate of the (A) CS and (B) CS-Au hydrogels

**Figure 5.8:** Thixotropy study demonstrating self-healing for the (A) CS and (B) CS-Au hydrogels

**Figure 5.9:** Re-swelling and pH sensitivity studies of the CS-Au hydrogel at pH 4.5, 7.4, and 10.5

**Figure 5.10:** Comparison of the weight loss of the CS-Au and CS-Au-5-FU hydrogels as a function of incubation time in PBS containing 1.5  $\mu\text{g}$  of lysozyme/ $\text{cm}^3$ , at 37 °C

**Figure 5.11:** *In vitro* drug release profile of 5-FU from the CS-Au-5-FU hydrogel at pH 4.5, 6.5, and 7.4, at 37 °C

**Figure 5.12:** Image illustrating the expansion of the CS-Au-5-FU at pH 4.5, 6.5, and 7.4

**Figure 5.13:** MTT cytotoxicity of the free 5-FU, CS-Au-5-FU, CS-Au, and CS hydrogels in HEK293 cells

**Figure 5.14:** MTT cytotoxicity of the free 5-FU, CS-Au-5-FU, CS-Au, and CS hydrogels in the HeLa cells

**Figure 5.15:** MTT cytotoxicity of the free 5-FU, CS-Au-5-FU, CS-Au, and CS hydrogels in the MCF-7 cells

**Figure 5.16:** Images displaying the migration of HEK293 cells for wound closure when treated with A (15.63  $\mu\text{g}/\text{ml}$ ), B (31.25  $\mu\text{g}/\text{ml}$ ), C (62.5  $\mu\text{g}/\text{ml}$ ), D (125  $\mu\text{g}/\text{ml}$ ) of the CS and CS-Au hydrogels on Day 0

**Figure 5.17:** Images displaying the migration of cells for wound closure when treated with A (15.63  $\mu\text{g}/\text{ml}$ ), B (31.25  $\mu\text{g}/\text{ml}$ ), C (62.5  $\mu\text{g}/\text{ml}$ ), D (125  $\mu\text{g}/\text{ml}$ ) of the CS and CS-Au hydrogels on Day 1

**Figure 5.18:** Images displaying the migration of cells for wound closure when treated with A (15.63  $\mu\text{g}/\text{ml}$ ), B (31.25  $\mu\text{g}/\text{ml}$ ), C (62.5  $\mu\text{g}/\text{ml}$ ), D (125  $\mu\text{g}/\text{ml}$ ) of the CS and CS-Au hydrogels on Day 2

**Figure 5.19:** Images displaying the migration of cells for wound closure when treated with A (15.63  $\mu\text{g}/\text{ml}$ ), B (31.25  $\mu\text{g}/\text{ml}$ ), C (62.5  $\mu\text{g}/\text{ml}$ ), D (125  $\mu\text{g}/\text{ml}$ ) of the CS and CS-Au hydrogels on Day 3

## List of Tables

**Table 2.1:** Characteristics of physical and chemical hydrogels

**Table 3.1:** Common wound dressings

**Table 3.2:** Some Commercially available hydrogels for wound healing

**Table 5.1:** DLS, zeta potential values of the CS-Au and CS-Au-5-FU hydrogels

**Table 5.2:** Kinetic parameters at pH 4.5, 6.5, and 7.4, where  $(r)^2$  is the coefficient and  $n^{(a)}$  is the Korsmeyer-Peppas release exponent

**Table 5.3:** Wound closure (%) after treatment with various concentrations of the CS hydrogel over a 3-day period

**Table 5.4:** Wound closure (%) after treatment with various concentrations of the CS-Au hydrogel over a 3-day period

## List of Abbreviations

|                   |  |
|-------------------|--|
| <b>AuNPs</b>      | <b>Gold Nanoparticles</b>  |
| <b>CS</b>         | <b>Chitosan</b>  |
| <b>CS-Au</b>      | <b>Gold nanoparticle cross-linked chitosan</b>                             |
| <b>5-FU</b>       | <b>5-Fluorouracil</b>  |
| <b>CS-Au-5-FU</b> | <b>5-Fluorouracil encapsulated gold nanoparticle cross-linked chitosan</b> |
| <b>HeLa</b>       | <b>Cervical carcinoma</b>  |
| <b>MCF-7</b>      | <b>Breast adenocarcinoma</b>   |
| <b>HEK293</b>     | <b>Embryonic kidney</b>  |
| <b>Mw</b>         | <b>Molecular weight</b>  |
| <b>g</b>          | <b>Gram</b>  |
| <b>DMSO</b>       | <b>Dimethyl sulfoxide</b>  |
| <b>FBS</b>        | <b>Foetal bovine serum</b>   |
| <b>mg</b>         | <b>Milligram</b>   |
| <b>ml</b>         | <b>Millilitre</b>  |
| <b>µl</b>         | <b>Microlitre</b>  |
| <b>nm</b>         | <b>Nanometre</b>   |
| <b>SPR</b>        | <b>Surface plasmon resonance</b>   |
| <b>TEM</b>        | <b>Transmission electron microscopy</b>                                    |
| <b>SEM</b>        | <b>Scanning electron microscopy</b>  |
| <b>DLS</b>        | <b>Dynamic light scattering</b>  |
| <b>TME</b>        | <b>Tumour micro-environment</b>  |
| <b>ECM</b>        | <b>Extracellular matrix</b>  |
| <b>FTIR</b>       | <b>Fourier transform infrared spectroscopy</b>                             |
| <b>NPs</b>        | <b>Nanoparticles</b>   |
| <b>ROS</b>        | <b>Reactive oxygen species</b>   |
| <b>MNPs</b>       | <b>Metal nanoparticles</b>   |
| <b>EPR</b>        | <b>Enhanced permeation and retention</b>                                   |
| <b>TGA</b>        | <b>Thermogravimetric analysis</b>  |

# **CHAPTER ONE**

## **INTRODUCTION**

## 1.1 Background and significance of the study

The human body is composed of trillions of specialized cells, each executing unique functions that are necessary for regulating physiological processes. Cancer is characterized by the uncontrolled proliferation of cells within the body, which then metastasize to other tissues and organs, driven by key hallmarks including diminished growth restriction, suppression of the immune system, angiogenesis, resistance to apoptosis, and genetic instability. These cancer formation pathways directly disrupt fundamental physiological processes, resulting in mortality (Hanahan, 2022). Significant progress in cancer identification and treatment has led to the creation of novel methodologies; nonetheless, chemotherapy continues to be the predominant strategy in cancer therapy. However, further improvements in chemotherapy are necessary to reduce the adverse effects due to poor administration techniques and a lack of therapeutic specificity for the cancer site.

5-Fluorouracil (5-FU) is a frequently used chemotherapeutic agent that has disadvantages, such as a rapid metabolism and a restricted ability to selectively target cancer cells, resulting in harm to healthy cells (Elgemeie and Mohamed-Ezzat, 2022). Consequently, it is essential to develop advanced techniques for 5-FU administration to overcome its limitations and improve its efficacy. Hydrogels are polymers characterized by hydrophilic attributes that undergo crosslinking to form three-dimensional networks. These networks can enlarge and absorb water many times its dry mass. They exhibit exceptional biocompatibility and possess the ability to efficiently encapsulate hydrophilic drugs owing to an elevated water content (Li *et al.*, 2023). The phenomenon of ‘smart’ hydrogels undergoing a conformational change in response to stimuli has been extensively studied to facilitate regulated drug release (Bordbar-Khiabani and Gasik, 2022).

The tumour microenvironment (TME) may serve as an area of interest for therapies that exploit the acidic characteristics of cancer cells attributed to acidosis. Hence, pH-sensitive hydrogels containing chitosan (CS) can be utilized for drug release in the acidic TME (Tiwari *et al.*, 2022). The therapeutic significance of CS is established by the abundance of positively charged amino groups. CS hydrogels exhibit swelling in the TME as a result of the protonation of amino groups at low pH. Due to the expansion of the pores between the intermolecular polymeric chains, biological fluid infiltrates the hydrogel, causing it to swell upon contact with the acidic TME. This releases the drug over time, specifically targeting cancer cells (Marques *et al.*, 2021). Several shortcomings, such as inadequate mechanical strength and dissolution in water, can be addressed by cross-linking.

Physical crosslinking is a suitable approach for the synthesis of hydrogels, as it creates a three-dimensional reversible network through the formation of non-covalent bonds, thereby improving mechanical strength and enabling injectability. Metal nanoparticles (NPs) are ideal physical crosslinkers, as they provide additional mechanical support. Gold nanoparticles (AuNPs) are non-toxic and biocompatible, providing a foundation for integration within a hydrogel (Huang *et al.*, 2023). The CS-Au hydrogel containing encapsulated 5-FU serves as an innovative treatment strategy, integrating the properties of AuNPs with CS hydrogels to enable the sustained release of 5-FU and mitigate adverse effects on patients.

While cancer is a major global scourge, the predicament of chronic and acute wounds has also impeded the social and economic climate, and much-needed change in healthcare is required to rectify these detrimental effects. The current strategies in wound healing have shortcomings in reducing recovery duration. Hence, a new and improved system is needed to overcome these incompetencies. Hydrogels have been presented as adequate wound dressings for chronic and acute wounds through their ideal properties, such as maintaining a moist environment, absorption of exudates and necrotic tissue, and flexibility in shape to cover wounds with different morphologies (Gounden and Singh, 2024). Hydrogels consist of natural or synthetic polymers. Synthetic polymers exhibit stability and convenience but lack biocompatibility, making natural polymers the preferred choice because their composition and properties closely resemble the fundamental features of bodily tissues (Satchanska *et al.*, 2024).

CS, a natural polymer is widely used in hydrogel formulations for wound healing owing to its beneficial attributes. CS resembles glycosaminoglycans in the extracellular matrix and its cationic nature contributes to its antibacterial properties (Rajinikanth *et al.*, 2024). The development of nanogels or NP crosslinked hydrogels has paved the way to effective wound treatments. Nanogels have attracted attention for their capacity to combine the physical attributes and increased water absorption properties of hydrogels with the tunable size and shape of nanomaterials for the conjugation of drugs and biomolecules (Altuntaş *et al.*, 2023). Gold nanogels have been sought after due to their inherent low toxicity, antibacterial properties through membrane disruption, increased stability, and photothermal potential due to their surface plasmon resonance (SPR) effect (Wang *et al.*, 2024).

The current study is focused on the *in situ* physical crosslinking of a CS hydrogel with AuNPs. This novel synergistic hydrogel may provide a dual purpose in drug delivery, by serving as a

potential solution for reducing the duration of wound healing, improving overall patient health, and reducing the load borne by the current healthcare system.

## 1.2 Aims and Objectives

The study aims to synthesize, characterize, and assess the potential of CS-Au hydrogels as *in vitro* drug delivery vehicles for 5-fluorouracil to cancer cells, as well as to assess its wound healing capabilities. By virtue of this design, the initiative is to improve the current status of anticancer drug delivery and wound healing to improve patient health and reduce adverse side effects.

The main objectives were to:

- Synthesize a CS hydrogel and physically cross-link AuNPs between polymer chains to produce a CS-Au hydrogel
- Characterize the CS-Au hydrogel using FTIR, TEM, DLS, and rheology to confirm synthesis and to determine nanoparticle size and stability.
- Evaluate the drug encapsulation efficiency and the drug release pharmacokinetics of the CS-Au hydrogel.
- Generate cytotoxicity profiles of the delivery system in three selected human cell lines; two cancer (HeLa and MCF-7) and one non-cancer (HEK293).
- Assess the wound healing capability of the CS-Au hydrogel on HEK293 cells using a scratch assay. Treatment was only conducted on the non-cancer HEK293 cells to assess the ability of the hydrogels to regenerate a monolayer of normal cells.

## 1.3 Outline of thesis

This thesis was written in the traditional format and is broken down as follows:

**Chapter One** - This chapter provides a brief background, the aims and objectives, and an outline of the dissertation.

**Chapter Two** - This chapter entails an introduction and literature review discussing topics supporting the CS-Au hydrogel as a drug delivery vehicle for 5-FU to enhance current chemotherapeutic treatments.

**Chapter Three** – This chapter provides a brief introduction and literature review that outline topics in relation to CS-Au hydrogel as a wound healing treatment. Part of the chapter has been published.

**Chapter Four** – This chapter focuses on the experimental procedures, namely the synthesis of the CS-Au hydrogel, and drug encapsulation of 5-FU. Characterization protocols, including UV-vis spectroscopy, FTIR, TEM and SEM, and rheology, are described. The methodology for the drug encapsulation efficiency, drug release, cytotoxicity assay, and scratch assay are also discussed.

**Chapter Five** - This chapter includes the results of the study and critically discusses them. The results are presented graphically or as tables.

**Chapter Six** - This chapter concludes and highlights the results of the study. Future studies are also outlined for the optimization of the therapeutic efficacy of the CS-Au hydrogel.

### 1.3 References

Altuntaş, E., Özkan, B., Güngör, S., & Özsoy, Y. (2023). Biopolymer-Based Nanogel Approach in Drug Delivery: Basic Concept and Current Developments. *Pharmaceutics*, 15(6). <https://doi.org/10.3390/pharmaceutics15061644>

Bordbar-Khiabani, A., & Gasik, M. (2022). Smart Hydrogels for Advanced Drug Delivery Systems. *Int J Mol Sci*, 23(7). <https://doi.org/10.3390/ijms23073665>

Elgemeie, G. H., & Mohamed-Ezzat, R. A. (2022). Chapter 4 - Pyrimidine-based anticancer drugs. In G. H. Elgemeie & R. A. Mohamed-Ezzat (Eds.), *New Strategies Targeting Cancer Metabolism* (pp. 107-142). Elsevier. <https://doi.org/https://doi.org/10.1016/B978-0-12-821783-2.00006-6>

Gounden, V., & Singh, M. (2024). Hydrogels and Wound Healing: Current and Future Prospects. *Gels*, 10(1). <https://doi.org/10.3390/gels10010043>

Hanahan, D. (2022). Hallmarks of Cancer: New Dimensions. *Cancer Discovery*, 12(1), 31-46. <https://doi.org/10.1158/2159-8290.Cd-21-1059>

Hong, F., Qiu, P., Wang, Y., Ren, P., Liu, J., Zhao, J., & Gou, D. (2024). Chitosan-based hydrogels: From preparation to applications, a review. *Food Chemistry: X*, 21, 101095. <https://doi.org/https://doi.org/10.1016/j.fochx.2023.101095>

Huang, H., Liu, R., Yang, J., Dai, J., Fan, S., Pi, J., Wei, Y., & Guo, X. (2023). Gold Nanoparticles: Construction for Drug Delivery and Application in Cancer Immunotherapy. *Pharmaceutics*, 15(7). <https://doi.org/10.3390/pharmaceutics15071868>

- Li, D.-Q., Xu, Y.-L., Xu, F., & Li, J. (2023). Chapter 8 - Eco-friendly and biodegradable cellulose hydrogels. In S. Thomas, B. Sharma, P. Jain, & S. Shekhar (Eds.), *Sustainable Hydrogels* (pp. 197-230). Elsevier. <https://doi.org/https://doi.org/10.1016/B978-0-323-91753-7.00002-8>
- Marques, A. C., Costa, P. J., Velho, S., & Amaral, M. H. (2021). Stimuli-responsive hydrogels for intratumoral drug delivery. *Drug Discovery Today*, 26(10), 2397-2405. <https://doi.org/https://doi.org/10.1016/j.drudis.2021.04.012>
- Rajinikanth, B. S., Rajkumar, D. S. R., K, K., & Vijayaragavan, V. (2024). Chitosan-Based Biomaterial in Wound Healing: A Review. *Cureus*, 16(2), e55193. <https://doi.org/10.7759/cureus.55193>
- Satchanska, G., Davidova, S., & Petrov, P. D. (2024). Natural and Synthetic Polymers for Biomedical and Environmental Applications. *Polymers (Basel)*, 16(8). <https://doi.org/10.3390/polym16081159>
- Tiwari, A., Trivedi, R., & Lin, S.-Y. (2022). Tumor microenvironment: barrier or opportunity towards effective cancer therapy. *Journal of Biomedical Science*, 29(1), 83. <https://doi.org/10.1186/s12929-022-00866-3>
- Wang, Y., Zhang, M., Yan, Z., Ji, S., Xiao, S., & Gao, J. (2024). Metal nanoparticle hybrid hydrogels: the state-of-the-art of combining hard and soft materials to promote wound healing. *Theranostics*, 14(4), 1534-1560. <https://doi.org/10.7150/thno.91829>
- Xing, R., Liu, K., Jiao, T., Zhang, N., Ma, K., Zhang, R., Zou, Q., Ma, G., & Yan, X. (2016). An Injectable Self-Assembling Collagen–Gold Hybrid Hydrogel for Combinatorial Antitumor Photothermal/Photodynamic Therapy. *Advanced Materials*, 28(19), 3669-3676. <https://doi.org/https://doi.org/10.1002/adma.201600284>

## **CHAPTER TWO**

### **A LITERATURE REVIEW OF THE CS-Au HYDROGEL IN ANTI-CANCER DRUG DELIVERY**

## 2.1 Introduction

As a worldwide epidemic, cancer is manifested by the unbridled proliferation of aberrant cells. Referred to as "*the plague of this generation*" (Mukherjee, 2011), cancer continues to be a major contributor to global mortality. In 2020, there were approximately 10 million deaths and 19.3 million new diagnoses worldwide. The present prognosis for the majority of cancers is a shortened lifespan of 5-7 years, with a remote possibility of attaining a complete cure, thus rendering patients with a bleak future outlook (Chhikara and Parang, 2023). Consequently, the availability of improved cancer therapies is imperative to reduce the severity of cancer. Conventional cancer treatments include chemotherapy, radiation, surgery, and photothermal therapy (Debela *et al.*, 2021). Chemotherapy employs an organizational-based therapeutic strategy utilizing drugs, either separately or in conjunction, with the objective of eradicating cellular proliferation in solid tumours and haemophilic malignancies. However, the constraints of chemotherapy, including its limited capacity to reach targeted regions in the body, poor bioavailability, and substantial harm to non-cancer tissue, pose a considerable threat to patient well-being (Yan *et al.*, 2023).

5-Fluorouracil (5-FU) is an extensively studied chemotherapeutic medication that is employed in antineoplastic treatment for a variety of carcinomas. Per contra, there remain adverse impediments to its application in medicine, such as inadequate tissue penetration, non-selective biodistribution, and undesirable dose-dependent side effects (Valencia-Lazcano *et al.*, 2023). The limitations in terms of sensitivity and specificity of 5-FU have necessitated an amelioration of the issues that accompany this therapeutic approach (Dongsar *et al.*, 2023).

The utilization of hydrogels can contribute immensely to the reduction of drug delivery deficiencies. Hydrogels are discussed in greater detail in Chapter 3. They are three-dimensional structural polymers of crosslinked hydrophilic chains that can absorb significant quantities of water (Wang *et al.*, 2023). These fluid and soft substances possess properties associated with solids, such as well-defined sizes and shapes, and liquids, due to the presence of an extensive amount of water that allows for the internal and external permeation of soluble substances (Dannert *et al.*, 2019). As a result of their soft, wet nature and systemic affinity, resembling the extracellular matrix (ECM), hydrogels are highly biocompatible and have many uses in the biomedical field, notably as drug carriers and wound dressings (Wang *et al.*, 2023). Fundamentally, the networks undergo an alteration in volume when water is integrated or ejected into the cavity owing to the contraction of the networks triggered by stimuli such as light, pH, and temperature (Liang *et al.*, 2022). This capacity to respond to stimuli renders them

suitable as drug delivery systems due to the release of pharmaceuticals through diffusion when stimuli are applied.

A variety of polymers with hydrophilic properties have been evaluated for hydrogel synthesis, with chitosan (CS), a naturally occurring polymer, being the most popular. CS, a linear, cationic polymer consisting of  $\beta$  (1 $\rightarrow$ 4) linked N-acetyl-D-glucosamine and D-glucosamine, contains  $\text{NH}_2$  and OH groups that facilitate the chelation of 5-FU (Guo *et al.*, 2024). The hydrogels exhibit ecological integrity, biodegradability, and biocompatibility and can transport 5-FU across biological borders with greater ease (Peers *et al.*, 2020). Despite their promise, hydrogels are challenged by poor mechanical rigidity, limited thermal stability, rapid deterioration, and a negligible propensity for self-healing following disruption (Wang *et al.*, 2023). CS hydrogels are frequently cross-linked through covalent bonding using glutaraldehyde and UV radiation. The covalently cross-linked hydrogels possess robust mechanical strength due to irreversible chemical cross-linkage (Rizzo and Kehr, 2021). However, hydrogels employed in biomedicine must exhibit quick self-healing post-injection and fluidity under shear strain. These techniques have a substantial magnitude of cross-linking and irreversibility that significantly reduces biodegradability and self-healing, which induces toxicity and adverse effects following injection (Rizzo and Kehr, 2021). Thus, a cross-linking process that provides improved mechanical strength and the ability to undergo shear-thinning is necessary. Paul Ehrlich's "*magic bullet*" concept, which targets diseases at their active sites (Ahmed *et al.*, 2023), and the benefits of nanotechnology in healthcare have led to the use of nanoparticles (NPs) as cross-linkers for hydrogels. These hydrogels are formed by physically cross-linking molecules using weak bonding forces such as Van der Waals or hydrogen bonds to form 'reversible' hydrogels (Rizzo and Kehr, 2021).

Gold nanoparticles (AuNPs) are nonpareil among the various NPs, primarily for their biocompatibility and minimal toxicity. In addition, the capability of AuNPs to harness infrared light has enabled the advancement of innovative, non-invasive treatments for cancer, such as photodynamic therapy (PDT). This therapy can be utilized in a drug delivery system alongside chemotherapy to enhance treatment outcomes (Gupta and Malviya, 2021).

This adaptation entails the utilization of the electrostatic interaction between the cationic chains of CS in acrylic acid and anionic  $\text{AuCl}_4^-$  ions, leading to the synthesis of AuNPs, which act as physical cross-linkers for the *in situ* assemblage of an adjustable and self-repairing hydrogel. The current research focuses on developing a smart drug delivery system that employs a gold

cross-linked chitosan (CS-Au) hydrogel for the precise administration and sustained release of 5-FU while exhibiting cancer cell-specific cytotoxicity *in vitro*.

## **2.2 Cancer**

The earliest documented diagnosis of cancer dates back to ancient Egyptian writing (2500 BC), which characterizes it as '*a bulging tumour in the breast, like touching a ball of wrappings*' (Mukherjee, 2011). According to global statistics, the fatalities resulting from cancer reveal that the primary contributors to cancer-related deaths were lung (1.79 million deaths), liver (830,000 deaths), stomach (769,000 deaths), and breast cancer (680,000 deaths) (Chhikara and Parang, 2023). Substantial progress has been made toward unveiling the genetics and biological mechanisms of tumours. Genetic instability, metabolic changes, and a cell's susceptibility to various microenvironmental stimuli significantly influence cancer development, owing to their capacity to diversify genes, and expediting the process. The accumulation of genetic alterations ultimately results in oncogene activation and tumour suppressor gene inactivation (Zimmerman and Weyemi, 2021). This facilitates the ability of cancer cells to evade growth inhibitors, sustain proliferative signalling, resist cell death, and promote invasion and metastasis, which are notable hallmarks of cancer (Figure 2.1) (Hanahan, 2022). The impact is further exacerbated by telomerase, which, through the continuous insertion of nucleotides into the telomere, inhibits its diminishment, yielding cancer (Lansdorp, 2022). Cancer, the uncontrolled, rapid growth of abnormal cells, culminates in the deterioration of the body's immunity. While cancer may be fatal, the tumour microenvironment presents as a potential avenue for treatment.

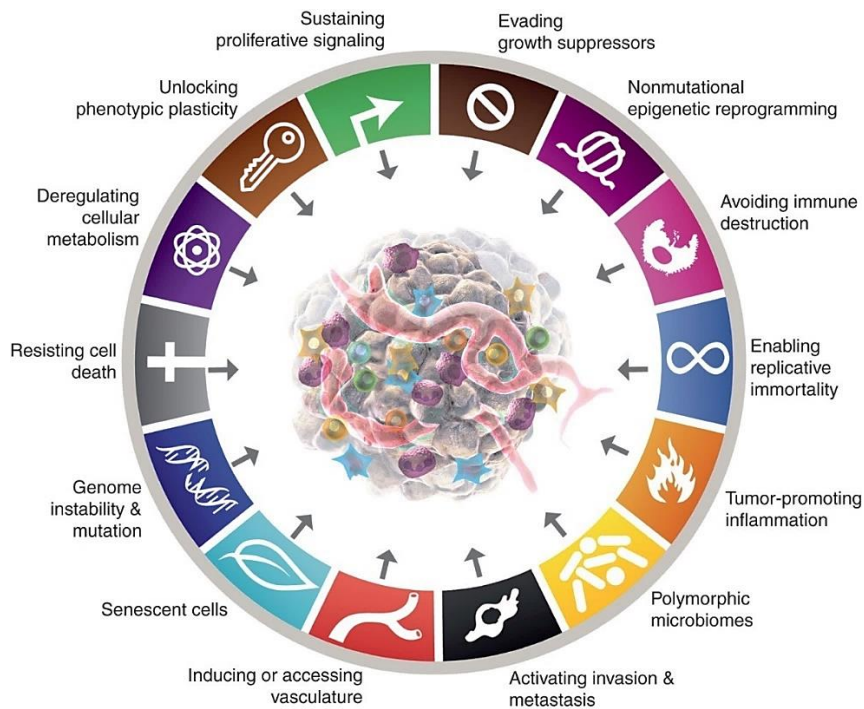


**Figure 2.1:** The Hallmarks of cancer (Hanahan, 2022).

### 2.2.1. The Tumour micro-environment (TME)

The tumour microenvironment (TME) is an intricate system in which cancer cells exist alongside and interact with non-cancer cells (stromal cells) and components that constitute the ECM (Elia and Haigis, 2021). Tumours produce enzymes that degrade the ECM, leading to the invasion of adjacent tissues. Solid tumours deplete their blood supply in order to fulfil the energy requirements of rapidly dividing tumour cells, resulting in either permanent or temporary oxygen and nutrition deprivation (hypoxia) (Fane and Weeraratna, 2020). Oxidative phosphorylation then ceases, and aerobic glycolysis begins as a metabolic response to hypoxia and inadequate nutrition. *'The Warburg effect'* is then engaged since cancer cells exhibit enhanced glucose absorption even when oxygen is available, and convert it into lactate (Zhong *et al.*, 2022). The elevated levels of lactic acid due to increased glycolysis lead to the tumour cells expressing additional acid-extruding transporters, which keep the intracellular pH neutral or slightly alkaline (Elia and Haigis, 2021). Solid tumours have a lower extracellular pH (usually 6.5 to 6.9) than normal tissues. Apart from their significance in the growth of cancers, acidosis, and hypoxia can be used to create novel therapeutic strategies (Singleton *et al.*, 2021).

### 2.2.2 Conventional Cancer Therapy

Cancer therapy is presently an area of complexity that requires collaboration among physicians, researchers, and biomedical engineers. Advances in identifying and treating cancer have resulted in the development of innovative approaches such as photothermal therapy, gene therapy, and immunotherapy. Nevertheless, the fundamental basis of cancer treatment is surgical intervention, radiation, and chemotherapy (Trayes and Cokenakes, 2021). The treatment plan is determined in accordance with the characteristics of the diagnosed cancer. Surgical intervention is effective in conventional therapy, in particular across the initial stages of cancer, as it may result in long-term remissions (Heymach *et al.*, 2018). Cancer has an extensive impact on the body as a whole, and the development of a tumour is a mere indication of this detrimental disease. Thus, addressing the symptom does not entirely relieve or cure the condition. Once malignancy has progressed to the point of metastasis, surgery is deemed ineffective (Heymach *et al.*, 2018). Radiotherapy works by eradicating the DNA within tumours and preventing further proliferation by employing high-energy ionizing radiation targeting the tumour microenvironments (Barazzuol *et al.*, 2020). Approximately 30% to 40% of individuals diagnosed with cancer undergo a treatment regimen that combines radiotherapy with chemotherapy (Damyanov *et al.*, 2018). However, the effectiveness of the treatment is greatly hindered by the damage inflicted on nearby healthy tissues (Barazzuol *et al.*, 2020).

Chemotherapy employs medications to specifically target rapidly dividing cells, including alkylating compounds, antimetabolites of purines and pyrimidines, and anthracyclines (Moodley and Singh, 2021). The chemotherapeutic compounds proceed through a primary and secondary mechanism of action (Figure 2.2). The primary mechanism is exerted through the intercalation of antimetabolites with DNA, which interfere with DNA and RNA synthesis. Topoisomerase (Top) inhibitors further halt DNA replication, thus impeding the formation of microtubules, which affect mitosis. The secondary mechanism of action occurs through the impediment of DNA and RNA synthesis due to enzyme inhibition by antimetabolites. Top inhibitors further impair mitochondria and produce reactive oxygen species (ROS) (Tilsed *et al.*, 2022). These processes ultimately result in cellular inhibition and death (Damyanov *et al.*, 2018). Chemotherapy is currently the predominant approach for anticancer treatment, as it addresses the entirety of the body as opposed to radiotherapy or surgery. However, there are negative consequences associated with this treatment, including anaemia, alopecia, and leukopenia (Moodley and Singh, 2021). Although significant developments and improvements have emerged in traditional cancer therapy, the adverse effects induced by the chemicals and

administration methods, and the lack of specificity for the tumour site, continue. Hence, it is essential to develop novel techniques to enhance patient care and complement conventional treatments.

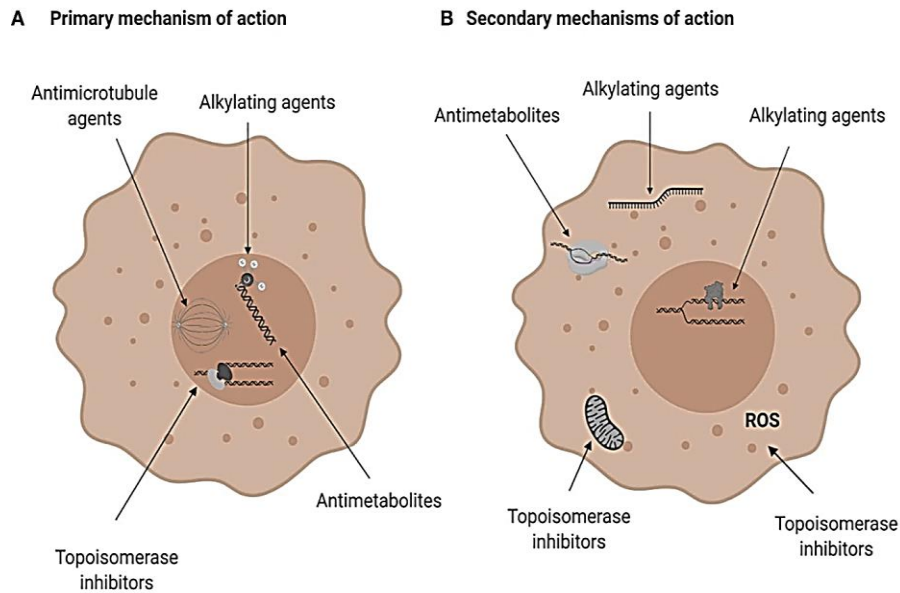


**Figure 2.2:** Primary (A) and secondary (B) mechanisms of chemotherapy (Tilsed *et al.*, 2022).

### 2.3 5-Fluorouracil (5-FU)

Researchers have specifically formulated and rigorously examined many potent chemotherapeutic drugs to combat cancer. The highly effective antimetabolite, 5-FU has been extensively used to treat various types of cancer, including cervical, colon, liver, and breast cancer (Sethy and Kundu, 2021). Chemotherapeutic regimens frequently consist of a combination of prescription drugs, often including 5-FU in conjunction with leucovorin or levamisole. Since 5-FU is a pyrimidine uracil analogue, its inclusion uses similar transport pathways and enzymatic processes for anabolism and catabolism. Cellular uptake and biochemical transformation are essential for 5-FU cytotoxicity (Vodenkova *et al.*, 2020).

One characteristic observed in malignancies is the ability to avoid apoptosis. Caspases, along with many upstream regulatory components, execute apoptosis. The principal approach of 5-FU is to render cancer cells more vulnerable to drug-induced apoptosis by triggering the caspase-6 pathway (Blondy *et al.*, 2020). The p53 tumour suppressor cascade is one of the signalling pathways for apoptosis. 5-FU induces ROS production in mitochondria via a mechanism that depends on the p53 protein. ROS leads to the degradation of mitochondria, prompting cell inhibition (Blondy *et al.*, 2020). Upon cellular absorption, 5-FU undergoes

anabolism to generate its cytotoxic derivative. Within cancer cells, 5-FU undergoes metabolism to form 5-fluorodeoxyuridine monophosphate (5-FdUMP), following which it competes for binding during thymidylate synthesis (Entezar-Almahdi *et al.*, 2020). This leads to deoxynucleotide imbalances and the exhaustion of essential components necessary for the synthesis and repair of DNA, causing the demise of the cell (Figure 2.3). 5-FU can impede RNA synthesis once converted to 5-fluorouridine triphosphate (5-FUTP) and can substitute uracil or thymine in RNA and DNA, leading to misincorporation. The overabundant disintegration of DNA repair systems ultimately eradicates cancer cells (Entezar-Almahdi *et al.*, 2020).

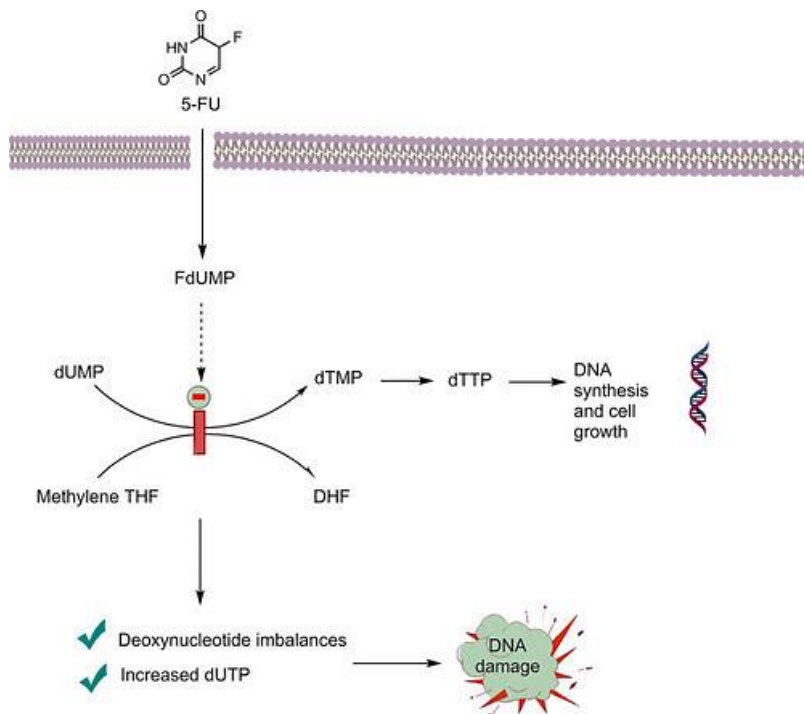


**Figure 2.3:** Mechanism of action of 5-FU (Entezar-Almahdi *et al.*, 2020).

Although 5-FU is a potent anticancer drug, it has limitations that reduce its effectiveness as a chemotherapeutic agent. These include a fast metabolism, a brief half-life, low bioavailability, damage to healthy cells, and a limited capacity to target cancer cells (Dongsar *et al.*, 2023). Oral preparations can also elicit severe gastrointestinal discomfort. Patients become susceptible to infection due to a compromised immune system and impaired organ function (Valencia-Lazcano *et al.*, 2023). Hence, it is vital to produce novel strategies for delivering 5-FU to address its limitations and enhance its efficiency as a chemotherapeutic agent.

### 2.3.1 Conventional drug delivery

Drug delivery refers to the controlled and precise administration of drugs in a specified region (Sultana *et al.*, 2022) and operates under the assumption of an ideal situation. Many available drugs have poor efficacy due to low solubility, high dosage demands, and non-specificity (Tewabe *et al.*, 2021). The advent of revolutionary drugs to increase effectiveness would be futile if the vectors responsible for their transportation remain inadequate.

Traditional drug delivery systems (Figure 2.4), such as tablets, capsules, and syrups, undergo rapid elimination from the body, resulting in poor maintenance of the desired dose within the therapeutic range (Adepu and Ramakrishna, 2021). Upon administration of a single standard dose, the drug undergoes an accelerated metabolism, resulting in an initial rise in drug concentration, which is subsequently accompanied by an exponential decline. The duration may not generate a substantial therapeutic impact and lead to a suboptimal response. Therefore, strategies have been pursued to preserve the drug's dosage in the blood plasma above the minimal effective concentration and below toxicity levels (Adepu and Ramakrishna, 2021).



**Figure 2.4:** Disadvantages of conventional drug delivery systems (Adepu and Ramakrishna, 2021).

Administering periodic doses may appear as an alternative to a single dose but can lead to variations in the drug concentration in the bloodstream (Hardenia *et al.*, 2019). It often results in levels below the desired level of effectiveness or above toxic tolerability. Administering multiple dosages in a single day also leads to inadequate adherence by patients. Alternatively, delivering a dosage that exceeds the recommended quantity results in unintended side effects (Hardenia *et al.*, 2019). Many anticancer medications cannot deeply infiltrate the tumour,

diminishing their efficacy in fully eliminating cancer cells. A further obstacle in anticancer treatment is the presence of P-glycoproteins embedded in the cell membranes of malignant cells. This protein operates as a pump that expels and prohibits drug buildup, leading to drug resistance (Tian *et al.*, 2023). Hence, there is a need for the innovation of ideal drug delivery systems that provide higher efficacy in treatment.

### **2.3.2 An ideal drug delivery system**

*"To liberate the drug at the right time in a right amount of concentration at a specified target site"* is the primary goal of a drug delivery system (Laffleur and Keckeis, 2020). An ideal drug delivery system should be convenient to employ and remove, biocompatible, mechanically robust, inert, able to sustain high drug loading, shielded from unintentional drug release, and straightforward to synthesize and sterilize (Liu *et al.*, 2023). Ideally, the system should bind the drug, protect it from degradation, provide a longer half-life, safely and efficiently transport the drug to the target site, and release the drug under optimal conditions (Jain, 2020). The adequacy of hydrogels and the rapid advancement of nanotechnology can significantly revolutionize the development and advancement of innovative drug delivery systems.

### **2.4 Hydrogels for drug delivery**

Hydrogels are polymers with hydrophilic properties subjected to physical or chemical cross-linking to develop three-dimensional mesh networks (Vigata *et al.*, 2020). These networks can expand and absorb water several times their dry weight, typically ranging from 70% to 99% in physiological conditions due to the ionization of hydrophilic functional groups such as carboxylic acid, sulphate, and hydroxyl moieties (Li and Mooney, 2016). The therapeutic potential of hydrogels stems from their unique traits, including high water retention, a flexible and malleable texture, minimal adhesion to bodily fluids, and biocompatibility (Kesharwani *et al.*, 2021). The extent and type of cross-linking have an immense impact on the characteristics exhibited. Hydrogels provide precise spatiotemporal control over numerous therapeutic substances, such as cells, large-molecule medications, and small-molecule drugs (Wang *et al.*, 2023). They are highly biocompatible and can effectively encapsulate hydrophilic medicines due to their high water content (Wang *et al.*, 2023). Synthesizing hydrogels in water-based solutions reduces the likelihood of drug decomposition and aggregation when exposed to an organic solvent (Jacob *et al.*, 2021). Conventionally, hydrogels are classified as being natural or synthetic. Hydrogels derived from natural sources encompass CS, alginate, gelatin, and hyaluronic acid, while typical synthetic hydrogels consist of polyethylene glycol or polyvinyl

alcohol (Vigata *et al.*, 2020). A third classification includes semi-synthetic hydrogels, such as gelatin methacryloyl hydrogels (Piao *et al.*, 2021). Despite the convenience of manipulating and fabricating synthetic hydrogels, natural hydrogels are preferred for their enhanced biocompatibility, which is crucial for patient health. These adaptable drug delivery platforms present the advantage of multiple routes of administration (Figure 2.5), such as oral, rectal, ocular, or transdermal administration (Kesharwani *et al.*, 2021). Due to their adjustable physicochemical features and ability to preserve labile drugs from degradation, hydrogels also serve as adequate vehicles to control drug release, facilitated through three unique mechanisms (Ezike *et al.*, 2023).

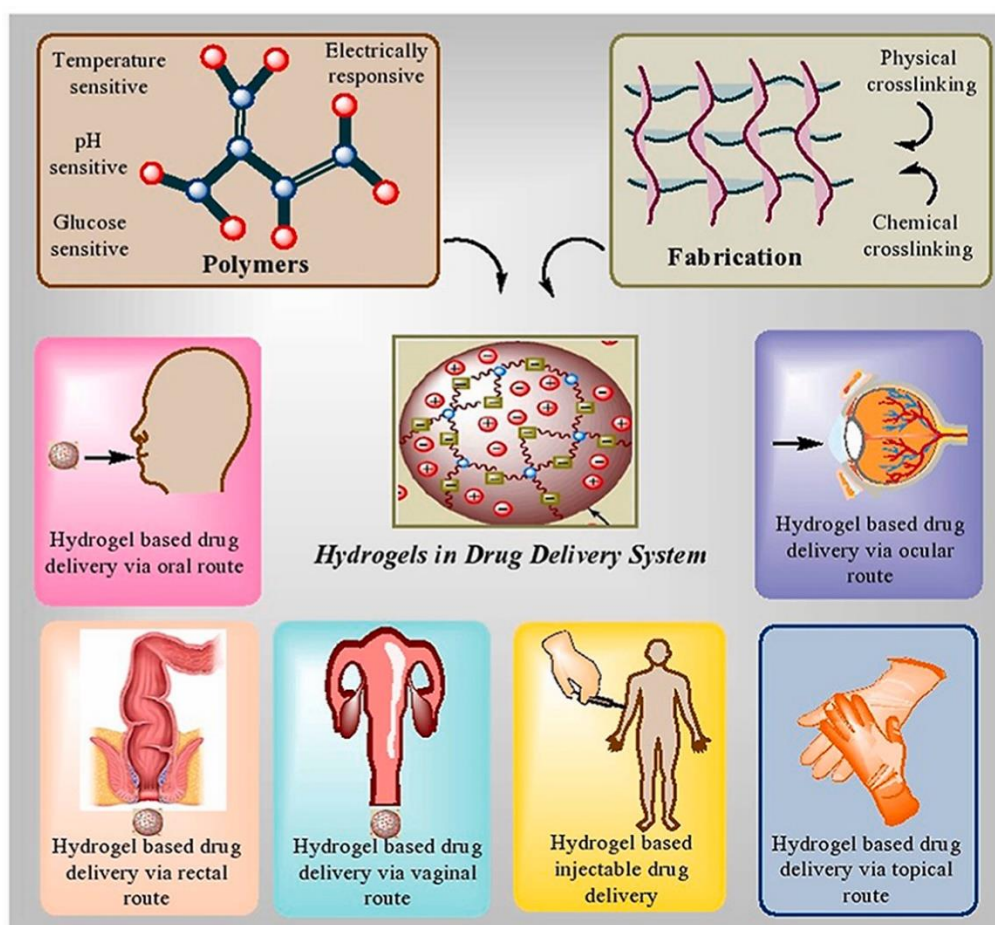


**Figure 2.5:** Hydrogel drug administration routes (Kesharwani *et al.*, 2021).

### 2.4.1 Mechanisms of hydrogel drug release

Similar to other methods of administration, the release of the drug from hydrogels is contingent upon the physicochemical characteristics of the encapsulated drug, such as its hydrophilic or hydrophobic nature, size, and dosage. It is also dependent on the properties of the polymer,

such as pore size, swelling, copolymers, excipients, and *in situ* gelling in a range of physiological fluids with varying pH and ion concentrations (Parhi, 2020). The following mechanisms govern the drug release from hydrogels containing chitosan. Diffusion, swelling, and erosion (Figure 2.6).

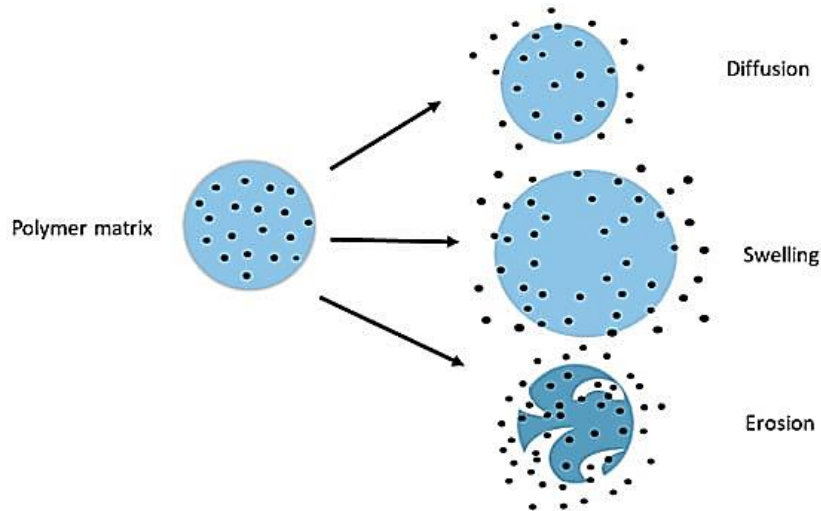


**Figure 2.6:** Mechanisms of drug release from a chitosan hydrogel (Mohammed *et al.*, 2017).

Diffusion utilizes a reservoir system, enclosing a drug in a hydrogel, where the polymer chains act as a rate-limiting membrane to regulate drug release. During the process of swelling, the drug is uniformly dispersed within a polymer matrix and undergoes diffusion through the polymer matrix (Mohammed *et al.*, 2017). Swelling is a process in which a hydrophilic polymer with cross-linked chains can absorb a significant amount of biological fluid or water without disintegrating it. This prompts the pores to expand and the polymer chains to detangle, thereby allowing for easier diffusion of drugs (Shaaban *et al.*, 2022). The synthesized CS-Au hydrogel will utilize swelling as a mechanism of drug release. The diffusion depends on the dimensions of the apertures and the level of porosity. A highly porous hydrogel facilitates diffusion readily, while less porous hydrogels require network disintegration to enable the drug to be effectively released (Narayanaswamy and Torchilin, 2020). Finally, erosion is the result of polymeric degradation. Surface erosion specifically refers to the erosion of the polymer surface, in which the rate of polymeric chain degradation is greater than the rate at which water flows into the hydrogel (Mohammed *et al.*, 2017). On the other hand, bulk erosion refers to erosion that occurs throughout the entire polymeric system, in which the flow of water into the system is greater than the rate of polymeric chain fracture (Parhi, 2020). "Smart "or stimuli-responsive hydrogels have recently been utilized to exploit the swelling mechanism of the hydrogel, resulting in a controlled release upon changes in temperature, pH, and ionic strength.

### 2.4.2 Stimuli-responsive hydrogels for drug delivery

The advancement of polymers responsive to external conditions or stimuli has led to the emergence of stimuli-responsive or "smart" drug delivery systems. The phenomenon of certain hydrogels conducting a phase transition or altering their conformation following stimuli has been thoroughly investigated with the objective of constructing drug depots and achieving controlled drug release (Tian and Liu, 2023). The ability to perceive these stimuli and respond through physical and chemical alterations has led to the coining of the term "smart" hydrogels. In particular, *in situ* gelling hydrogels have garnered close interest due to their ability to exist in an unswollen state at ambient temperature and transform into a swollen state upon application to the body, triggered by different stimuli. The reversibility of these conformational changes is attributed to the ability of stimuli-responsive polymers to revert to their original state once the stimulus ceases (Alvarez-Lorenzo *et al.*, 2020). Stimuli are biological, physical, or chemical based on their inherent properties. Stimuli-responsive hydrogels in drug delivery can undergo a volume-phase transition, swelling or shrinking, or assembly or disassembly when exposed to external triggers such as light (Figure 2.7) or internal stimuli in the tumour microenvironment such as pH and redox (Kasiński *et al.*, 2020). These hydrogels offer enhanced control over the location and duration of drug release in comparison to conventional hydrogels. Such hydrogels have various benefits for the delivery of cancer drugs, depending on the stimulation.

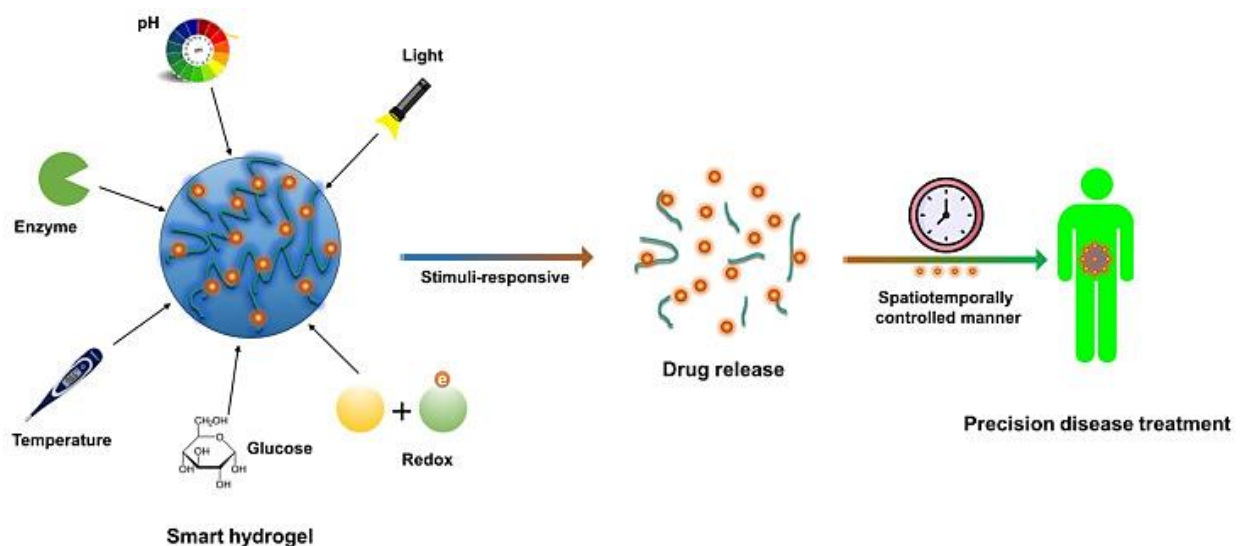


**Figure 2.7:** Stimuli-responsive drug release by "smart" hydrogels (Zhang and Wu, 2023).

### 2.4.3 Targeted drug release mechanism of pH-responsive hydrogels in the tumour-microenvironment (TME)

The TME, as previously mentioned, is a phenomenon produced by the interaction of cancer cells with stromal cells. It may be used as a treatment targeting route due to its characteristics, such as the acidic nature of cancer cells, which is induced by acidosis. Therefore, pH-sensitive hydrogels, particularly the swelling nature of cationic hydrogels in acidic pH, may release drugs in the acidic TME. Cationic hydrogels swell at low pH (acidic medium) due to the protonation of amino and imine groups. These protonated, positively charged moieties cause repulsion and are responsible for swelling (Rizwan *et al.*, 2017). Once in contact with the TME, the biological fluid permeates the surface of the hydrogel due to the open pores between their intermolecular chains. The fluid influx exerts stress, which prompts the polymer chains to be less rigid, leading to the enlargement of pores and subsequent swelling (Zhang and Wu, 2023). The pH-responsive hydrogels transition from an unswollen state to a swollen state when in contact with the acidic TME and gradually release the drug through diffusion over a prolonged period (Figure 2.8) (Xin and Naficy, 2022). Its ideal applicability is realized as the cationic polymer theoretically may not fully swell and release the drugs in healthy tissue as the amine groups may not be protonated, inhibiting the influx of biological fluid and drug diffusion (Rizwan *et al.*, 2017). This bodes well for patient health, as the adverse effects of chemotherapy may be severely reduced. Switching a stimulus on and off allows for a cancer-specific and sustained drug release, with minimal release occurring during the off state (in healthy tissue), which is beneficial for cancer treatment (Marques *et al.*, 2021). CS is a pH-sensitive polymer with favourable characteristics for use in "smart" drug delivery systems.

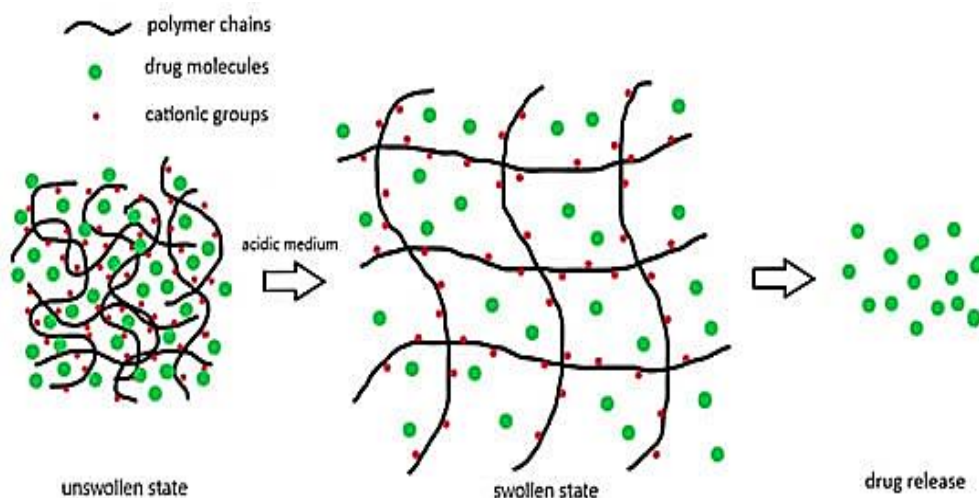


**Figure 2.8:** Swelling of a cationic polymer hydrogel to facilitate drug release (Xin and Naficy, 2022).

#### 2.4.4 Chitosan in hydrogels

CS is a derivative of chitin (Figure 2.9) that has undergone partial deacetylation and is mainly extracted from crustacean exoskeletons (Peers *et al.*, 2020). A  $\beta$  (1 $\rightarrow$ 4) glycosidic bond connects the two subunits of this linear copolymer, D-glucosamine and N-acetyl-D-glucosamine, facilitating facile chemical alteration with superior flexibility, elasticity, and reduced inflammatory response (Do *et al.*, 2022). The functional value of CS is determined by the presence of an amino group, which provides a positive charge, and a hydroxyl group, which bears a negative charge (Peers *et al.*, 2022). Due to the amino groups, CS exhibits a pH-dependent solubility and dissolves when the pH is lower than the pKa value of 6.5 but is insoluble when the pH is higher. This feature has been harnessed for developing stimuli-responsive hydrogels (McCarthy *et al.*, 2021). The primary hydroxyl group is important in hydrogel synthesis as it is the point of attachment for chain substitution to yield branched polymers or copolymers necessary for physical or chemical cross-linking to alter mechanical characteristics (Saeedi *et al.*, 2022).

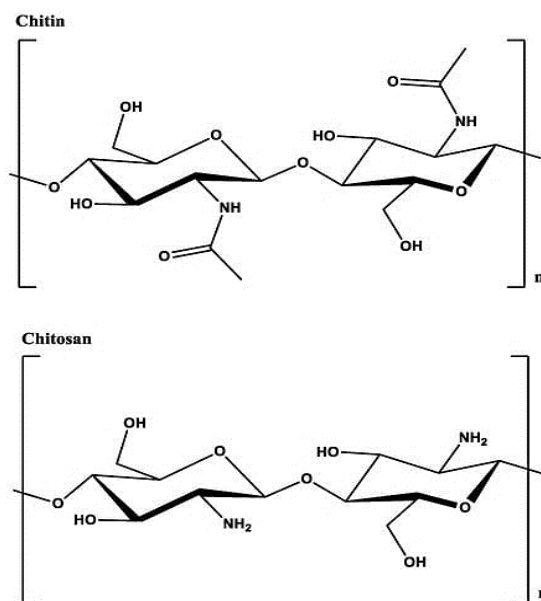


**Figure 2.9:** Structure of chitin and chitosan (McCarthy *et al.*, 2021).

CS distinguishes itself from other biomaterials because of its availability, adaptability, and unique attributes, including hydrophilicity, anti-inflammatory response, biodegradability, and non-toxicity (Saeedi *et al.*, 2022). The positive charge allows for the attachment to negatively charged cell membranes, facilitating drug release. Notably, the breakdown of CS results in non-toxic amino sugars that may be fully assimilated by the human body, thus providing a competent polymer without adverse effects, which is crucial for patient health. CS in drug

delivery further exhibits an enhanced drug-carrying capacity, chelating ability with 5-FU, compatibility with targeting ligands, moldability into multiple configurations, and flexibility of an interconnected porous structure (Peers *et al.*, 2020). It can be utilized as a multi-stimuli-responsive drug delivery vehicle to allow for a targeted, sustained release (Figure 2.10). Hence, CS is a suitable polymer for hydrogel synthesis, with remarkable potential for drug delivery.

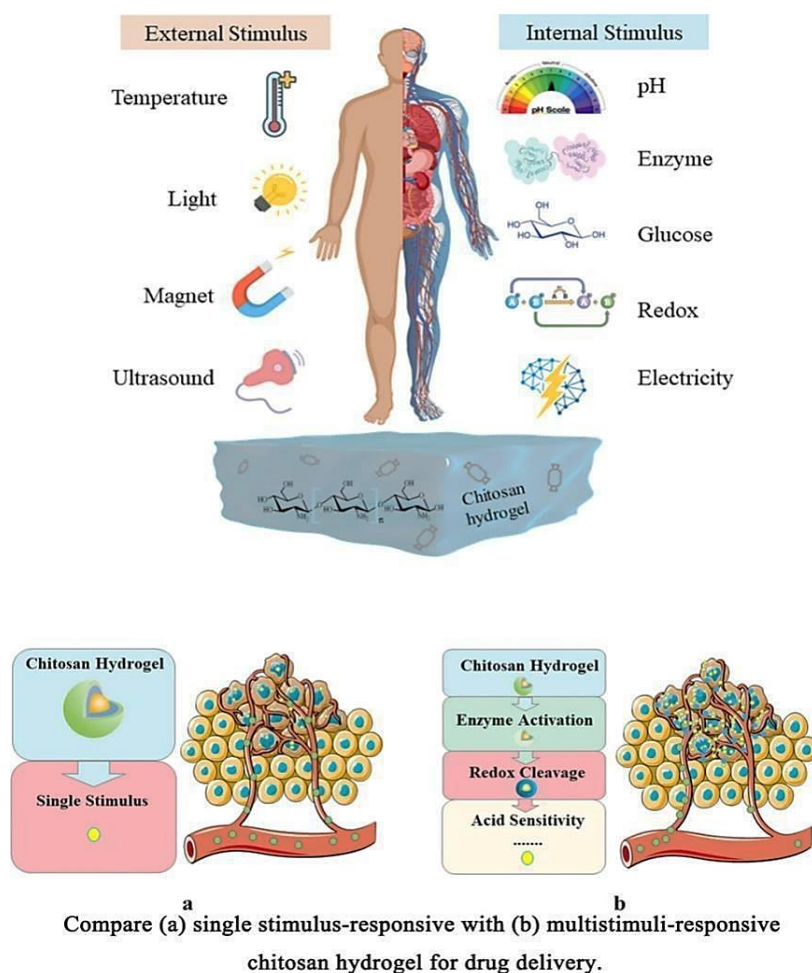


**Figure 2.10:** Single and multi-stimuli responsive application of chitosan hydrogels in cancer therapy (Tian and Liu, 2023).

CS has shown anticancer effects that may enhance its applicability with 5-FU in cancer therapy. It was reported that higher degrees of deacetylation and a lower molecular weight of CS, enhance anticancer efficacy (Park *et al.*, 2011). It was demonstrated that CS and its derivatives have a significant anticancer impact due to their capacity to eliminate free radicals from cancer cells and antiangiogenic and apoptotic pathways, which is promising for developing anticancer treatments (Shakil *et al.*, 2021). CS-based hydrogels present many advantages, but on their own, they may face inefficiencies that can inhibit their efficacy as a drug delivery vehicle. Such

disadvantages include poor mechanical rigidity and solubility in water. This can be overcome by including a cross-linking matrix.

#### **2.4.5 Cross-linking of hydrogels**

Hydrogels constitute a network of polymer chains. Cross-links are necessary to prevent the polymer chains from dissolving in the solution. Cross-linking is used in polymer chemistry to stabilize a polymer by extending its chains to various dimensions, giving rise to a network arrangement. A cross-link is a chemical link that connects different polymer chains ionically or covalently. Cross-linking constrains the molecular mobility of the free-flow chains of a liquid polymer, transforming it into a "gel" (Maitra and Shukla, 2014). Cross-linked polymers are significant due to their considerable mechanical strength and resistance to heat, disintegration, and solvent attack (Parhi, 2017). Their rigidity can be adjusted within a range of 0.5 kPa to 5 mPa, enabling their physical characteristics to align with various soft tissues in the human body. The interconnected network may inhibit the entry of different proteins, thereby safeguarding bioactive therapies against untimely disintegration caused by enzymes that diffuse within. This characteristic is especially crucial for macromolecular medications prone to instability (such as monoclonal antibodies and recombinant protein-based therapies), which comprise a growing proportion of newly approved drugs (Li and Mooney, 2016). The degree of cross-linking in hydrogels directly impacts their internal framework, leading to alterations in their swelling and physical properties. Generally, an increased level of crosslinking in hydrogels is associated with greater compression and tensile strength and a slower rate of swelling at equilibrium (Akhtar *et al.*, 2016). This may reduce the size of the pores and drug diffusion. Hence, the degree and nature of cross-linking can impact not only the mechanical characteristics but also the drug-release kinetics and the rheological attributes of hydrogels (Parhi, 2017). When cross-linking is absent, water-soluble polymeric solutions often behave in a "Newtonian" manner. The introduction of cross-links can produce networks that exhibit viscoelastic "non-Newtonian" behaviour (Peppas and Barr-Howell, 2019). Hydrogel synthesis involves utilizing two primary types of cross-linking, namely physical and chemical cross-linking (Figure. 2.11). Due to the intrinsic chemistry involved, these mechanisms endow hydrogels with distinct properties and suitability for numerous applications.

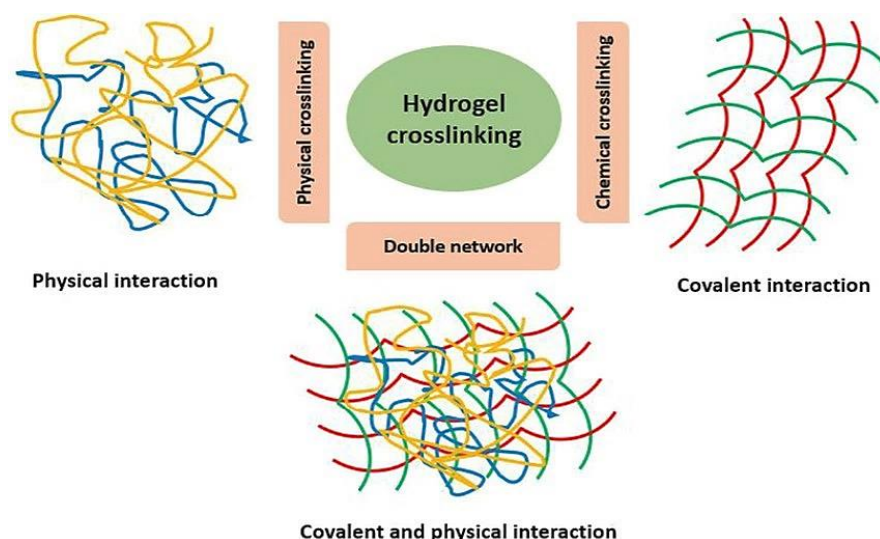


**Figure 2.11:** Physical, chemical, and double network hydrogel cross-linking (Zafar *et al.*, 2021).

#### 2.4.6 Chemically cross-linked hydrogels

Chemical cross-linking constructs a three-dimensional network by forging covalent links between the polymer chains. These hydrogels are often called "permanent hydrogels" because their bonding is irreversible (Ho *et al.*, 2022). Several methods, including polymer-polymer cross-linking, high-intensity radiation, and enzyme integration, can create chemically cross-linked hydrogels (Parhi, 2017). For this, chemical crosslinking compounds or the addition of functional groups that can react and generate covalent bonds with the polymer chains are required. These cross-linkers include genipine, glutaraldehyde, diisocyanate, palladium cation, and acrylic acid (Ahmadi *et al.*, 2015). The crosslinking agent and the polymers, or complementary functional groups, undergo a chemical reaction. In terms of the free-radical synthesis of hydrogels, free radicals are generated by high-energy irradiation (Figure 2.12), such as gamma rays or electronic beams, and polymerization is facilitated by UV excitation and enzymes (Zafar *et al.*, 2021). Once established, the cross-links are robust and permanent. Chemically cross-linked hydrogels demonstrate superior mechanical strength, durability, and ability to withstand dissolution. However, cross-linking may require hazardous conditions and toxic substances, restricting their use in biomedical applications.

The incompatibility between the cross-linkers and therapeutic agents and the presence of unreacted cross-linkers poses an additional obstacle that limits their usage (Hu *et al.*, 2019). Furthermore, the irreversibility and strength of its covalent bonds raise concerns about its injectability. A hydrogel must experience shear-thinning (disassembly) when injected using a

syringe and, after that, perform self-healing (re-assembly) when shear pressures are eliminated (Loebel *et al.*, 2017). Hence, physical cross-linking may offer a better strategy for producing injectable hydrogels.

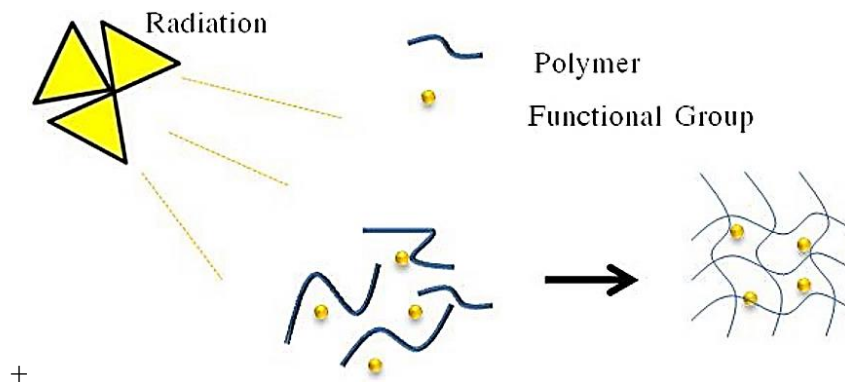


**Figure 2.12:** Synthesis of hydrogels using high-energy radiation (MohanKumar *et al.*, 2021).

#### 2.4.7 Physically cross-linked hydrogels

Physical cross-linking involves forming a structural network through reversible, non-covalent bonds between polymer strands. Polymer chains may physically entangle, form hydrogen bonds, hydrophobically interact, or be bound by electrostatic interactions (Parhi, 2017). The physical crosslinks, albeit not permanent, are adequate to render hydrogels insoluble in water. Physical hydrogels can absorb water; however, they may experience anomalies or network irregularities due to unbound chain ends or loops (Maitra and Shukla, 2014). Compared to chemical bonding, physical cross-links can be reversed due to the dynamic interplay between pro-assembly forces, such as hydrophobic interactions, and anti-assembly forces, such as electrostatic repulsion (Loebel *et al.*, 2017). Hence, they are frequently called "reversible" hydrogels (Table 2.1). Physical hydrogels are commonly formed by integrating two oppositely charged polyelectrolytes in a solution.

CS-based hydrogels are formed by electrostatic attraction between either negative or positive functional groups of the polymer and the amine units of CS (Thirupathi *et al.*, 2023). The primary benefit of a physical cross-link is its high level of biomedical safety due to the absence of chemical crosslinking agents, which could be cytotoxic. Such hydrogels can be engineered to function as bioactive hydrogels, capable of encapsulating living cells and delivering therapeutic compounds for medicinal purposes (Hu *et al.*, 2019).

**Table 2.1:** Characteristics of physical and chemical hydrogels (Zafar et al., 2021).

| <b>Physical Hydrogels</b>   | <b>Chemical Hydrogels</b>                                    |
|---|--|
| Reversible hydrogels formed by non-covalent interactions and entanglements. | Permanent hydrogels produced through covalent bonding.       |
| Lower stability against degradation.  | Higher stability against degradation.                        |
| Exhibition of poor mechanical properties.                                   | Relatively adequate mechanical properties.                   |
| Allows for injectability.   | Hydrogels are incapable of injectability.                    |
| Homogenous and synthesized without cross-linkers.                           | Non-homogenous and requires the cross-linkers for synthesis. |

Physically cross-linked hydrogels, however, often exhibit inferior mechanical strength compared to covalently cross-linked hydrogels. Physical crosslinking techniques provide benefits such as non-hazardous conditions for processing and the flexibility to modify the properties and organization of the network by adjusting to the surrounding environment. Significantly, physically cross-linked hydrogels exhibit stimuli-responsive behaviour and the ability to self-repair and be injected at room temperature (Parhi, 2017). The stimuli-responsiveness is displayed through swelling or shrinking according to environmental fluctuations, owing to their nature of bond reversibility (Hu *et al.*, 2019).

Some hydrogels can undergo pre-gelation before injection and then be injected by applying shear force. These shear-thinning hydrogels exhibit a property where they become less viscous when subjected to shear tension during injection. However, they rapidly regain their original stiffness once the shear force is removed from the body. This shear-thinning characteristic can be attributed to the reversible physical cross-links (Loebel *et al.*, 2017). While physically cross-linked hydrogels offer numerous advantageous drug-delivery routes, it has been noted that hydrogels with a low tensile strength might allow for leaching of drugs, thus releasing the payload before reaching the target site (Al-Mayahy and Hameed, 2023). Therefore, scientists have ventured into incorporating nanotechnology to maintain the positive attributes of the physically cross-linked hydrogels and account for the lack of mechanical strength. Nanotechnology produces therapeutically effective compounds, including nanoparticles (NPs), nanocapsules, conjugates, and micellar systems. These preparations offer multiple benefits for administering drugs, with the fundamental advantage being enhanced drug safety and efficacy. NPs, in particular, may also provide additional mechanical support through the reinforcement of the hydrogel skeleton (Wang *et al.*, 2023).

## 2.5 Nanotechnology and Nanomedicine

Nanotechnology is the formulation, analysis, manufacture, and utilization of materials and systems within a 1-100 nanometre (nm) range (Nasrollahzadeh *et al.*, 2019). Nanomedicine is the use of nanotechnology in conjunction with cellular and molecular components to diagnose and treat diseases (Soares *et al.*, 2018). Nanotechnology has facilitated novel approaches for confronting hurdles across diverse fields with the potential to identify, mitigate, and treat human diseases (Malik *et al.*, 2023). The ability to precisely modify NPs to interact with biological systems is highly appealing in biomedical sciences. NPs are currently under development to regulate and monitor molecular interactions and mechanisms to facilitate the delivery of diagnostic material and drugs across physiological barriers, that are dictated by their chemical features, structure, and size (Jiang *et al.*, 2020).

Nanoformulations can address the limitations of conventional therapy by enhancing drug localization, improving drug solubility, and enabling sustained release of the payload (Soares *et al.*, 2018). As drug delivery vehicles, NPs have proven to be highly effective in encapsulating one or more drugs, rendering them suitable for combination drug delivery. Compared to macroscopic materials, NPs have an increased surface area-to-volume ratio (Figure 2.13). They can be engineered to possess diverse geometries, dimensions, and surface chemical configurations, advancing cutting-edge clinical imaging technology, diagnostic apparatus, and drug delivery vehicles (Jiang *et al.*, 2020).

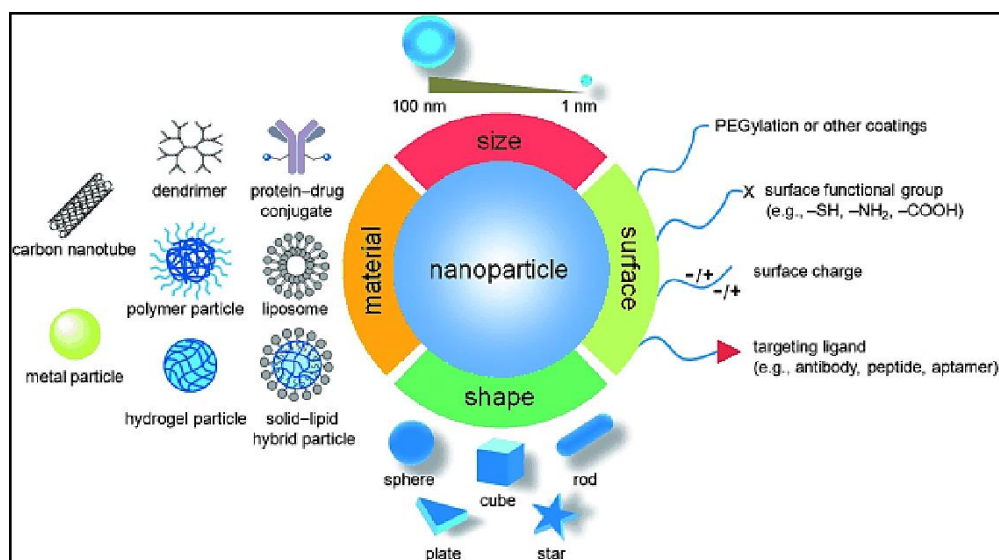


**Figure 2.13:** Favourable characteristics of nanoparticles for drug delivery (Pardhiya and Paulraj, 2016).

Current chemotherapy has been likened to "dousing an entire garden of roses in poison to remove a single weed" (Zahr and Pishko, 2009). Nanotechnology surpasses conventional procedures by targeting cancer cells and minimizing harm to healthy cells. The small dimensions of NPs have been extensively employed in the transportation of cancer drugs due to their ability to easily pass through leaky blood vessels by extravasation due to their improved permeability and retention (EPR) effect (Golombek *et al.*, 2018). Hence, they tend to accumulate primarily in tumour tissues. Active, targeted delivery systems can be created by combining NPs with different moieties, including aptamers, peptides, antibodies, and other small molecules (Rosenblum *et al.*, 2018). Studies conducted *in vitro* and *in vivo* indicate that NPs specifically designed to target specific cells or tissues can be more effective than conventional drugs. This enhanced activity leads to improved treatment outcomes and safety (Muhamad *et al.*, 2018). Furthermore, the physical, magnetic, electrical, and chemical characteristics of NPs can be customized, allowing for synergistic cancer treatments. These characteristics can be integrated to produce NP-crosslinked hydrogels.

### 2.5.1 Nanoparticle-crosslinked hydrogels

NP hydrogels, or "nanogels," consist of saturated, cross-linked polymers containing NPs (Dannert *et al.*, 2019). Notable progress has been achieved in NP and hydrogel innovations in recent years. By merging the benefits of these technologies, NP hydrogels have been constructed that can be employed for drug administration (Figure 2.14) (Umeyor *et al.*, 2024).

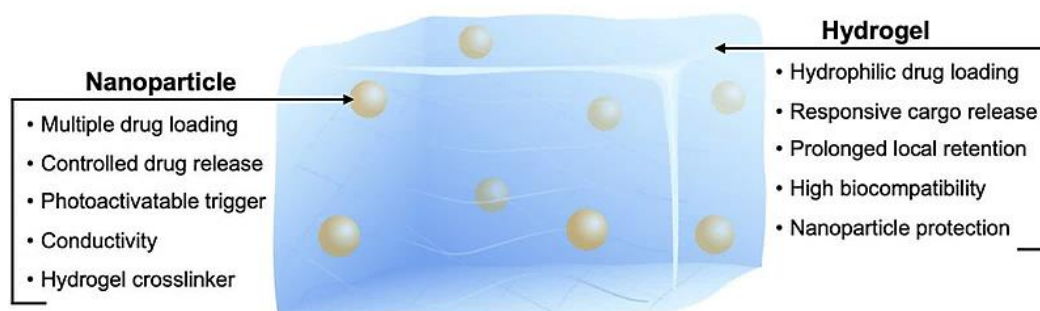


**Figure 2.14:** Combined advantages of a nanoparticle cross-linked hydrogel (Jiang *et al.*, 2020).

Nanogels can swell and absorb significant amounts of water or biological fluids, similar to hydrogels, while maintaining their structural integrity. Nanogels exhibit superior drug encapsulation, biological uniformity, enhanced stability, and heightened responsiveness to diverse environmental stimuli compared to other nanocarriers (Gao *et al.*, 2016). Incorporating

NPs into hydrogels allows drugs to be loaded in a nanosized range. This enables them to readily penetrate physiological barriers, enhancing the bioavailability of the drugs. Their nanosize also allows them to be easily injected using a needle (1 mm in diameter) (Wang *et al.*, 2023). Nanogels demonstrate exceptional mechanical characteristics. Their stiffness is significantly increased without compromising their dynamics, indicating their apparent supremacy as scaffolds for tissue repair or drug delivery. The improvement in mechanical characteristics is attributed to the sturdiness of the nanomaterial, which supports the gel skeleton. Hydrogels, in turn, stabilize the enclosed NPs and reduce agglomeration while also providing additional engineering flexibility to improve the overall effectiveness of the treatment (Wang *et al.*, 2023).

NPs can be incorporated into a hydrogel network by blending them with a monomer solution, which is then solidified by gelation (Gao *et al.*, 2016). Alternatively, NPs can be introduced into the gel after synthesis by allowing the pores of the gel to expand and, absorb and entrap the NPs (Figure 2.15). This method is particularly beneficial when NPs disrupt the gelation process (Fadilah *et al.*, 2022). However, the most favourable approach involves using inorganic NPs to grow within a gel matrix by injecting NP precursors into the gel and subsequently carrying out the reduction processes to generate the NPs (Fadilah *et al.*, 2022).

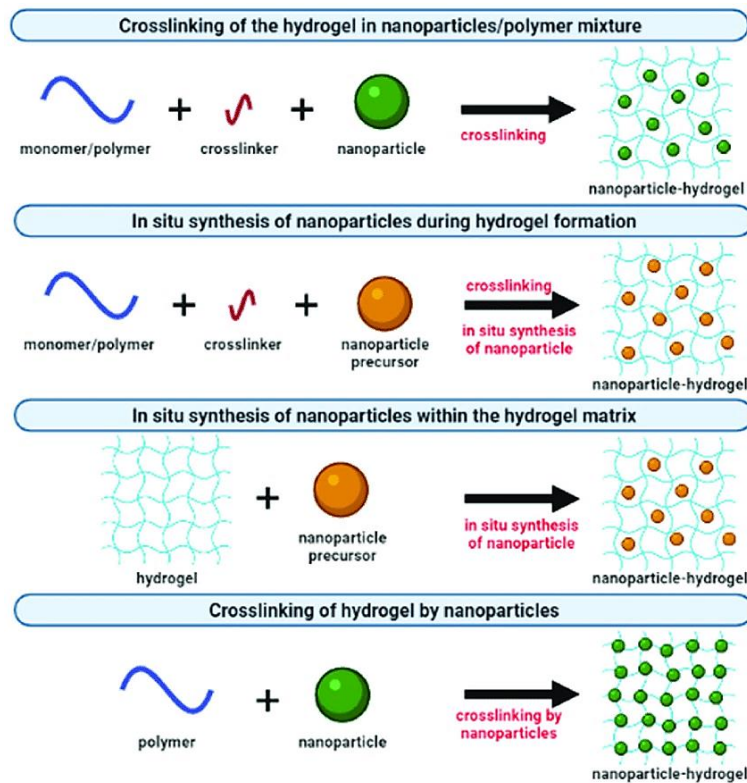


**Figure 2.15:** Different methods used to synthesize nanoparticle hydrogels (Fadilah *et al.*, 2022).

Metallic NPs are inorganic NPs with exceptional properties suitable for formulating NP-crosslinked hydrogels.

### 2.5.2 Metallic Nanoparticles

Metal NPs (MNPs) have demonstrated several compelling traits, unveiling their prospects as vehicles for targeted drug delivery. MNPs include silver NPs (AgNPs), gold NPs (AuNPs), zinc oxide NPs (ZnONPs), and iron oxide NPs (IONPs) (Ibrahim Fouad, 2021). Experiments using MNPs are being implemented for the preclinical screening and treatment of several illnesses (Farinha *et al.*, 2021). Hence, MNPs are considered important due to their ability to modify their photothermal and optical properties and ease of surface customization (Azharuddin *et al.*, 2019). Biological and chemical synthesis may efficiently yield MNPs. Modifying their size, shape, and delivery methods enables the adjustment of their pharmacokinetic properties (Chandrakala *et al.*, 2022). This introduces favourable characteristics such as anti-bacterial, anti-microbial, and anti-oxidative properties (Figure 2.16) (Ibrahim Fouad, 2021).

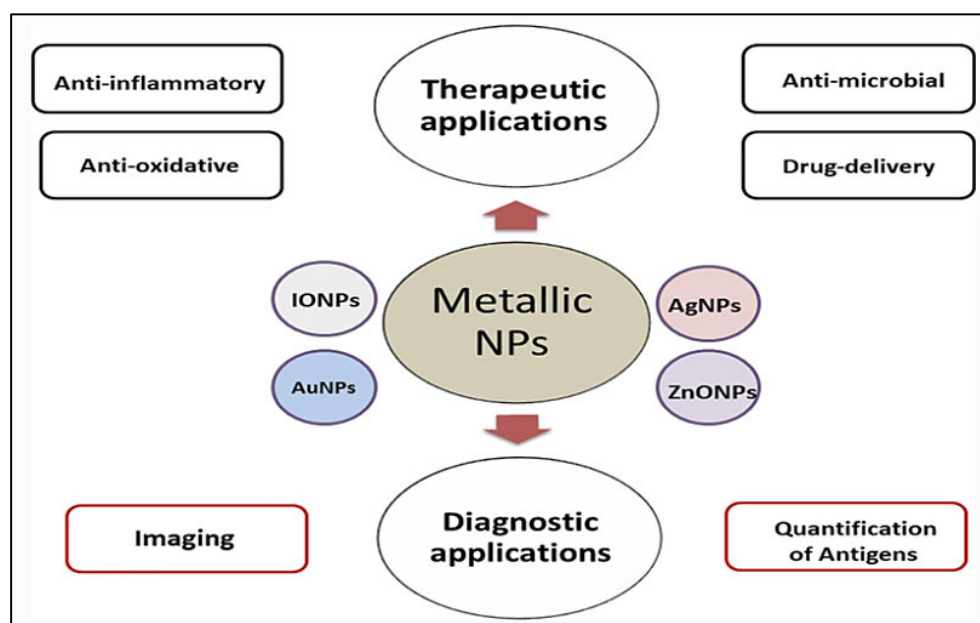


**Figure 2.16:** Types and therapeutic benefits of metal nanoparticles (Ibrahim Fouad, 2021).

Surface functionalization allows the attachment of targeted moieties and biomolecules through covalent, hydrogen, and ionic interactions (Azharuddin *et al.*, 2019). The modified MNPs can rapidly disintegrate in the acidic TME and undergo absorption through several metabolic routes without causing injury to healthy tissues (Chandrakala *et al.*, 2022). They can increase the

duration of drug circulation in the blood, improve drug solubility, and decrease or prevent the rapid clearance of drugs by the kidneys. By virtue of their unique properties, such as precise targeting and efficient absorption into cells, magnetic NPs have been shown to enhance the bioavailability and efficacy of drug carriers while reducing adverse effects (Azharuddin *et al.*, 2019). Gold nanoparticles (AuNPs) have gained immense attention for their inherent properties facilitating traditional cancer treatment and drug delivery.

### 2.5.2 Gold Nanoparticles (AuNPs)

The concept of gold as a medicinal agent dates back 5000 years to the dawn of Egypt, where gold was ingested to cleanse both mind and spirit (David *et al.*, 2023). In our modern society, the concept remains influential, mainly due to the use of gold in nanotechnology and nanomedicine. Among the approaches to nanomedicine, AuNPs provide screening, visualization, and delivery benefits. AuNPs possess non-toxic and biocompatible properties, which render them ideal as delivery vehicles and for incorporation into hydrogels (Sani *et al.*, 2021). AuNPs also possess multifunctionality, surface plasmon resonance, stability, surface chemistry, and ease of manufacture. This enables the easy production of gold of various sizes (1-150 nm), allowing for efficient penetration into cells and tissues (Sarfranz and Khan, 2021). AuNPs with distinct shapes, including rods, stars, diamonds, and spheres, have been developed for medical purposes (Figure 2.17) (Gerosa *et al.*, 2020).

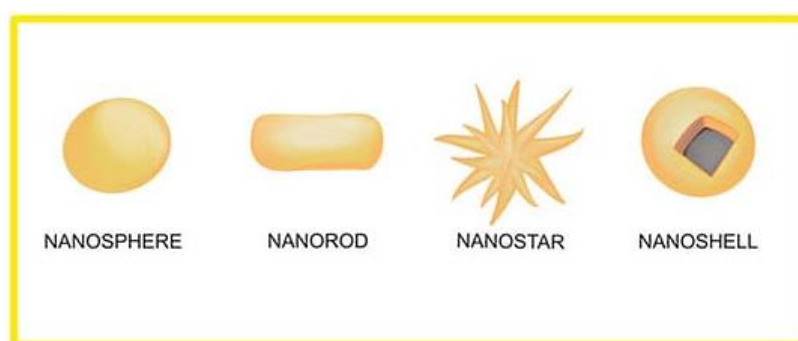


**Figure 2.17:** The different shapes of gold nanoparticles that can be synthesized (Gerosa *et al.*, 2020).

AuNPs have the capacity to absorb and scatter infrared and visible light when excited by plasmon oscillation. They exhibit an effect known as "localized surface plasmon resonance" (LSPR) that prompts them to absorb light at a maximum wavelength of 520 nm (Sarfranz and Khan, 2021). By modifying the dimensions or configuration of the NPs, it is feasible to control

the LSPR and create NPs with optical properties tailored for specific uses. The LSPR phenomenon of AuNPs has been commonly applied in cancer therapy (Gerosa *et al.*, 2020).

Oncologists adopt the term '*the Midas touch*' to describe the incorporation of AuNPs with pertinent antitumor properties into anticancer therapies, revolutionizing the oncology field (Gerosa *et al.*, 2020). The unique proclivity of AuNPs to accumulate in cancer cells is essential for the effectiveness of gold-based methods in oncology. LSPR allows for the detection of the intense light scattering produced by AuNPs in tumour tissue, which facilitates the visualization and diagnosis of tumours. Photothermal therapy and radiotherapy can be combined with AuNPs (Figure 2.18). They function as photosensitizers and radiosensitizers, amplifying the absorption of infrared light and X-rays. This leads to the destruction of DNA and the induction of local hypothermia, which is used for tumour ablation (Albarwary *et al.*, 2021). The application of AuNPs in chemotherapeutic drug delivery is where we observe their greatest potential.

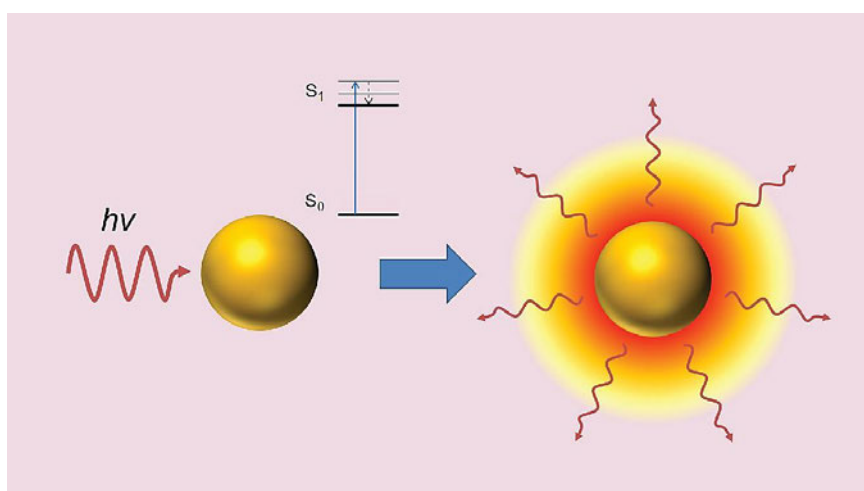


**Figure 2.18:** Photothermal effect of gold nanoparticles (Guerrero *et al.*, 2014).

### 2.5.3 Gold nanoparticles in drug delivery

The multitude of characteristics mentioned earlier render AuNPs suitable for use in drug delivery systems. AuNPs have a greater surface-area-to-volume ratio compared to other NPs. This enables the binding of a large number of ligands to load drugs or to target cells. AuNPs with a diameter of 2 nm can accommodate around 100 ligands per NP. Furthermore, the fabrication of multifunctional monolayers can be readily accomplished through ligand place-exchange processes (Stordy *et al.*, 2022). This allows for the insertion of multiple functional and/or targeting moieties with fewer obstacles in synthesis compared to other types of NPs.

The gold core is non-toxic and inert, providing an optimal framework for carrier fabrication. This enables adequate hydrogel integration and *in vivo* application (Sani *et al.*, 2021). Hydrogels have also been noted to shield the AuNPs and reduce their toxicity even further (Wang *et al.*, 2023). AuNPs have been utilized in various delivery strategies due to their ease of functionalization. AuNPs can be chemically bonded to prodrugs using linkers that are readily disassembled (Figure 2.19).

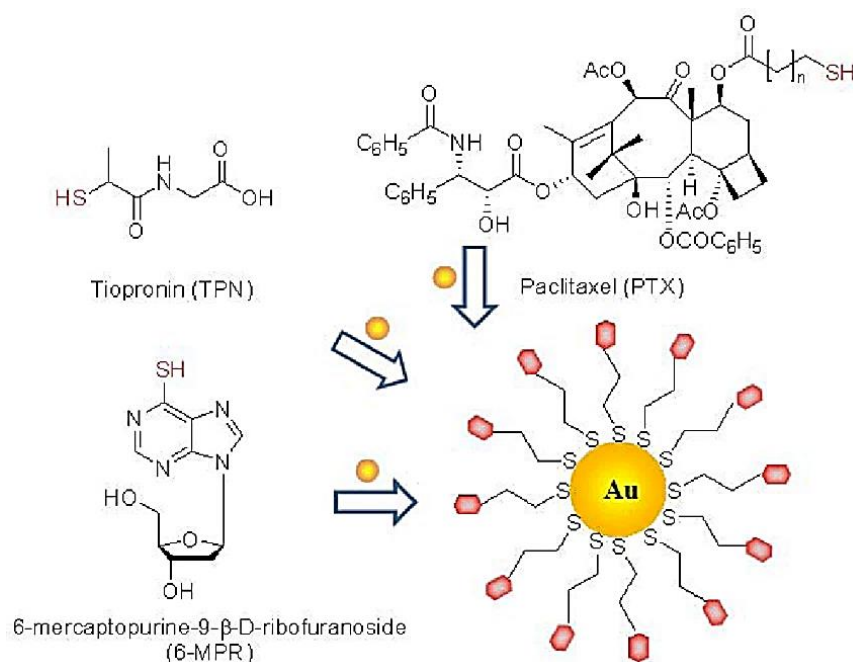


**Figure 2.19:** Attachment of drugs on AuNPs through covalent bonds (Liang *et al.*, 2014).

Hydrophobic drugs can be loaded onto AuNPs through non-covalent bonding, allowing for conjugation without altering the drug structure (Amina and Guo, 2020). It is crucial to note that hydrophilic polymers such as CS may not be suitable for encapsulating hydrophobic substances. Therefore, introducing AuNPs broadens the variety of drugs that may be encapsulated. Once loaded, external (light) or internal (glutathione) stimuli may trigger AuNP payloads to be ejected. In both techniques' the release of the therapeutic depends on the AuNP monolayer's versatility, which serves as a functional foundation for external release mechanisms and allows for customization of internal release mechanisms (Yang and Dai, 2024). In addition to the pH release of the CS hydrogel, the drug release induced by light stimulation offers an additional release mechanism, enabling an alternate route for administration. Therefore, AuNPs are ideal for integration into a CS hydrogel, providing many highly desirable features when paired with the hydrogel.

### 2.5.4 Mechanism of formation of the gold nanoparticle cross-linked chitosan hydrogel

Various techniques were devised to produce AuNP-CS hydrogels. In this study, the CS gel matrix is injected with the AuNP precursor ( $\text{HAuCl}_4$ ), which is then allowed to grow and undergo reduction (Figure 2.20).

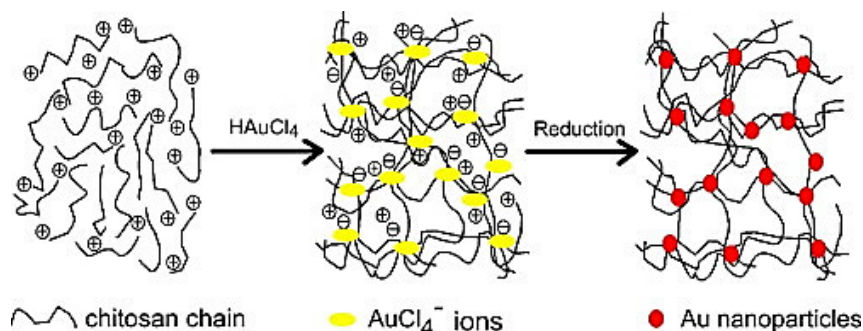


**Figure 2.20:** Gold nanoparticle formation and physical cross-linking of chitosan (Chen *et al.*, 2012).

CS is dissolved in an acrylic acid solution, resulting in positively charged amino groups. Upon injection of chloroauric acid into the system, an abundance of negatively charged  $\text{AuCl}_4^-$  ions is introduced (Chen *et al.*, 2012). These ions neutralize the positively charged amino groups of CS, leading to a decrease in the water solubility of CS. This establishes a strong electrostatic interaction between CS and  $\text{HAuCl}_4$ . When these two elements are combined, an instantaneous viscous solution is produced (Wang *et al.*, 2023), which transforms from yellow to wine red, forming a solid hydrogel within the solution. This colour change signifies that AuNPs are forming inside the hydrogel (Chen *et al.*, 2012). In a heated acidic solution, the CS reduces  $\text{AuCl}_4^-$  ions to zerovalent AuNPs. The hot, acidic CS hydrogel serves as a nucleation site, facilitating the formation of AuNPs (Xing *et al.*, 2016).

Owing to the strong attraction of Au to amine groups, the neutralized amine groups in the CS molecules are critical for stabilizing the reduced Au. Since the surface charge of AuNPs is negative, the protonated amino groups further shield the Au domains by means of electrostatic contact, prompting them to separate from the solution. As the duration of heating increases, an increasing number of  $\text{AuCl}_4^-$  ions reduces to zerovalent  $\text{Au}^0$  and is deposited onto the existing Au domains (Xing *et al.*, 2016). This leads to an increase in the size of the Au regions and their transformation into AuNPs. The solution forms a CS-Au hydrogel due to the electrostatic bonds between the amino groups and AuNPs, which function as physical cross-linking points. The CS-Au hydrogel with encapsulated 5-FU functions as an enhanced, novel chemotherapeutic

regimen incorporating the characteristics of AuNPs and CS-hydrogels for the sustained release of 5-FU and the reduction of side effects to improve the quality of life of patients. The advantages of the CS-Au hydrogel are noted in its *in vivo* applicability.

## 2.6 Prevention of opsonization

Nanogels have been tailored to provide prolonged circulatory half-lives of their payload and the capacity to transport that cargo to the target location. They enhance the longevity of the drugs by impeding their rapid elimination or metabolic degradation (Soni *et al.*, 2016). To achieve this, a nanogel must overcome numerous obstacles through oral and pulmonary routes, especially when not administered intravenously.

Nanogels first encounter the reticuloendothelial system (RES) and blood-stream-circulating macrophages, whose primary function is to remove foreign particles from the body. This is accomplished through opsonization via opsonin proteins (Keskin *et al.*, 2021). Opsonins bind to foreign bodies through ionic interactions and van der Waals forces. Macrophages in circulation detect the opsonin proteins that encase the foreign object and eliminate them through the mononuclear phagocyte system (MPS) (Bewersdorff *et al.*, 2019). The Au-CS hydrogel escapes this as the CS component enhances stealth qualities by increasing surface hydrophilicity, prohibiting exposure of the core charge, and producing steric hindrance that prevents binding to serum proteins (Figure 2.21) (Wani *et al.*, 2020).

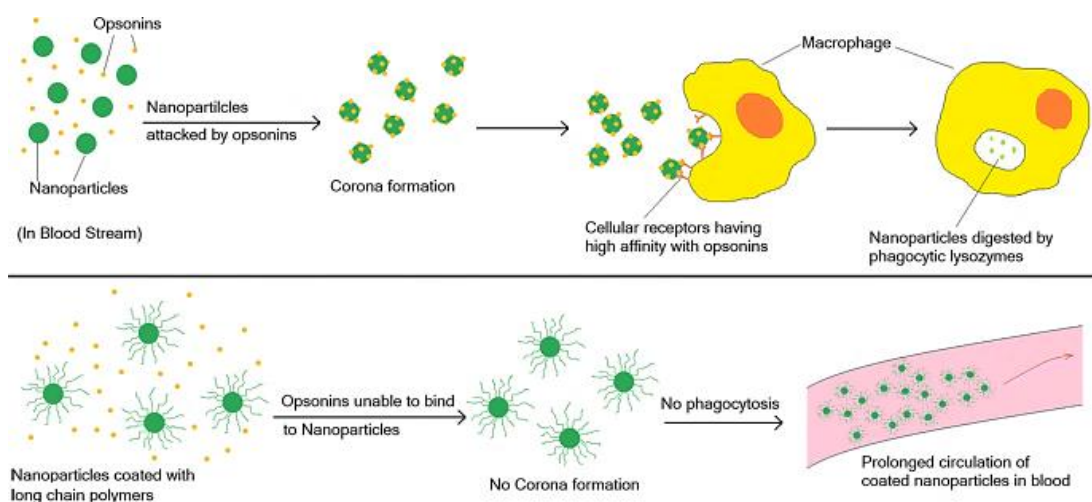


**Figure 2.21:** Evasion of nanoparticle opsonization with polymers (Wani *et al.*, 2020).

The CS-Au hydrogel possesses prolonged circulation characteristics and mitigates MPS absorption. Nevertheless, opsonization and subsequent macrophage clearance inevitably transpire. Nanogels may also be able to evade spleen clearance, due to their unique properties, which include their high swelling ratio, softness, and deformability (Keskin *et al.*, 2021). These biomimetic features of nanogels offer significant benefits for *in vivo* applications. The portion of nanogels that evades elimination through the above-mentioned methods is transmitted through the bloodstream to different organs for cellular uptake.

## 2.7 Cellular Uptake

Nanogels are typically unable to traverse the tight junctions of the normal endothelium due to their large size (Brianna *et al.*, 2024). However, they can effectively accumulate in solid tumours or inflamed tissues with distinct structural characteristics, such as malfunctioning, leaking, loosely compacted vasculature, and diminished drainage of lymphatic fluid. This accumulation is attributed to the EPR as mentioned previously (Figure 2.22) (Passi *et al.*, 2020).

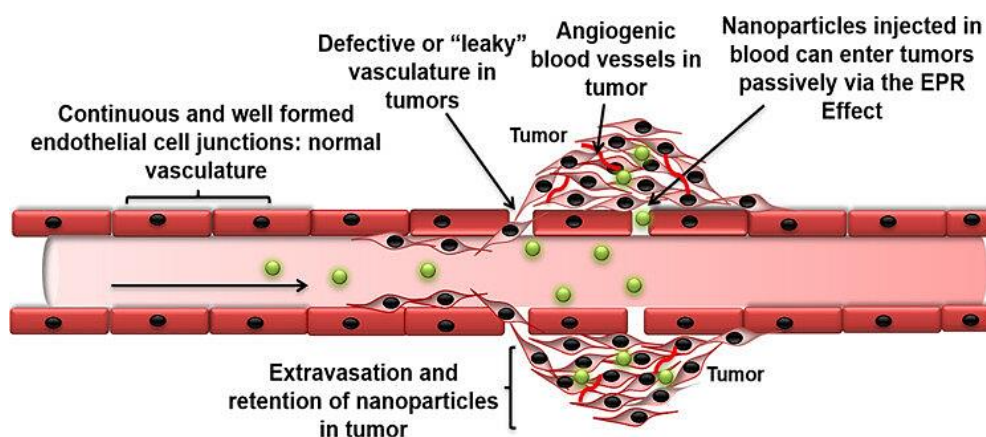


**Figure 2.22:** The enhanced permeability and retention effect in cancer tissue (Passi *et al.*, 2020).

It has been proposed that high concentrations of vascular mediators, including prostaglandins, nitric oxide, vascular endothelial growth factors, and bradykinin, may be the root cause of leaky tumour angiogenic blood vessels. The EPR effect is induced by such infrastructure and inadequate lymphatic drainage (Passi *et al.*, 2020). The nanogel can penetrate the vessels via passive diffusion or convection. The EPR effect has two components: extended plasma half-life and modified biodistribution (Brianna *et al.*, 2024). The modified biodistribution of nanogels results in an elevated nanogel level in tumour tissue compared to healthy tissue. The longer plasma half-life is attributed to the larger size of the drug-containing nanogels, which

exceeds the threshold for renal elimination (David *et al.*, 2023). Passive targeting has the benefit of increasing drug bioavailability, particularly at the tumour site. This is due to tumours having larger voids (up to 800 nm) in their blood vessels and a disjointed structure, in contrast to the blood vessels in healthy tissue (Shi *et al.*, 2020). A disadvantage of this method is that it could lead to heightened cytotoxicity in healthy tissue.

Active targeting, in contrast, entails the process of attaching targeting molecules to the nanogel. These targeted ligands are selected based on the specific type of receptor present and upregulated in particular tumour cells (Subhan *et al.*, 2021). Active targeting enables enhanced drug retention at the desired location by leveraging the ability of nanogels to penetrate biological barriers through molecular recognition (Shi *et al.*, 2020). Incorporating a targeted ligand into the CS-Au hydrogel has the potential to augment its therapeutic efficacy. Following extravasation from the bloodstream, nanogels must diffuse through the tissue matrix within the interstitial space to navigate to the targeted cells. The nanogels are then internalized by several endocytotic processes, which vary based on nanogel shape, size, texture, charge, surface qualities, specific cell type, and target receptor (Soni *et al.*, 2016).

### **2.7.1 Intracellular trafficking**

Internalization of the nanogel is an elaborate procedure that may occur through multiple pathways. However, endocytosis predominantly packages the NPs into intracellular vesicles, which are transported to the endosomes and eventually to the lysosomes (Sousa de Almeida *et al.*, 2021). During these processes, nanogels are exposed to different pH levels in the endosomal/lysosomal lumen, and degrading enzymes are commonly used as triggers to release the drug from the nanogels (Soni *et al.*, 2016). 5-FU is released at this stage, as CS is sensitive to acidic pH. There is an increasing trend to using nanogels composed of bioresponsive polymers that permit escape from intracellular organelles using pH-responsive or reducible cross-linkers to destabilize the nanogels after internalization, thereby enhancing delivery efficiency (Sousa de Almeida *et al.*, 2021). Degradation occurs within the cycle and is crucial for reducing the harmful effects of the buildup of the delivery vehicle in the body (Figure 2.23). Au-CS-nanogels with encapsulated 5-FU can be highly efficient and biocompatible drug delivery vehicles with the potential to reduce the adverse effects of chemotherapeutic drugs.

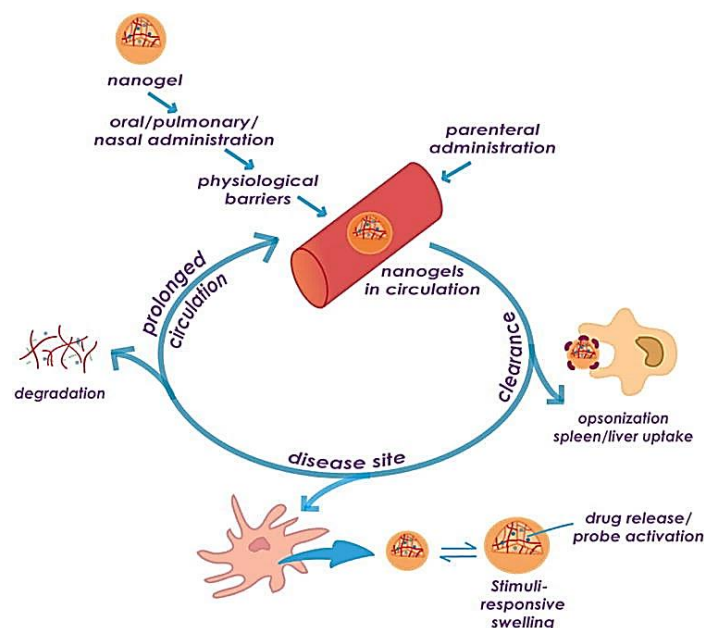


**Figure 2.23:** *In vivo* behaviour and fate of nanogels (Soni *et al.*, 2016).

## 2.8 References

- Adepu, S., & Ramakrishna, S. (2021). Controlled Drug Delivery Systems: Current Status and Future Directions. *Molecules*, 26(19), 5905. <https://www.mdpi.com/1420-3049/26/19/5905>
- Ahmadi, F., Oveisi, Z., Samani, S. M., & Amoozgar, Z. (2015). Chitosan based hydrogels: characteristics and pharmaceutical applications. *Res Pharm Sci*, 10(1), 1-16.
- Ahmed, B., Sharma, A., Usmani, Z., Sharma, G., Singh, J., Yadav, R., Sharma, I., & Kaur, I. P. (2023). Magic shotgun over magic bullet for treatment of ovarian cancer via polymeric nanoparticles. *Journal of Drug Delivery Science and Technology*, 104945.
- Akhtar, M. F., Hanif, M., & Ranjha, N. M. (2016). Methods of synthesis of hydrogels... A review. *Saudi Pharmaceutical Journal*, 24(5), 554-559.
- Albarwary, S. A., Kibarar, A. G., Mustapha, M. T., Hamdan, H., & Ozsahin, D. U. (2021). The Efficiency of AuNPs in Cancer Cell Targeting Compared to Other Nanomedicine Technologies Using Fuzzy PROMETHEE. *J Healthc Eng*, 2021, 1566834. <https://doi.org/10.1155/2021/1566834>
- AL-Mayahy, M. H., & Hameed, H. I. (2023). Hydrogels and Nanogels as a Promising Carrier for Drug Delivery. In *Hydrogels and Nanogels-Applications in Medicine*. IntechOpen.

Alvarez-Lorenzo, C., Grinberg, V. Y., Burova, T. V., & Concheiro, A. (2020). Stimuli-sensitive cross-linked hydrogels as drug delivery systems: Impact of the drug on the responsiveness. *International Journal of Pharmaceutics*, *579*, 119157.

Amina, S. J., & Guo, B. (2020). A Review on the Synthesis and Functionalization of Gold Nanoparticles as a Drug Delivery Vehicle. *Int J Nanomedicine*, *15*, 9823-9857. <https://doi.org/10.2147/ijn.S279094>

Azharuddin, M., Zhu, G. H., Das, D., Ozgur, E., Uzun, L., Turner, A. P. F., & Patra, H. K. (2019). A repertoire of biomedical applications of noble metal nanoparticles. *Chem Commun (Camb)*, *55*(49), 6964-6996. <https://doi.org/10.1039/c9cc01741k>

Barazzuol, L., Coppes, R. P., & van Luijk, P. (2020). Prevention and treatment of radiotherapy-induced side effects. *Molecular Oncology*, *14*(7), 1538-1554. <https://doi.org/https://doi.org/10.1002/1878-0261.12750>

Bewersdorff, T., Gruber, A., Eravci, M., Dumbani, M., Klinger, D., & Haase, A. (2019). Amphiphilic nanogels: Influence of surface hydrophobicity on protein corona, biocompatibility and cellular uptake. *International journal of nanomedicine*, 7861-7878.

Blondy, S., David, V., Verdier, M., Mathonnet, M., Perraud, A., & Christou, N. (2020). 5-Fluorouracil resistance mechanisms in colorectal cancer: From classical pathways to promising processes. *Cancer Science*, *111*(9), 3142-3154. <https://doi.org/https://doi.org/10.1111/cas.14532>

Brianna, Anwar, A., Teow, S.-Y., & Wu, Y. S. (2024). Nanogel-based drug delivery system as a treatment modality for diverse diseases: Are we there yet? *Journal of Drug Delivery Science and Technology*, *91*, 105224. <https://doi.org/https://doi.org/10.1016/j.jddst.2023.105224>

Chandrakala, V., Aruna, V., & Angajala, G. (2022). Review on metal nanoparticles as nanocarriers: Current challenges and perspectives in drug delivery systems. *Emergent Materials*, *5*(6), 1593-1615.

Chen, R., Chen, Q., Huo, D., Ding, Y., Hu, Y., & Jiang, X. (2012). In situ formation of chitosan–gold hybrid hydrogel and its application for drug delivery. *Colloids and Surfaces B: Biointerfaces*, *97*, 132-137. <https://doi.org/https://doi.org/10.1016/j.colsurfb.2012.03.027>

Chhikara, B. S., & Parang, K. (2023). Global Cancer Statistics 2022: the trends projection analysis. *Chemical Biology Letters*, *10*(1), 451-451.

Damyantov, C., Maslev, I., Pavlov, V., & Avramov, L. (2018). Conventional treatment of cancer realities and problems. *Ann Complement Altern Med*, 1(1), 1002.

Dannert, C., Stokke, B. T., & Dias, R. S. (2019). Nanoparticle-Hydrogel Composites: From Molecular Interactions to Macroscopic Behavior. *Polymers (Basel)*, 11(2). <https://doi.org/10.3390/polym11020275>

David, L.L.; Daniels, A.; Habib, S.; Singh, M. (2023) Gold Nanoparticles in Transferrin-targeted dual-drug delivery in vitro. *Journal of Drug Delivery Science and Technology*. 90, 105168. <https://doi.org/10.1016/j.jddst.2023.105168>

Debela, D. T., Muzazu, S. G., Heraro, K. D., Ndalama, M. T., Mesele, B. W., Haile, D. C., Kitui, S. K., & Manyazewal, T. (2021). New approaches and procedures for cancer treatment: Current perspectives. *SAGE Open Med*, 9, 20503121211034366. <https://doi.org/10.1177/20503121211034366>

Do, N. H. N., Truong, Q. T., Le, P. K., & Ha, A. C. (2022). Recent developments in chitosan hydrogels carrying natural bioactive compounds. *Carbohydrate polymers*, 294, 119726. <https://doi.org/https://doi.org/10.1016/j.carbpol.2022.119726>

Dongsar, T. T., Dongsar, T. S., Gupta, N., Almalki, W. H., Sahebkar, A., & Kesharwani, P. (2023). Emerging potential of 5-Fluorouracil-loaded chitosan nanoparticles in cancer therapy. *Journal of Drug Delivery Science and Technology*, 104371.

Elia, I., & Haigis, M. C. (2021). Metabolites and the tumour microenvironment: from cellular mechanisms to systemic metabolism. *Nature metabolism*, 3(1), 21-32.

Entezar-Almahdi, E., Mohammadi-Samani, S., Tayebi, L., & Farjadian, F. (2020). Recent advances in designing 5-fluorouracil delivery systems: a stepping stone in the safe treatment of colorectal cancer. *International journal of nanomedicine*, 5445-5458.

Ezike, T. C., Okpala, U. S., Onoja, U. L., Nwike, C. P., Ezeako, E. C., Okpara, O. J., Okoroafor, C. C., Eze, S. C., Kalu, O. L., Odoh, E. C., Nwadike, U. G., Ogbodo, J. O., Umeh, B. U., Ossai, E. C., & Nwanguma, B. C. (2023). Advances in drug delivery systems, challenges and future directions. *Heliyon*, 9(6), e17488. <https://doi.org/10.1016/j.heliyon.2023.e17488>

Fadilah, N. I., Mohd Isa, I. L., Zaman, W., Tabata, Y., & Mb, F. (2022). The Effect of Nanoparticle-Incorporated Natural-Based Biomaterials towards Cells on Activated Pathways: A Systematic Review. *Polymers*, 14, 476. <https://doi.org/10.3390/polym14030476>

- Fane, M., & Weeraratna, A. T. (2020). How the ageing microenvironment influences tumour progression. *Nature Reviews Cancer*, 20(2), 89-106.
- Farinha, P., Coelho, J. M. P., Reis, C. P., & Gaspar, M. M. (2021). A Comprehensive Updated Review on Magnetic Nanoparticles in Diagnostics. *Nanomaterials (Basel)*, 11(12). <https://doi.org/10.3390/nano11123432>
- Gao, W., Zhang, Y., Zhang, Q., & Zhang, L. (2016). Nanoparticle-Hydrogel: A Hybrid Biomaterial System for Localized Drug Delivery. *Ann Biomed Eng*, 44(6), 2049-2061. <https://doi.org/10.1007/s10439-016-1583-9>
- Gerosa, C., Crisponi, G., Nurchi, V. M., Saba, L., Cappai, R., Cau, F., Faa, G., Van Eyken, P., Scartozzi, M., Floris, G., & Fanni, D. (2020). Gold Nanoparticles: A New Golden Era in Oncology? *Pharmaceuticals*, 13(8), 192. <https://www.mdpi.com/1424-8247/13/8/192>
- Golombek, S. K., May, J. N., Theek, B., Appold, L., Drude, N., Kiessling, F., & Lammers, T. (2018). Tumor targeting via EPR: Strategies to enhance patient responses. *Adv Drug Deliv Rev*, 130, 17-38. <https://doi.org/10.1016/j.addr.2018.07.007>
- Guerrero, A. R., Hassan, N., Escobar, C. A., Albericio, F., Kogan, M. J., & Araya, E. (2014). Gold nanoparticles for photothermally controlled drug release. *Nanomedicine*, 9 13, 2023-2039.
- Guo, Y., Qiao, D., Zhao, S., Liu, P., Xie, F., & Zhang, B. (2024). Biofunctional chitosan–biopolymer composites for biomedical applications. *Materials Science and Engineering: R: Reports*, 159, 100775.
- Gupta, N., & Malviya, R. (2021). Understanding and advancement in gold nanoparticle targeted photothermal therapy of cancer. *Biochimica et Biophysica Acta (BBA)-Reviews on Cancer*, 1875(2), 188532.
- Hanahan, D. (2022). Hallmarks of Cancer: New Dimensions. *Cancer Discovery*, 12(1), 31-46. <https://doi.org/10.1158/2159-8290.Cd-21-1059>
- Hardenia, A., Maheshwari, N., Hardenia, S. S., Dwivedi, S. K., Maheshwari, R., & Tekade, R. K. (2019). Scientific rationale for designing controlled drug delivery systems. In *Basic Fundamentals of Drug Delivery* (pp. 1-28). Elsevier.
- Heymach, J., Krilov, L., Alberg, A., Baxter, N., Chang, S. M., Corcoran, R. B., Dale, W., DeMichele, A., Magid Diefenbach, C. S., & Dreicer, R. (2018). Clinical cancer advances 2018:

annual report on progress against cancer from the American Society of Clinical Oncology. *Journal of Clinical Oncology*, 36(10), 1020-1044.

Ho, T. C., Chang, C. C., Chan, H. P., Chung, T. W., Shu, C. W., Chuang, K. P., Duh, T. H., Yang, M. H., & Tyan, Y. C. (2022). Hydrogels: Properties and Applications in Biomedicine. *Molecules*, 27(9). <https://doi.org/10.3390/molecules27092902>

Hu, W., Wang, Z., Xiao, Y., Zhang, S., & Wang, J. (2019). Advances in crosslinking strategies of biomedical hydrogels [10.1039/C8BM01246F]. *Biomaterials Science*, 7(3), 843-855. <https://doi.org/10.1039/C8BM01246F>

Ibrahim Fouad, G. (2021). A proposed insight into the anti-viral potential of metallic nanoparticles against novel coronavirus disease-19 (COVID-19). *Bulletin of the National Research Centre*, 45. <https://doi.org/10.1186/s42269-021-00487-0>

Jacob, S., Nair, A. B., Shah, J., Sreeharsha, N., Gupta, S., & Shinu, P. (2021). Emerging role of hydrogels in drug delivery systems, tissue engineering and wound management. *Pharmaceutics*, 13(3), 357.

Jain, K. K. (2020). An Overview of Drug Delivery Systems. In K. K. Jain (Ed.), *Drug Delivery Systems* (pp. 1-54). Springer New York. [https://doi.org/10.1007/978-1-4939-9798-5\\_1](https://doi.org/10.1007/978-1-4939-9798-5_1)

Jiang, Y., Krishnan, N., Heo, J., Fang, R. H., & Zhang, L. (2020). Nanoparticle-hydrogel superstructures for biomedical applications. *J Control Release*, 324, 505-521. <https://doi.org/10.1016/j.jconrel.2020.05.041>

Kasiński, A., Zielińska-Pisklak, M., Oledzka, E., & Sobczak, M. (2020). Smart hydrogels—synthetic stimuli-responsive antitumor drug release systems. *International journal of nanomedicine*, 4541-4572.

Kesharwani, P., Bisht, A., Alexander, A., Dave, V., & Sharma, S. (2021). Biomedical applications of hydrogels in drug delivery system: An update. *Journal of Drug Delivery Science and Technology*, 66, 102914. <https://doi.org/https://doi.org/10.1016/j.jddst.2021.102914>

Keskin, D., Zu, G., Forson, A. M., Tromp, L., Sjollem, J., & van Rijn, P. (2021). Nanogels: A novel approach in anti-microbial delivery systems and anti-microbial coatings. *Bioactive Materials*, 6(10), 3634-3657. <https://doi.org/https://doi.org/10.1016/j.bioactmat.2021.03.004>

- Laffleur, F., & Keckeis, V. (2020). Advances in drug delivery systems: Work in progress still needed? *International Journal of Pharmaceutics*, *590*, 119912. <https://doi.org/10.1016/j.ijpharm.2020.119912>
- Lansdorp, P. M. (2022). Telomeres, Telomerase and Cancer. *Archives of Medical Research*, *53*(8), 741-746. <https://doi.org/10.1016/j.arcmed.2022.10.004>
- Li, H., Zimmerman, S. E., & Weyemi, U. (2021). Chapter Six - Genomic instability and metabolism in cancer. In U. Weyemi & L. Galluzzi (Eds.), *International Review of Cell and Molecular Biology* (Vol. 364, pp. 241-265). Academic Press. <https://doi.org/10.1016/bs.ircmb.2021.05.004>
- Li, J., & Mooney, D. J. (2016). Designing hydrogels for controlled drug delivery. *Nature Reviews Materials*, *1*(12), 16071. <https://doi.org/10.1038/natrevmats.2016.71>
- Li, J., & Mooney, D. J. (2016). Designing hydrogels for controlled drug delivery. *Nat Rev Mater*, *1*(12). <https://doi.org/10.1038/natrevmats.2016.71>
- Liang, J.-J., Zhou, Y.-Y., Wu, J., & Ding, Y. (2014). Gold Nanoparticle-Based Drug Delivery Platform for Antineoplastic Chemotherapy. *Current drug metabolism*, *15*. <https://doi.org/10.2174/1389200215666140605131427>
- Liang, Y., Li, M., Yang, Y., Qiao, L., Xu, H., & Guo, B. (2022). pH/Glucose Dual Responsive Metformin Release Hydrogel Dressings with Adhesion and Self-Healing via Dual-Dynamic Bonding for Athletic Diabetic Foot Wound Healing. *ACS Nano*, *16*(2), 3194-3207. <https://doi.org/10.1021/acsnano.1c11040>
- Liu, R., Luo, C., Pang, Z., Zhang, J., Ruan, S., Wu, M., Wang, L., Sun, T., Li, N., & Han, L. (2023). Advances of nanoparticles as drug delivery systems for disease diagnosis and treatment. *Chinese chemical letters*, *34*(2), 107518.
- Loebel, C., Rodell, C. B., Chen, M. H., & Burdick, J. A. (2017). Shear-thinning and self-healing hydrogels as injectable therapeutics and for 3D-printing. *Nat Protoc*, *12*(8), 1521-1541. <https://doi.org/10.1038/nprot.2017.053>
- Maitra, J., & Shukla, V. K. (2014). Cross-linking in hydrogels-a review. *Am. J. Polym. Sci*, *4*(2), 25-31.
- Malik, S., Muhammad, K., & Waheed, Y. (2023). Nanotechnology: A Revolution in Modern Industry. *Molecules*, *28*(2). <https://doi.org/10.3390/molecules28020661>

- Marques, A. C., Costa, P. J., Velho, S., & Amaral, M. H. (2021). Stimuli-responsive hydrogels for intratumoral drug delivery. *Drug Discovery Today*, 26(10), 2397-2405.
- McCarthy, P. C., Zhang, Y., & Abebe, F. (2021). Recent Applications of Dual-Stimuli Responsive Chitosan Hydrogel Nanocomposites as Drug Delivery Tools. *Molecules*, 26(16), 4735. <https://www.mdpi.com/1420-3049/26/16/4735>
- Mohammed, M. A., Syeda, J. T. M., Wasan, K. M., & Wasan, E. K. (2017). An Overview of Chitosan Nanoparticles and Its Application in Non-Parenteral Drug Delivery. *Pharmaceutics*, 9(4), 53. <https://www.mdpi.com/1999-4923/9/4/53>
- MohanKumar, B., Priyanka, G., Rajalakshmi, S., Sankar, R., Sabreen, T., & Ravindran, J. (2021). Hydrogels: potential aid in tissue engineering—a review. *Polymer Bulletin*, 79, 1-31. <https://doi.org/10.1007/s00289-021-03864-x>
- Moodley, T., & Singh, M. (2021). Current stimuli-responsive mesoporous silica nanoparticles for cancer therapy. *Pharmaceutics*, 13(1), 71.
- Muhamad, N., Plengsuriyakarn, T., & Na-Bangchang, K. (2018). Application of active targeting nanoparticle delivery system for chemotherapeutic drugs and traditional/herbal medicines in cancer therapy: a systematic review. *Int J Nanomedicine*, 13, 3921-3935. <https://doi.org/10.2147/ijn.S165210>
- Mukherjee, S. (2011). *The emperor of all maladies: a biography of cancer*. Large Print edn (Thorndike Press, 2010).
- Narayanaswamy, R., & Torchilin, V. P. (2020). Hydrogels and their applications in targeted drug delivery. *The Road from Nanomedicine to Precision Medicine*, 1117-1150.
- Nasrollahzadeh, M., Sajadi, S. M., Sajjadi, M., & Issaabadi, Z. (2019). Chapter 1 - An Introduction to Nanotechnology. In M. Nasrollahzadeh, S. M. Sajadi, M. Sajjadi, Z. Issaabadi, & M. Atarod (Eds.), *Interface Science and Technology* (Vol. 28, pp. 1-27). Elsevier. <https://doi.org/https://doi.org/10.1016/B978-0-12-813586-0.00001-8>
- Pardhiya, S., & Paulraj, R. (2016). Nanotechnology in Drug Delivery 21 2 Role of nanoparticles in targeted drug delivery system.
- Parhi, R. (2017). Cross-Linked Hydrogel for Pharmaceutical Applications: A Review. *Adv Pharm Bull*, 7(4), 515-530. <https://doi.org/10.15171/apb.2017.064>

- Parhi, R. (2020). Drug delivery applications of chitin and chitosan: a review. *Environmental Chemistry Letters*, 18(3), 577-594. <https://doi.org/10.1007/s10311-020-00963-5>
- Park, J. K., Chung, M. J., Choi, H. N., & Park, Y. I. (2011). Effects of the molecular weight and the degree of deacetylation of chitosan oligosaccharides on antitumor activity. *International journal of molecular sciences*, 12(1), 266-277.
- Passi, M., Shahid, S., Chockalingam, S., Sundar, I., & Packirisamy, G. (2020). Conventional and Nanotechnology Based Approaches to Combat Chronic Obstructive Pulmonary Disease: Implications for Chronic Airway Diseases. *International journal of nanomedicine*, Volume 15, 3803-3826. <https://doi.org/10.2147/IJN.S242516>
- Peers, S., Montembault, A., & Ladaviere, C. (2022). Chitosan hydrogels incorporating colloids for sustained drug delivery. *Carbohydrate polymers*, 275, 118689.
- Peers, S., Montembault, A., & Ladavière, C. (2020). Chitosan hydrogels for sustained drug delivery. *Journal of Controlled Release*, 326, 150-163.
- Peppas, N. A., & Barr-Howell, B. D. (2019). Characterization of the cross-linked structure of hydrogels. In *Hydrogels in medicine and pharmacy* (pp. 27-56). CRC press.
- Piao, Y., You, H., Xu, T., Bei, H.-P., Piwko, I. Z., Kwan, Y. Y., & Zhao, X. (2021). Biomedical applications of gelatin methacryloyl hydrogels. *Engineered Regeneration*, 2, 47-56. <https://doi.org/https://doi.org/10.1016/j.engreg.2021.03.002>
- Rizwan, M., Yahya, R., Hassan, A., Yar, M., Azzahari, A. D., Selvanathan, V., Sonsudin, F., & Abouloula, C. N. (2017). pH Sensitive Hydrogels in Drug Delivery: Brief History, Properties, Swelling, and Release Mechanism, Material Selection and Applications. *Polymers (Basel)*, 9(4). <https://doi.org/10.3390/polym9040137>
- Rizzo, F., & Kehr, N. S. (2021). Recent Advances in Injectable Hydrogels for Controlled and Local Drug Delivery. *Advanced Healthcare Materials*, 10(1), 2001341. <https://doi.org/https://doi.org/10.1002/adhm.202001341>
- Rosenblum, D., Joshi, N., Tao, W., Karp, J. M., & Peer, D. (2018). Progress and challenges towards targeted delivery of cancer therapeutics. *Nat Commun*, 9(1), 1410. <https://doi.org/10.1038/s41467-018-03705-y>
- Saedi, M., Vahidi, O., Moghbeli, M. R., Ahmadi, S., Asadnia, M., Akhavan, O., Seidi, F., Rabiee, M., Saeb, M. R., Webster, T. J., Varma, R. S., Sharifi, E., Zarrabi, A., & Rabiee, N.

(2022). Customizing nano-chitosan for sustainable drug delivery. *Journal of Controlled Release*, 350, 175-192. <https://doi.org/https://doi.org/10.1016/j.jconrel.2022.07.038>

Sani, A., Cao, C., & Cui, D. (2021). Toxicity of gold nanoparticles (AuNPs): A review. *Biochem Biophys Rep*, 26, 100991. <https://doi.org/10.1016/j.bbrep.2021.100991>

Sarfraz, N., & Khan, I. (2021). Plasmonic Gold Nanoparticles (AuNPs): Properties, Synthesis and their Advanced Energy, Environmental and Biomedical Applications. *Chem Asian J*, 16(7), 720-742. <https://doi.org/10.1002/asia.202001202>

Sethy, C., & Kundu, C. N. (2021). 5-Fluorouracil (5-FU) resistance and the new strategy to enhance the sensitivity against cancer: Implication of DNA repair inhibition. *Biomedicine & Pharmacotherapy*, 137, 111285.

Shaaban, E., Ellakwa, D., Elaraby, N., Amr, K., & Mohamadin, A. (2022). The effect of insulin-loaded gold and carboxymethyl chitosan nanoparticles on gene expression of glucokinase and pyruvate kinase in rats with diabetes type 1. *Journal of Food Biochemistry*, 46. <https://doi.org/10.1111/jfbc.14447>

Shakil, M. S., Mahmud, K. M., Sayem, M., Niloy, M. S., Halder, S. K., Hossen, M. S., Uddin, M. F., & Hasan, M. A. (2021). Using Chitosan or Chitosan Derivatives in Cancer Therapy. *Polysaccharides*, 2(4), 795-816. <https://www.mdpi.com/2673-4176/2/4/48>

Shi, Y., van der Meel, R., Chen, X., & Lammers, T. (2020). The EPR effect and beyond: Strategies to improve tumor targeting and cancer nanomedicine treatment efficacy. *Theranostics*, 10(17), 7921-7924. <https://doi.org/10.7150/thno.49577>

Singleton, D. C., Macann, A., & Wilson, W. R. (2021). Therapeutic targeting of the hypoxic tumour microenvironment. *Nature reviews Clinical oncology*, 18(12), 751-772.

Soares, S., Sousa, J., Pais, A., & Vitorino, C. (2018). Nanomedicine: Principles, Properties, and Regulatory Issues [Review]. *Frontiers in Chemistry*, 6. <https://doi.org/10.3389/fchem.2018.00360>

Soni, K. S., Desale, S. S., & Bronich, T. K. (2016). Nanogels: An overview of properties, biomedical applications and obstacles to clinical translation. *J Control Release*, 240, 109-126. <https://doi.org/10.1016/j.jconrel.2015.11.009>

- Sousa de Almeida, M., Susnik, E., Drasler, B., Taladriz-Blanco, P., Petri-Fink, A., & Rothen-Rutishauser, B. (2021). Understanding nanoparticle endocytosis to improve targeting strategies in nanomedicine. *Chem Soc Rev*, 50(9), 5397-5434. <https://doi.org/10.1039/d0cs01127d>
- Stordy, B., Zhang, Y., Sepahi, Z., Khatami, M. H., Kim, P. M., & Chan, W. C. W. (2022). Conjugating Ligands to an Equilibrated Nanoparticle Protein Corona Enables Cell Targeting in Serum. *Chemistry of Materials*, 34(15), 6868-6882. <https://doi.org/10.1021/acs.chemmater.2c01168>
- Subhan, M. A., Yalamarty, S. S. K., Filipczak, N., Parveen, F., & Torchilin, V. P. (2021). Recent Advances in Tumor Targeting via EPR Effect for Cancer Treatment. *J Pers Med*, 11(6). <https://doi.org/10.3390/jpm11060571>
- Sultana, A., Zare, M., Thomas, V., Kumar, T. S. S., & Ramakrishna, S. (2022). Nano-based drug delivery systems: Conventional drug delivery routes, recent developments and future prospects. *Medicine in Drug Discovery*, 15, 100134. <https://doi.org/https://doi.org/10.1016/j.medidd.2022.100134>
- Tewabe, A., Abate, A., Tamrie, M., Seyfu, A., & Abdela Siraj, E. (2021). Targeted drug delivery—from magic bullet to nanomedicine: principles, challenges, and future perspectives. *Journal of Multidisciplinary Healthcare*, 1711-1724.
- Thirupathi, K., Raorane, C. J., Ramkumar, V., Ulagesan, S., Santhamoorthy, M., Raj, V., Krishnakumar, G. S., Phan, T. T. V., & Kim, S.-C. (2023). Update on Chitosan-Based Hydrogels: Preparation, Characterization, and Its Anti-microbial and Antibiofilm Applications. *Gels*, 9(1), 35. <https://www.mdpi.com/2310-2861/9/1/35>
- Tian, B., & Liu, J. (2023). Smart stimuli-responsive chitosan hydrogel for drug delivery: A review. *International Journal of Biological Macromolecules*, 235, 123902.
- Tian, Y., Lei, Y., Wang, Y., Lai, J., Wang, J., & Xia, F. (2023). Mechanism of multidrug resistance to chemotherapy mediated by P-glycoprotein. *International Journal of Oncology*, 63(5), 1-19.
- Tilsed, C. M., Fisher, S. A., Nowak, A. K., Lake, R. A., & Lesterhuis, W. J. (2022). Cancer chemotherapy: insights into cellular and tumor microenvironmental mechanisms of action. *Frontiers in oncology*, 12, 960317.

- Trayes, K. P., & Cokenakes, S. E. (2021). Breast cancer treatment. *American family physician*, *104*(2), 171-178.
- Umeyor, C., Uronnachi, E., & Kakade, P. (2024). Hydrogels and Nanogels-Applications in Medicine.
- Valencia-Lazcano, A. A., Hassan, D., Pourmadadi, M., Behzadmehr, R., Rahdar, A., Medina, D. I., & Díez-Pascual, A. M. (2023). 5-Fluorouracil nano-delivery systems as a cutting-edge for cancer therapy. *European Journal of Medicinal Chemistry*, *246*, 114995.
- Vigata, M., Meinert, C., Hutmacher, D. W., & Bock, N. (2020). Hydrogels as drug delivery systems: A review of current characterization and evaluation techniques. *Pharmaceutics*, *12*(12), 1188.
- Vodenkova, S., Buchler, T., Cervena, K., Veskrnova, V., Vodicka, P., & Vymetalkova, V. (2020). 5-fluorouracil and other fluoropyrimidines in colorectal cancer: Past, present and future. *Pharmacology & therapeutics*, *206*, 107447.
- Wang, Q., Zhang, Y., Ma, Y., Wang, M., & Pan, G. (2023). Nano-crosslinked dynamic hydrogels for biomedical applications. *Materials Today Bio*, 100640.
- Wani, T. U., Raza, S. N., & Khan, N. A. (2020). Nanoparticle opsonization: forces involved and protection by long chain polymers. *Polymer Bulletin*, *77*(7), 3865-3889. <https://doi.org/10.1007/s00289-019-02924-7>
- Xin, H., & Naficy, S. (2022). Drug Delivery Based on Stimuli-Responsive Injectable Hydrogels for Breast Cancer Therapy: A Review. *Gels*, *8*(1), 45. <https://www.mdpi.com/2310-2861/8/1/45>
- Xing, R., Liu, K., Jiao, T., Zhang, N., Ma, K., Zhang, R., Zou, Q., Ma, G., & Yan, X. (2016). An Injectable Self-Assembling Collagen–Gold Hybrid Hydrogel for Combinatorial Antitumor Photothermal/Photodynamic Therapy. *Advanced Materials*, *28*(19), 3669-3676. <https://doi.org/https://doi.org/10.1002/adma.201600284>
- Yan, M., Wu, S., Wang, Y., Liang, M., Wang, M., Hu, W., Yu, G., Mao, Z., Huang, F., & Zhou, J. (2023). Recent progress of supramolecular chemotherapy based on host–guest interactions. *Advanced Materials*, 2304249.
- Yang, Y., & Dai, X. (2024). Current status of controlled onco-therapies based on metal organic frameworks. *RSC Adv*, *14*(18), 12817-12828. <https://doi.org/10.1039/d4ra00375f>

Zafar, S., Hanif, M., Azeem, M., Mahmood, K., & Gondal, S. A. (2021). Role of cross-linkers for synthesizing biocompatible, biodegradable and mechanically strong hydrogels with desired release profile. *Polymer Bulletin*, 79. <https://doi.org/10.1007/s00289-021-03956-8>

Zahr, A. S., & Pishko, M. V. (2009). Nanotechnology for Cancer Chemotherapy. In M. M. de Villiers, P. Aramwit, & G. S. Kwon (Eds.), *Nanotechnology in Drug Delivery* (pp. 491-518). Springer New York. [https://doi.org/10.1007/978-0-387-77668-2\\_16](https://doi.org/10.1007/978-0-387-77668-2_16)

Zhang, Y., & Wu, B. M. (2023). Current Advances in Stimuli-Responsive Hydrogels as Smart Drug Delivery Carriers. *Gels*, 9(10). <https://doi.org/10.3390/gels9100838>

Zhong, X., He, X., Wang, Y., Hu, Z., Huang, H., Zhao, S., Wei, P., & Li, D. (2022). Warburg effect in colorectal cancer: the emerging roles in tumor microenvironment and therapeutic implications. *Journal of hematology & oncology*, 15(1), 160.

## CHAPTER THREE

### A LITERATURE REVIEW OF THE CS-AU HYDROGEL AS A WOUND SCAFFOLD

---

**Part of this chapter has been published.**

Gounden, V.; Singh, M. (2024). Hydrogels and Wound Healing: Current and future prospects. *Gels*. 10 (1), 43; <https://doi.org/10.3390/gels10010043>. (**Appendix A**)

---

### 3.1 Introduction

Wounds have plagued patients for millennia, imposing a substantial burden on their caregivers, thus earning its designation as the 'silent epidemic' (Lindholm and Searle, 2016). Approximately 4 million cutaneous wounds have been documented to occur annually in affluent countries, with the number in developing nations in ascendance (Chen *et al.*, 2023). Skin injury compromises the integrity of the skin's framework, leading to a wound-healing process that is characterized by a well-coordinated series of cellular and molecular reactions that aim to recuperate or replace the injured tissue (Gonzalez *et al.*, 2016). Wounds that are distinguished by synergistic and ordered processes, leading to uninterrupted wound regeneration, are commonly referred to as 'acute wounds.' Although minor cutaneous injuries can recuperate, several variables frequently impact wound rehabilitation. These include severe oxidative stress, infection, and underlying medical conditions that result in the development of "chronic or inert wounds" (Xiang *et al.*, 2020). Chronic wounds exhibit distinctive attributes, including recurrent infections, a heightened inflammatory phase, and impaired responsiveness of epidermal cells to reparative signals (Firlar *et al.*, 2022).

In addition to the impact on psychological, social, and physical health, diminished productivity and high treatment costs impose a financial strain on the healthcare sector, emphasizing the need for efficient wound treatment. The current industry-standard therapies include skin grafts and flaps, dermal substitutes, and skin growth procedures. However, these procedures encounter significant challenges, such as a scarcity of sites for donors and the development of hypertrophied scars, resulting in physiological complications (Tavakoli and Klar, 2020). Hence, there is a dire need for an efficient alternative system that can overcome the present limitations.

Hydrogels can be described as intricate three-dimensional structures composed of hydrophilic polymer chains and exhibit a quick swelling response upon contact with water, forming a partially solid material (Ahmed, 2015). More than 90% of the hydrogel framework is composed of water, thereby rendering it possible to sustain a moist environment adjacent to the wound's surface, facilitating tissue repair (Xiang *et al.*, 2020). Hydrogels possess numerous properties that make them ideal for use as wound dressings. These include firm adhesion, shape adaptability, and mechanical protection, which enable sufficient coverage and safeguarding of the wound (Fan *et al.*, 2021). Hydrogel-based dressings possess the advantage of being readily tuneable, allowing for the incorporation of antibacterial and antimicrobial agents, cells, biomolecules, and growth factors (Aswathy *et al.*, 2020). This augmentation aims to expedite

the processes of wound contraction and healing. A hydrogel can be constructed using any hydrophilic polymer through a tailored cross-linking technique. These water-soluble polymers can be natural or synthetic. Synthetic materials provide unique features pertaining to their highly modifiable physical attributes and adhesive characteristics. However, natural polymers exhibit enhanced biocompatibility and biodegradability in comparison to synthetic polymers, rendering them more suitable for wound healing applications (Sheokand *et al.*, 2023).

Chitosan (CS) is a natural polymer that exhibits beneficial pharmacological qualities, including anti-inflammatory, antibacterial, and skin regeneration effects, in addition to proficient water absorption and retention capabilities (Feng *et al.*, 2021). Owing to these advantageous properties, this research will entail the employment of CS as the fundamental polymer in the synthesized hydrogel. Additionally, integrating nanomaterials *in situ* has led to the formation of "smart" nanogels that possess a customized functionality, facilitating the application of hydrogels in treating deep or irregular wounds due to *in situ* induction (Chandel *et al.*, 2017). Gold nanoparticles (AuNPs) are widely recognized and utilized in the field of medicine due to their innate inert core producing negligible side effects upon application, as well as some antibacterial effects.

Therefore, this research involves the synthesis of a CS hydrogel cross-linked with AuNPs *in situ*, with the aim of advancing wound healing interventions and ultimately improving the quality of life for numerous patients affected by wounds and their associated ramifications.

### **3.2 The Skin**

The skin is the most remarkable multifunctional organ in the human body. It plays a crucial role in protecting against a wide range of exterior hazards while preserving the internal environment. In virtue of its physical and sensory functions, this multilayered, complex organ

is essential for the body's defence. Human skin comprises three distinct layers: the epidermis, dermis, and hypodermis (Figure 3.1).

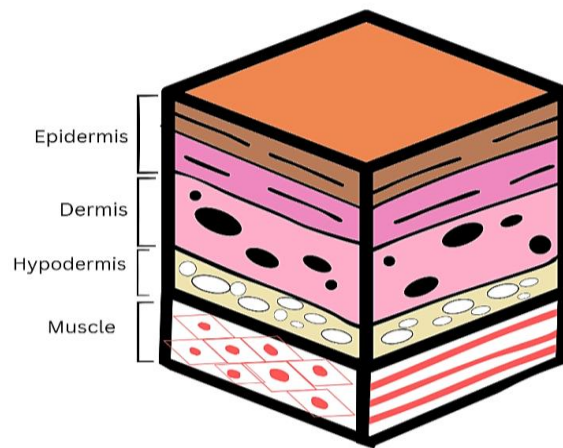


**Figure 3.1:** The structure of the skin illustrating the three layers: epidermis, dermis, and hypodermis.

The epidermis, mainly consisting of keratinocytes, is an integral contributor to the skin's cutaneous protective barrier function (Abdo *et al.*, 2020). The second layer is the dermis, which is the most substantial stratum of the integumentary system, measuring between 1.5 and 4 mm in thickness. Fibroblasts are the predominant cellular component within the dermis, responsible for the synthesis of collagen and elastin, which contribute to the rigidity and flexibility of the skin. The hypodermis, located beneath the dermis, consists predominantly of adipose and connective tissue, which assists in the provision of strength (Rittie, 2016). Due to the skin's slight acidity, it is protected against pathogens. In addition, Langerhans cells, which reside within the epidermis, protect against harmful infections (Clayton *et al.*, 2017). Despite these protective properties, the skin is susceptible to breakage. A wound is characterized by the impairment or disturbance of the body tissue's anatomical and physiological integrity (Sharma *et al.*, 2021). Once the disruption has occurred, the skin undergoes a complex and synchronized regeneration process to restore its physical integrity.

### 3.2.1 Wound Healing Phases

The natural wound repair process is a fundamental physiological mechanism that entails the coordinated interaction of several cellular strains with their respective products (Gonzalez *et al.*, 2016). It is essential to maintain the skin's integrity. To effectively navigate the wound toward complete healing succession, an intricate biological healing process of hemostasis, inflammation, proliferation, and remodeling must be accomplished (Figure 3.2).

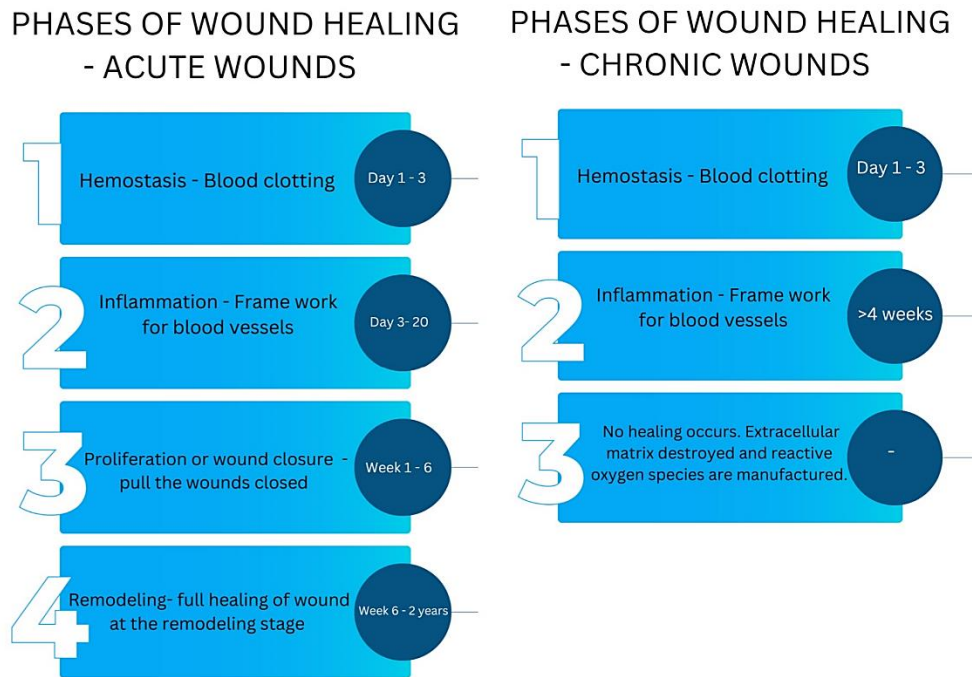


**Figure 3.2:** The four phases of wound healing and their approximate duration for acute and chronic wounds.

It is imperative that all four physiological phases, which are closely interconnected, interdependent, and sometimes overlapping, occur in the appropriate sequence and within an acceptable duration (Velnar *et al.*, 2009). Hemostasis initiates the wound-healing process, which occurs when ruptured tissue enables the influx of blood to enter the open lesion. Upon sustaining an injury, the initial physiological response is the restriction of blood vessels, known as vasoconstriction, which impedes the bleeding process (Dorgalaleh *et al.*, 2023). Platelets aggregate upon exposure to collagen and are subsequently released in conjunction with fibrin to form a thrombus, which serves to occlude the punctured blood vessels, preventing bleeding. Additionally, this process provides a provisional structure for the infiltration of cells necessary to repair the lesion (Rodrigues *et al.*, 2019).

Inflammation follows hemostasis, which commences within the initial 72 hours post-cellular injury. The cellular response during the period of inflammation is distinguished by the migration of leukocytes into the vicinity of the lesion. A complex cascade of signaling molecules facilitates the influx of neutrophils and macrophages into the region of injury. Neutrophils are mobilized and directed to the wound within the initial 24-hour period, where they remain for a duration ranging from 2 to 5 days (Singh *et al.*, 2017). These phagocytic cells are responsible for releasing reactive oxygen species (ROS) and lysozymes to eliminate

surrounding microorganisms and remove necrotic tissues. Macrophages often migrate to the site of injury within approximately 3 days. They are responsible for the secretion of many growth factors, cytokines facilitating cellular growth, and the formation of molecules within the extracellular matrix (ECM) (Dorgalaleh *et al.*, 2023).

The transition from the period of inflammation to the proliferative state is vital in wound healing. The objective of proliferation is to reduce the area of damaged tissue through angiogenesis and fibroplasia, thus producing an effective epithelial screen that can stimulate the activation of keratinocytes for wound closure. These processes commence within an initial 48-hour period and may continue until the 14th day following the emergence of injury (Gonzalez *et al.*, 2016). The last stage of the healing process involves remodeling, which commences around 2 to 3 weeks following the initiation of the wound and may persist for one year (Landen *et al.*, 2016). The primary objective of the remodeling phase is to optimize elasticity and restore the typical tissue structure through reorganization, disintegration, and reconstruction of the matrix surrounding the cells. The granulation tissue undergoes a slow remodeling process, forming scar tissue (Ellis *et al.*, 2018). Although the process of wound healing is highly efficient, various factors, such as infection and disease, can cause impairment, resulting in an increase in healing time and recurrent wounds.

### **3.2.2 Acute and Chronic Wounds**

Acute and chronic wounds are determined based on the healing period after the initial injury and, more significantly, by the presence of physiological damage. Acute wounds are breaches in the epidermis integrity that repair completely, with minor scarring (Figure 3.3), while progressing through a structured process of recovery that takes about 8 to 12 weeks (Tavakoli and Klar, 2020). The etiology of these injuries primarily stems from mechanical trauma, such as abrasive interaction and incisions performed during surgical procedures, thermal traumas, chemical burns, and electrical accidents (Percival, 2002).

A wound that fails to advance through the standard phases of inflammation and regeneration is classified as a chronic wound. This classification is frequently assigned once the wound exhibits minimal indications of improvement beyond three months (Nagle *et al.*, 2023). Around 15% of wounds fail to heal within one year following their initial manifestation due to asynchronous wound-healing phases (Lindholm and Searle, 2016).

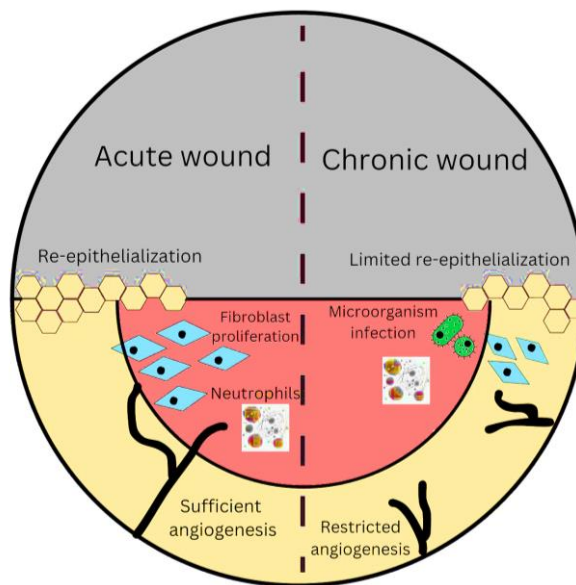


**Figure 3.3:** Illustration of the differences in acute and chronic wounds during wound healing.

The principal risk factors associated with the development of chronic wounds include age, immunological status, malnutrition, infection, low oxygen levels or perfusion, tobacco use, underlying disorders, drugs, exposure to radiation, and chemotherapy (Gantwerker and Hom, 2011). The primary idea of significance pertains to prolonged hyper-inflammation, a common pathophysiological feature that perpetuates a destabilized environment within a wound, rendering it resistant to the healing process. The dysfunction of macrophages also plays a crucial role in deviating from the normal healing process (Sen, 2021). Bacterial infection, such as with *Staphylococcus aureus* (*S.aureus*) and *Escherichia coli* (*E.coli*), has emerged as a significant factor in the development of chronic wounds. Chronic wounds are frequently infested by bacteria that create complex communities known as polymicrobial biofilms.

Biofilm, when present on a wound, induces a surplus of neutrophils that are incapable of engulfing the bacteria bound to the biofilm. However, these neutrophils continue to release enzymes (cytokines and proteases) and ROS, which disrupt the migration of cells, hinder wound healing, and compromise the nearby tissue (Zhao *et al.*, 2016). In cases of long-lasting infections, there is a harmful cycle of continued inflammation induced by ongoing biofilm, resulting in excessive and continuous NETosis which leads to tissue damage and an increase in biofilm production. The formation and accumulation of dead tissue and exudate serve as a constant source of essential nutrients for the biofilm, allowing it to thrive over the host (Hurlow and Bowler, 2022). The rise in bacterial infections can be attributed to the rise in nosocomial

infections post-surgery. Surgical site infections account for 2 million nosocomial infections in the United States, and this is a result of both endogenous flora present in mucous membranes as well as exogenous flora in theatre. The rise in infections ultimately increases the likelihood of chronic wounds (Zabaglo and Sharman, 2020). Chronic wounds are commonly classified as vascular ulcers, including venous or arterial ulcers, diabetic ulcers, and pressure ulcers (Firlar *et al.*, 2022).

### **3.2.3 Socio-economic Impact of Chronic Wounds**

A large proportion of individuals who endure chronic wounds typically present with concomitant medical disorders, particularly obesity and diabetes. Globally, approximately 463 million individuals have diabetes, with projections indicating a surge to 783 million individuals by 2045 (Sen, 2021). The prevalence of obesity is relatively proportional, as it is projected that by 2030, obesity will impact over 1 billion adults, constituting approximately one-sixth of the global population (Tham *et al.*, 2023). In contrast, the wound healing process is impaired among the senior demographic. Aging results in a reduction in collagen production, causing the epidermis to regenerate at a decreased rate. By 2050, the global population of individuals aged 60 or above is anticipated to surpass the population of youth aged 10–24, with an estimated count of 2.1 billion compared to 2.0 billion, respectively (Rudnicka *et al.*, 2020). The notable rise in diseases and the aging population pose significant concerns regarding the future occurrence of chronic wounds in patients.

According to research, 70% to 80% of people with wounds receive treatment primarily from community nurses (Lindholm and Searle, 2016). Health systems must develop more effective ways to cope with the additional workload, which fosters immense and perhaps unsustainable pressure on the already overworked nursing personnel. From an economic perspective, it has been projected that the management of wounds constitutes approximately 3% of the total medical expenditure. In the United States, it has been projected that venous ulcers result in the forfeiture of roughly two million working days each year and a projected expenditure of 2.5 to 3.5 billion dollars a year for the healthcare system. According to the evaluation, the worldwide wound management industry is expected to attain a value of 18.7 billion dollars by 2027 (Sen, 2021). Hence, there is a dire need for more efficient treatments to reduce the social and economic strain placed on individuals and health.

### 3.3 Current treatment methods

#### 3.3.1 Dressings

Various forms of dressings for wounds have been reported (Table 3.1). However, their suitability differs based on the characteristics of the lesion. The selection of dressing is determined by several variables, including depth, location, size, exudate volume, inflammation, and adhesion to the wound (Rezvani *et al.*, 2019). In comparison to dry dressings, moist dressings possess the capacity to enhance the process of wound repair. Moisture-retentive dressings can protect wounds, reduce the risk of infection, and promote granulation tissue formation. These substances are categorized as gauzes, films, or gels based on their physical characteristics. Dry dressings can cause additional pain and tissue damage as they may adhere to wounds.

**Table 3.1:** Common wound dressings.

| Type of wound                      | Treatment        | Function                        | Advantages  | Disadvantages  | References  |
|------------------------------------|------------------|---------------------------------|---|--|---|
| <b>Infected</b>                    | Gauze            | Dries wounds                    | Removes necrotic tissue, used with other topical products, can pack wounds                | Adherence hinders healing, frequent change in dressing, secondary dressing necessary | (Dabiri <i>et al.</i> , 2016; Baranoski, 2008; Boateng, 2008)               |
| <b>High exudate</b>                | Foam             | Absorbs high levels of exudates | Provides a moist environment, easy to apply, and non-adherent                             | Adherence hinders healing, not recommended for eschar or non-draining wounds         | (Dabiri <i>et al.</i> , 2016; Baranoski, 2008; Dhivya <i>et al.</i> , 2015) |
| <b>Superficial skin disruption</b> | Transparent film | Allows for gaseous exchange     | Stabilizes the wound site; removal is not needed for visualization, autolytic debridement | Damages newly formed tissue does not absorb moisture, peri-wound maceration          | (Dabiri <i>et al.</i> , 2016; Baranoski, 2008; Sood <i>et al.</i> , 2014)   |
| <b>Eschar</b>                      | Hydrocolloid     | Absorbs high levels of exudates | Provides a moist environment, insulation, autolytic debridement, waterproof               | Promotes granulated tissue, cannot be used for infected wounds                       | (Dabiri <i>et al.</i> , 2016; Baranoski, 2008; Dhivya <i>et al.</i> , 2015) |

### **3.3.2 Negative Pressure Therapy**

Negative pressure wound therapy (NPWT) is a non-invasive therapy that employs regulated negative pressure to generate a vacuum. This vacuum system facilitates the removal of debris and fluid from the site of injury by implementing a closed or foam covering connected to an extraction vessel. This methodology effectively improves the degree of oxygen and moisture in the vicinity of the lesion, thereby facilitating wound repair. NPWT is not recommended in wounds associated with cancer, osteomyelitis, or necrotic tissue in conjunction with eschar. Additionally, NPWT restricts the patient's range of motion (Kantak *et al.*, 2017).

### **3.3.3 Surgery**

Surgery includes direct wound closure, skin flaps and grafts, and musculocutaneous flaps. The selection of the surgical intervention is contingent upon various factors, including the precise anatomical site, concurrent medical conditions, and the desired outcomes of the medical procedure (Ho *et al.*, 2020). The long-term effects of surgical interventions exhibit variations determined by bed rest and preoperative risk factors. Implementing this procedure necessitates the involvement of medical specialists who possess the expertise required and have access to well-equipped healthcare facilities. In addition, surgery is not a cost-effective method.

### **3.3.4 Hyperbaric Oxygen Therapy**

Patients are administered 100% oxygen within a compression chamber with a maintenance pressure exceeding sea level. The improved degree of oxygen delivery to the wound increases the regeneration efficiency, leading to a reduction in the duration required for the healing process (Wenhui *et al.*, 2021). Hyperbaric oxygen therapy (HBOT) is currently employed as a treatment modality for managing non-healing wounds. Implementing HBOT necessitates expensive, specialized equipment and is a time-intensive process. Furthermore, its application is typically restricted to wounds associated with diabetes and pressure-induced ulcers. Although HBOT yields many advantages, it is crucial to acknowledge the notable hazards associated with this treatment. These hazards encompass the possible occurrence of pneumothorax and detrimental effects on the eardrums (Kantak *et al.*, 2017).

### 3.4 Ideal wound healing system

While numerous conventional wound treatments are available, they exhibit various drawbacks, necessitating the exploration of an alternate treatment strategy. An optimal system should demonstrate antibacterial and antimicrobial characteristics to mitigate infections. During an infection, bacteria infiltrate the site of injury and secrete compounds that impede the ability of immune cells to eliminate these bacteria, thereby prolonging the course of healing (Holloway and Harding, 2022). The system must possess biodegradability, biocompatibility, and non-toxicity while also ensuring the provision and maintenance of a moist environment (Figure 3.4). Moist conditions facilitate the healing procedure by supporting angiogenesis and collagen formation and providing non-adherence, thus reducing pain and scab formation (Varaprasad *et al.*, 2020). In addition, the system needs to possess the capacity to absorb wound exudates and facilitate the exchange of gases between the wounded tissue and the surrounding environment. This is crucial, as oxygen is critical in cell growth and angiogenesis (Sheokand *et al.*, 2023). Lastly, the treatment must enhance tissue regeneration mechanisms while demonstrating cost-effectiveness.

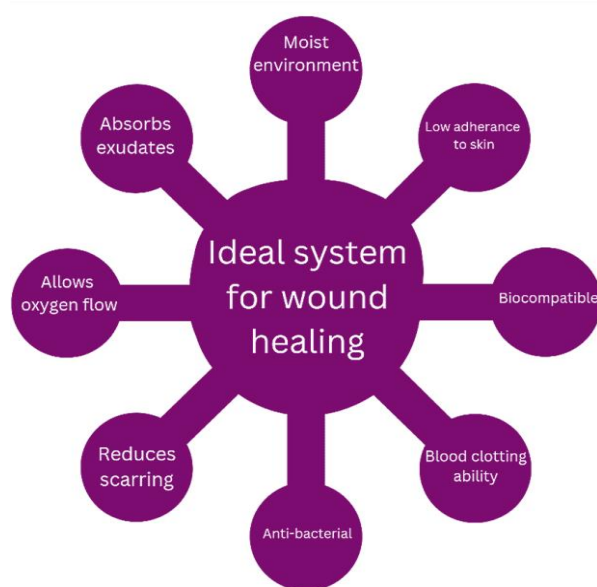


**Figure 3.4:** Properties required for an ideal wound healing system.

#### 3.4.1 Hydrogels in wound-healing

Hydrogels are a category of substances that have extensive applications in the field of skin regeneration. They are polymeric structures that exist in a three-dimensional structure, formed through physical or chemical cross-linking of hydrophilic polymer chains (Koehler *et al.*, 2018). They can be synthesized using several techniques, including radiation, freeze-thawing,

or chemical processes. Hydrogels are referred to as "reversible" or "physical" gels when the structural integrity is maintained through molecular entanglements or ionic and hydrogen bonds. They are referred to as "permanent" or "chemical" gels when composed of covalent bonds (Figure 3.5). These networks can potentially undergo water expansion until reaching a state of equilibrium while maintaining their initial structure. This results in a notable capacity to absorb exudates from wounds, facilitate oxygen flow and sustain a heightened moisture content at the injury site. This accelerates the healing process (Van Vlierberghe *et al.*, 2011).

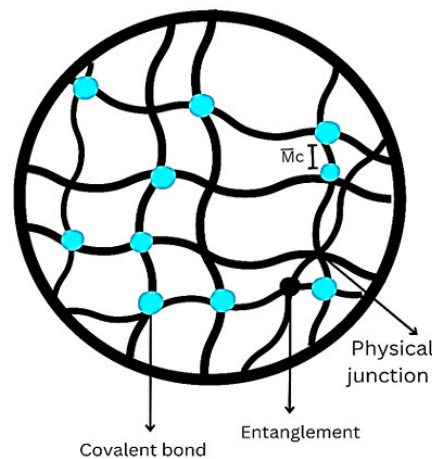


**Figure 3.5:** Different types of cross-linking in hydrogels.

These distinctive physical qualities enable the fabrication of hydrogels into diverse sizes and forms, thereby facilitating the complete covering of irregular-shaped wounds (Bilici *et al.*, 2016). Hydrogels possess biodegradability and biocompatibility, allowing them to serve as a temporary template throughout the re-epithelialization and remodeling of chronic wounds. Additionally, hydrogels demonstrate sufficient bioadhesivity, which is crucial in ensuring sustained stability. This property enhances hemostasis and maintains optimal moisture levels in the wound (Maaz Arif *et al.*, 2021). Furthermore, hydrogels provide a versatile framework for incorporating various components such as antibacterial and antimicrobial agents, drugs, and other supplemental biomolecules, enhancing their overall efficacy in promoting wound healing. Hence, it can be concluded that hydrogel-based materials exhibit the highest suitability level as dressings for covering skin wounds.

### 3.4.2 Hydrogels as a replicate extracellular matrix (ECM)

Another essential characteristic of hydrogels is their capacity to replicate the ECM. The ECM is harmed in acute or chronic injury or damage. The ECM facilitates cellular adhesion, tissue

anchorage, cellular signaling, and cell recruitment. The primary components of the ECM include polysaccharides, proteins, and water (Potekaev *et al.*, 2021). Hydrogels can imitate the rigidity of an ECM due to their primary elements being water and polymers. Additionally, hydrogels can imitate the ECM functionally, as they can incorporate cells and other macromolecules in the ECM (Sivaraj *et al.*, 2021). Theoretically, once a hydrogel is placed on the wounded area, it acts as a dermal matrix that can replicate the structure and function of unwounded skin, thereby preventing the ensuing scar by approximating the strength of tensile contraction and elastic retraction of an intact, unwounded dermis. This is believed to promote the development of cells, the deposition of extracellular matrix, the creation of new tissue, and enhancing wound healing. Hyaluronic acid, collagen, and alginate hydrogels are valuable for creating ECM structures (Ho *et al.*, 2022).

### **3.4.3 Hydrogels as a first aid for burn wounds**

Within the initial 15 minutes of a thermal burn, the heat generated is stored in the epidermis and can subsequently be transmitted to the underlying layers. Applying a cooling agent to the skin diminishes the severity of the damage and minimizes scarring (Wright *et al.*, 2019). Hydrogels are crucial in burn therapy as primary dressings for first aid. Water in hydrogels provides an essential function in the cooling process, as water helps maintain a stable temperature in the wound. Hydrogels serve the dual purpose of cooling the burn site and alleviating pain while safeguarding the wound region from infection (Shu *et al.*, 2021). Hence, they are highly suitable as dressings for transportation in ambulances. Compared to paraffin dressings, hydrogels offer quicker recovery and are safe first-aid treatment options for paediatric patients. Ambulances worldwide and the US Marine Corps have hydrogel sheets (96% water) for emergencies (Surowiecka *et al.*, 2022). Carbomer 940 is an affordable and effective hydrogel used for burns. It can enhance blood flow to tissues and reduce the extent of necrotic tissue (Chouhan *et al.*, 2018).

### 3.5 Natural and Synthetic Hydrogels

Hydrogel wound dressings are developed using diverse natural and synthetic polymers (Figure 3.6). Synthetic polymers include polyethylene glycol, polyvinyl pyrrolidone, polyethylene oxide, and polyvinyl alcohol. Natural polymers include CS, gelatin, hyaluronic acid, and alginate. Hydrogels can be highly elastic, which reduces its mechanical power. Therefore, multipolymeric hydrogels have been introduced for improved mechanical power and absorption. Combining a naturally occurring polymer with a synthetic polymer promises to be a viable approach for generating materials with the desired thermal and mechanical attributes. Advancements in the field have been achieved by harnessing the inherent features of polymers, leading to the development of novel technologies such as sprayable hydrogels, "smart hydrogels," and nanogels.

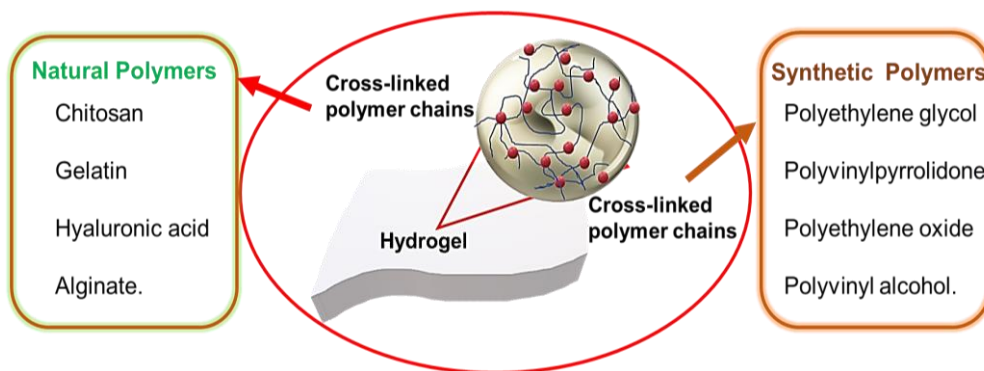


**Figure 3.6:** Natural and synthetic polymers being used in hydrogel dressings.

#### 3.5.1 Synthetic Hydrogels

Synthetic polymers have demonstrated considerable efficacy in biomedical applications due to their mechanical properties, capacity for facile shaping into various configurations, and manufacturing cost-effectiveness (Rausch *et al.*, 2021). These polymers exhibit stability and ease of use but are inhibited by limited biocompatibility. In contrast to their naturally occurring equivalents, synthetic polymers possess the advantage of being conveniently manufactured on an industrial level. Furthermore, their inherent adaptability enables them to be employed in various forms that promote the ideal development of tissues. The ability to precisely manipulate both the hydrophilic and hydrophobic regions of synthetic polymers additionally permits the fabrication of more homogenous frameworks and an improved capacity for the retention of water (Güiza-Argüello *et al.*, 2022). Hybrid polymers (blended), which exhibit favourable physicochemical characteristics, can be achieved through their combination with biopolymers.

The positive attributes of blended hydrogels fabricated from synthetic polymers are further improved using bioactive substances derived from naturally occurring substances. Blended hydrogels serve as a solution for future wound treatment by combining their favourable characteristics.

### **3.5.1.1 Polyethylene glycol (PEG)**

Polyethylene glycol (PEG) is a polymer that possesses hydrophilic properties, resulting in it being capable of interacting favorably with water. PEG is characterized by its flexibility and is composed of ether-based units.

The use of PEG-based hydrogels in constructing biological systems has been motivated by their remarkable biocompatibility and ability to thwart protein attachment. The addition of functional groups may generate PEG derivatives like PEG dimethacrylate (PEGDM) and PEG diacrylate (PEGDA), which can then be chemically cross-linked to create long-lasting matrices that permit the connecting or integrating of biomolecules to support tissue repair (Güiza-Argüello *et al.*, 2022). Polymethacrylic acid (PMA) and polyacrylic acid (PAA) can combine with PEG to create complexes due to hydrogen bonding between the carboxylic groups of PMA and the oxygen of PEG. This interaction facilitates the absorption of liquids by the complex and causes it to expand at low pH, forming a gel. PEG may also be used as an adequate cross-linker due to its rigidity, water solubility, and low immunogenicity (Maitra and Shukla, 2014). Growth factors, such as epidermal growth factor (EGF) and PEG macromers, have a favourable attraction and can form chemical bonds with each other. These can be specifically directed to the site of injury. PEG's mechanical, thermal, and crystalline attributes can be enhanced by including CS in the polymer blends (Mir *et al.*, 2018). PEG-based hydrogels have been used for the treatment of lesions in individuals with diabetes. These hydrogels facilitate wound repair by stimulating the multiplication and development of skin cells. The application of such dressings has been observed to decrease scar development.

A wound closure study using PEG-based hydrogels on 1.5 cm long incisions in Sprague-Dawley rats was conducted by Chen *et al.* (2018). Applying the PEG-based hydrogels stopped the haemorrhaging from the cuts and the incision apertures, which closed within minutes (Chen *et al.*, 2018). Hence, the use of PEG-based hydrogels can exhibit a positive impact on the wound-healing process.

### **3.5.1.2 Polyvinyl alcohol (PVA)**

Polyvinyl alcohol (PVA) is a hydrophilic polymer whose properties have garnered considerable attention from the biomedical industry. It is biocompatible, biodegradable, and semi-crystalline. PVA can undergo physical cross-linking using several freeze-thaw cycles, called cryogelation. Additionally, PVA can be chemically cross-linked by employing glutaraldehyde or epichlorohydrin. Both methods of production produce PVA hydrogels that are remarkably hydrophilic and chemically stable (Figueroa-Pizano *et al.*, 2020). Moreover, PVA can be altered with glycidyl methacrylate or acryloyl chloride to produce reactive acrylate groups via the pendant hydroxyl groups. These can then be cross-linked and polymerized to create hydrogels (Maitra and Shukla, 2014). PVA hydrogels serve as effective wound dressings by protecting them from external environmental stimuli and mechanical forces, reducing the risk of secondary injuries. PVA hydrogels also exhibit favourable characteristics such as excellent water and oxygen permeability and an elevated moisture level (Muchová *et al.*, 2020). These attributes are advantageous in wound healing, as they facilitate maintaining a moist environment, promoting the formation of new tissue, and improving the overall wound healing process. However, PVA hydrogels lack inherent antibacterial activity, necessitating the augmentation of their antibacterial efficacy when employed as a therapeutic (Li *et al.*, 2017).

Through the coupling of CS/Fe<sup>3+</sup> and carboxylated PVA, a double-cross-linked hydrogel was synthesized that exhibited exceptional features, including enhanced rigidity (78 kPa) and adherence traits, as well as a reduced duration for self-healing (5 minutes). These changes were observed to align with the dynamic nature of lesions. The hydrogel demonstrated antibacterial efficacy and enhanced hemostatic ability throughout the wound recovery phase. It was further proposed that the hydrogel could reduce skin repair duration to 14 days (Liu *et al.*, 2022).

### **3.5.1.3 Polyvinylpyrrolidone (PVP)**

Polyvinylpyrrolidone (PVP) is a crystalline polymer soluble in water and polar solutions. PVP is a highly appealing polymer for the manufacture of hydrogels due to its diverse qualities, including its non-toxic nature, ability to form films, and adequate adhesion. A promising technique for the cross-linking of PVP hydrogels is the use of radiation. PVP is often mixed with PEG and agar to form a reaction mixture that undergoes cross-linking through irradiation under a linear electron accelerator. Radiation cross-linking removes the need for an initiator and cross-linking agent, allowing ease in manipulating the hydrogel properties (Irmukhametova *et al.*, 2014). PVP can absorb water up to one hundred times its mass, which

facilitates the preservation of moisture (Shahrousvand *et al.*, 2023). The semi-permeable nature of PVP enables the selective permeation of oxygen while effectively impeding the ingress of bacteria and other contaminants. The utilization of PVP is beneficial in the debridement process, as it effectively absorbs exudate and necrotic tissue. PVP can potentially protect wounds from further injury or onset of infection (Xu *et al.*, 2023).

Hydrogel fibre mats using PVP with ferulic and p-coumaric acid have been synthesized. The biocompatibility studies conducted on erythrocytes from humans, A549 cells, and HaCaT cells demonstrated the absence of any adverse effects. The *ex-vivo* experiments on human skin revealed evidence of skin regrowth and effective regulation of inflammation, as seen by the presence of minimal quantities of pro-inflammatory cytokines, specifically IL-6 and IL-8. The results obtained from the study suggested that PVP-based fibre hydrogels have the potential for application in wound treatment (Contardi *et al.*, 2021).

### **3.5.2 Natural hydrogels**

While synthetic polymers demonstrate stability and ease of use, they are inhibited by limited biocompatibility. This notable shortcoming negatively impacts the mitigation of issues related to wound healing management. Therefore, natural hydrogels are the preferred therapeutic alternative. Natural hydrogels primarily comprise proteins and ECM constituents, rendering them intrinsically biocompatible, bioactive, and potentially well-suited for various biomedical applications due to their ability to enhance numerous cellular activities (Catoira *et al.*, 2019). The makeup and attributes of these materials resemble the inherent characteristics of tissue layers. Nevertheless, they are subject to some restrictions, primarily from the challenges associated with their manipulation arising from variations between different batches. Hydrogel variants exhibit unique properties that render them appropriate for their proposed purpose.

#### **3.5.2.1 Gelatin**

Gelatin is a renowned, naturally occurring, inexpensive vascular polymer with beneficial features for tissue development, including low immunogenicity and significant degradability. Gelatin is derived by disrupting the triple helical structure of collagen, resulting in the development of the sequence of amino acids known as RGD (Arg/Gly/Asp). This sequence can facilitate the adhesion of cells and create a favourable environment for cell proliferation. This material's fibroblast adhesion, proliferative features, and low antigenicity render it highly promising for clinical use (Mousavi *et al.*, 2019). Nevertheless, its suboptimal strength and

breakage susceptibility restrict its hydrogel use. Therefore, this hydrophilic protein requires cross-linking (Dash *et al.*, 2013). Gelatin has also been employed as an adhesive for coatings to enhance cell adhesion, facilitating the regrowth of vascular tissues. The absorption of wound exudates and moisture maintenance by porous gelatin matrices contribute to wound recovery. Despite its potential as a biopolymer for wound healing, gelatin lacks antibacterial properties that could effectively avoid infections. Therefore, it is typically combined with antibacterial agents or hybrid polymers (Xu and Zhou, 2008). Gelatin is often cross-linked with aldehydes, such as glutaraldehyde and formaldehyde, similar to CS, due to the presence of amino groups. Another frequently used method is cross-linkers such as 1-ethyl-3-(3-dimethylaminopropyl) carbodiimide hydrochloride (EDC) that are not incorporated into the gelatin matrix. EDC activates the carboxyl groups in gelatin, reacting directly and forming bonds with the adjacent amino groups (Skopinska-Wisniewska *et al.*, 2021).

Wang and coworkers (2023) developed a bilayer gelatin hydrogel with photothermal properties to eradicate biofilms and provide extensive therapy for chronic wounds. To enhance the attachment and growth of fibroblasts, gelatin methacryloyl (GelMA) with favourable rigidity was synthesized by optical cross-linking on the outermost layer of the hydrogel. EGF was introduced into GelMA to enhance tissue repair and re-establish the wound's epithelial layer. Scanning electron microscopy (SEM) revealed a significant reduction in the biofilm layer within the lesion after photothermal therapy. After a 12-day treatment period, the *E.coli*-afflicted wound exhibited a reduction to 7.9% of its initial area (Wang *et al.*, 2023).

### **3.5.2.2 Hyaluronic acid**

Hyaluronic acid (HA) is a glycosaminoglycan lacking sulfonate groups and is a naturally occurring anionic polysaccharide. It comprises a series of disaccharides, specifically  $\beta$ -D-glucuronic acid and N-acetyl-D-glucosamine, interlinked by alternate  $\beta$ -1, 3, and  $\beta$ -1, 4-glucosidic linkages. HA is found within the vitreous humor of humans, umbilical cords, and connective tissues and is synthesized via fermentation by microbes (Fallacara *et al.*, 2018). HA does not undergo hydrogel formation through conventional physical cross-linking methods. However, this polymer can undergo chemical modifications to its hydroxyl and carboxyl moieties. As a result, it is widely used in the construction of hydrogels, making it one of the most commonly employed polymers. The hydrophilicity of hyaluronic acid can be attributed to the presence of these functional groups, and this characteristic allows it to soak up exudate and enhance cell adhesion efficiently (Highley *et al.*, 2016). A widely used cross-linking

method for HA is the formation of thiol-modified HA hydrogels. The cross-linking system entails the conjunction of oxidized glutathione with an HA-based hydrogel through a thiol-disulfide exchange reaction. The thioether-sulfone bond is highly stable, not readily susceptible to hydrolysis, and unsuitable for hydrogel formation (Khunmanee *et al.*, 2017). Hydrogel wound dressings based on HA exhibit features such as reduction in inflammation, amplification of angiogenesis, and the promotion of endothelial cell growth, making them an option for addressing all four phases of wound healing (Della Sala *et al.*, 2022).

Li *et al.* (2022) developed a hydrogel that used HA as its primary constituent. HA was cross-linked using benzaldehyde-functionalized PEG co-polyglycerol caprate (PEGSB) to form a hydrogel with both elasticity and regeneration abilities. The aldehyde group of PEGSB can undergo a chemical reaction with those found in the wounds, thereby facilitating adequate adhesion. A three-minute exposure to near-infrared (NIR) irradiation at 808 nm effectively eradicated *E.coli* and methicillin-resistant *S. aureus* (MRSA). After a 14-day therapy regimen targeting hip wounds in mice, a near-complete healing of the lesion was observed. The hydrogel showed promise for practical use in the treatment of infections in wounds due to its excellent biocompatibility (Li *et al.*, 2022).

### **3.5.2.3 Alginate**

Alginate is a polymer found in brown algae cell walls and certain bacteria capsules. Its structure is built from blocks of two distinct monomers, D-manuronate (M) and L-glucuronate (G). Alginate's substantial G block concentration may produce stiff hydrogels when bound to divalent cations like  $\text{Ca}^{2+}$ . This is referred to as the "egg-box model". Alginate with an elevated M block concentration demonstrates reduced adhesiveness and immunostimulatory properties (Sanchez *et al.*, 2021). The calcium ions in an alginate-containing dressing exchange with sodium ions as they come into contact with the exudate from the wound. The alginate fibres undergo expansion, partial dissolution, and solidification, forming a protective coating that facilitates wound repair (Zhang *et al.*, 2020). A direct method of cross-linking is typically utilised, wherein alginate is directly treated with calcium chloride, calcium sulphate, or calcium carbonate. Internal gelation occurs upon mixing as the cations penetrate the alginate gel through diffusion. Divalent ionic bonding with zinc oxide has also been a notable cross-linking method, providing antibacterial properties (Jang *et al.*, 2014). Alginate can activate macrophages and promote the production of interleukin-6 (IL-6) and tumour necrosis factor  $\alpha$  (TNF- $\alpha$ ) by monocytes, thereby accelerating chronic wound healing. Dry alginate dressings

can soak up wound fluids, resulting in the formation of gels. These gels subsequently release water, which can benefit the hydration of dry wounds. The gelation property of alginate facilitates the painless and safe removal of dressings (Lee and Mooney, 2012). Many commercial hydrogels contain alginate as the primary component (Table 3.2).

**Table 3.2:** Some commercially available hydrogels for wound healing (Firlar *et al.*, 2022).

| <b>Product</b>             | <b>Company</b>                  | <b>Constituent</b>   | <b>Use</b>  |
|----------------------------|---------------------------------|--|---|
| <b>DermaSyn®</b>           | DermaRite Industries            | Primary wound dressing with vitamin E                          | Partial and full-thickness chronic wounds   |
| <b>Neoheal® Hydrogel</b>   | Kikgel                          | Polyethylene glycol, polyvinylpyrrolidone, Agar, and 90% water | Low-exuding scabs, abrasions, dry scabs, first-, second- and third-degree burns, and ulcers   |
| <b>Restore Hydrogel</b>    | Hollister Incorporated          | Gauze pad, Hyaluronic acid                                     | Partial and full-thickness chronic wounds   |
| <b>ActivHeal®</b>          | Advanced Medical Solutions Ltd. | Primary wound dressing with 85% water                          | Cavity wounds, Pressure ulcers, Diabetic foot ulcers, and leg ulcers                          |
| <b>NU-GEL™</b>             | Systagenix                      | Sodium alginate primary wound dressing                         | Diabetic foot ulcers, leg ulcers, venous ulcers   |
| <b>Purilon®</b>            | Coloplast                       | Calcium alginate, sodium carboxymethyl cellulose               | Pressure ulcers, first and second-degree burns, non-infected diabetic foot ulcers, leg ulcers |
| <b>Simpurity™ Hydrogel</b> | Safe n' Simple                  | Acrylate, polyvinyl alcohol, polyethylene oxide, polyurethane  | First- and second-degree partial-thickness burns, low exuding chronic wounds                  |

To improve the repair of wounds, a dual-network hydrogel using platelet-rich plasma (PRP) and sodium alginate (SA) was synthesized using a thrombin activation method. EGF and vascular endothelial growth factor (VEGF) were observed in a hydrogel maintained in phosphate-buffered saline (PBS), suggesting the potential for cellular growth and the redevelopment of blood vessels. The hydrogel showed efficacy in promoting wound closure when administered directly to the cutaneous wounds of rats (Wang *et al.*, 2023). Alginate

hydrogels present a viable strategy for addressing the limitations associated with traditional wound dressings.

#### **3.5.2.4 Chitosan (CS)**

CS has been discussed briefly in Chapter 2. Chitin is the primary building block of arthropod exoskeletons. It is partially deacetylated to make chitosan, a linear polysaccharide of beta (1-4)-linked D-glucosamine and N-acetyl-D-glucosamine groups. CS exhibits a structural resemblance to glycosaminoglycans inside the ECM. The molecular weight and level of deacetylation of CS are directly related to its physical and mechanical characteristics (Chen *et al.*, 2022). CS possesses a cationic charge and exhibits specific antimicrobial activity through electrostatic interactions (Sahariah *et al.*, 2023). Its positive charge has made it a polymer of choice for coating nanoparticles for enhanced stability (Joseph *et al.*, 2022, Akinyelu *et al.*, 2022). The potential advantages of CS-based hydrogels in wound healing applications include the creation of a hydrated wound environment, protection from infections, promotion of leukocyte activity for wound exudate disposal, regulation of degradation through a change in the level of deacetylation, and a reduction in scar tissue (Liu *et al.*, 2018). These properties highlight the significant promise of CS in wound healing. The susceptibility of the hydrogel to external factors, such as pH and temperature, can be attributed to the presence of hydroxyl and amino groups. One of the drawbacks associated with this material is its suboptimal mechanical strength and challenges in manufacturing fibrous wound dressings (Catoira *et al.*, 2019). Nevertheless, this issue can be effectively addressed by implementing cross-linking techniques. The most prominent cross-linking technique is the utilization of glutaraldehyde or genipine cross-linkers, which will typically embed themselves between CS polymer chains by cross-linking with the amino groups of CS. Another method often utilized is cross-linking CS with tripolyphosphate (TPP). The phosphates present in TPP ionically bind to the amine groups of the CS through a process known as ionic gelation (Ahmadi *et al.*, 2015).

An injectable CS-based hydrogel for repairing wounds has been reported. This hydrogel exhibited antimicrobial activity against bacterial strains *Pseudomonas aeruginosa* and *S.aureus*, with a terminating efficiency of 96.4% and 95.0%, respectively. Hydrogel-treated wounds showed 99.8% sealing after two weeks. Evaluation of the hydrogel's hemostatic properties demonstrated prompt attachment to the adjacent tissue of the bleeding region, thereby establishing a protective covering that mitigated hemorrhaging (Du *et al.*, 2019). Hence, hydrogels derived from CS can promote the healing of wounds as well as the prevention

of infection. Recently, an injectable carboxymethyl CS (CMCS) hydrogel was developed to modulate cellular responses and facilitate the complete recovery of diabetic wounds. CMCS was synthesized by modifying CS to improve its solubility in water. The CMCS hydrogel exhibited a significant swelling rate of 132% at 37 °C. This property enabled it to efficiently soak up a substantial amount of tissue exudate and regulate the moisture levels at the lesion. The hydrogel was administered intradermally into the wounds of mice with diabetes. The hydrogel promptly attaches to the location of the wound, effectively halting hemorrhaging and establishing a favourable environment for the healing process, which takes 14 days for 99% wound healing (Hao *et al.*, 2022). Hence, it can be concluded that hydrogels constructed from carboxymethyl CS exhibit properties that closely resemble the conditions of the ECM, demonstrating their efficacy in wound healing.

This research investigates using a CS hydrogel, in virtue of the substantial evidence supporting its therapeutic efficacy in wound healing.

### **3.5.3 Advanced Hydrogels**

#### **3.5.3.1 Sprayable hydrogels**

Attempts have been made to address the shortcomings of traditional dressings used in healthcare by employing "*in situ*" forming wound dressings such as sprayable hydrogels. These hydrogels provide many benefits, including ease of use without needing specialized assistance, patient approval, and manufacturing cost-effectiveness (Tavakoli and Klar, 2020). Furthermore, applying a spray can enhance the permeation of the hydrogel into the injured region, improving the administration of medicinal formulations or active substances. An ideal viscosity is thus needed to allow the sprayability of these hydrogels (Tavakoli *et al.*, 2019).

A methacrylate gelatin (GelMA) hydrogel is an example of a sprayable hydrogel. Cheng and coworkers (2021) functionalized the GelMA hydrogels with DOPA, resulting in an increased affinity for binding to the wound surfaces. The GelMA-DOPA hydrogel was also loaded with cerium oxide nanoparticles (CeONs) and an antimicrobial peptide (AMP HHC-36) to grant the hydrogel antibacterial and ROS-scavenging properties. This hydrogel exhibited several advantageous properties, including sprayability, adequate adhesion, antibacterial activity, ROS-scavenging, and wound repair capabilities. These attributes have the potential to effectively alleviate the medical and financial obstacles related to the care and handling of chronic wounds (Cheng *et al.*, 2021). A few constraints associated with sprayable hydrogels include the control of drug dispersity and uniform spraying, balancing rheological properties

while maintaining physical and mechanical characteristics, and the inhibition of precursors during gel formation by bioactive molecules (Tan *et al.*, 2023).

### 3.5.3.2 “Smart” hydrogels

Conventional wound therapies cannot offer insights into the overall progress of healing. This served as a catalyst for advancing sensor-based hydrogels, commonly called "smart" hydrogels. These hydrogels can present significant insights into the state of a wound, encompassing factors such as the concentration of bacteria, oxygen levels, inflammatory intensity, pH, and temperature (Figure 3.7).

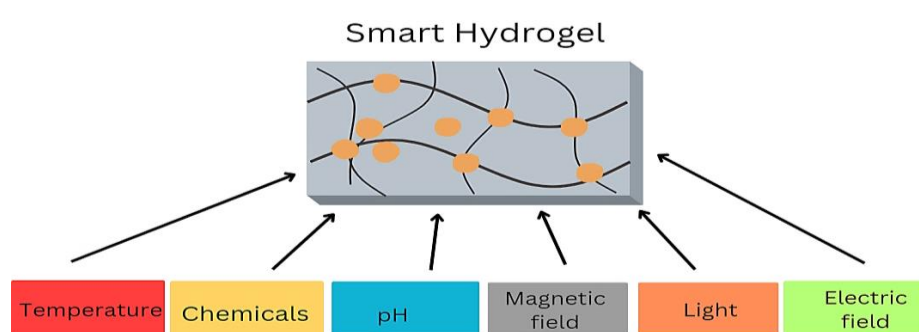


**Figure 3.7:** Sensors detected by "smart" hydrogels.

Many sensors have been created to quantify the pH level, moisture, temperature, oxygen supply, and mechanical and enzymatic activity (Tavakoli and Klar, 2020). Each sensor must be non-toxic, biocompatible, and flexible enough to conform to the hydrogel. Temperature has been identified as a handy parameter for the early identification of infection within the wound, as aberrant fluctuations in wound temperature can serve as an initial indicator of an infection before the manifestation of any other symptoms (Derakhshandeh *et al.*, 2018). However, concerns associated with thermosensitive hydrogels include weak mechanical properties, poor biocompatibility, and a delayed temperature response (Khan *et al.*, 2023).

A "smart" hydrogel consisting of a polycation and alginate was formulated and demonstrated remarkable antibacterial properties against *S.aureus* and *E.coli*. Treatment with this hydrogel promoted the healing of infected wounds in rats, with a recovery rate of 96.49%. The hydrogel also reacted to stress, temperature, and pressure, demonstrating its potential for reliable wound monitoring (Dong *et al.*, 2022).

### 3.5.3.3 Nanogels

Nanogels are hydrogels composed of cross-linked polymer networks in three-dimensional configurations at the nanoscale. The nanogels primarily exhibit a spherical shape and can be constructed to possess a core-shell or core-shell-corona structure (Figure 3.8).

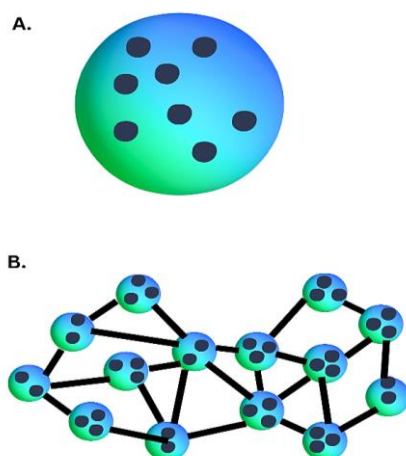


**Figure 3.8:** (A) Nanoparticles embedded in a hydrogel. (B) Cross-linking between polymer particles.

Nanogels have garnered significant interest due to their ability to integrate the characteristics of hydrogels, such as substantial water retention and adaptable physical characteristics, with the customizable size and expansive surface area of nanoparticles for the conjugation of active compounds (Soni *et al.*, 2016). Nanogels that demonstrate a response to stimuli enable the controlled release of therapeutic agents (antibacterial agents, cytokines, and growth factors) in response to illness-induced fluctuations in pH and temperature, which are commonly associated with infection. Additionally, nanogels have the potential to significantly contribute to the precise adjustment of the texture of the scaffold and its mechanical features, which is crucial for cell regulation (Grimaudo *et al.*, 2019).

Metal nanocomposite hydrogels have recently gained attention as promising nanogels for enhancing wound healing while protecting against bacterial infections. The nanomaterial's moist state can effectively inhibit wound dehydration, which impedes wound recovery. The nanoparticles incorporated within the hydrogels function as an antibacterial agent, hindering the development and proliferation of bacteria or fungi (Dzulkharnien and Rohani, 2022). Haseeb and colleagues synthesized linseed hydrogels (LSH) containing silver nanoparticles (LSH-AgNPs) that effectively suppressed the proliferation of numerous bacteria and fungi. Furthermore, 100% wound closure in rabbits was exhibited on day 15, demonstrating its

therapeutic efficacy (Haseeb *et al.*, 2017). Some issues that hinder the progression of nanogels include degradation and batch-to-batch reproducibility (Soni *et al.*, 2016).

#### **3.5.3.3.1 Gold nanoparticle hydrogels**

While gold is typically considered inert, gold nanoparticles (AuNPs) have diverse biological properties and have been extensively employed in the medical domain. In contrast to other metal nanoparticle carriers, such as copper and silver, AuNP carriers exhibit negligible toxicity in human tissues. When integrated with hydrogels, they form biomaterials with improved mechanical stability, environmental adaptability, biocompatibility, conductivity, and antibacterial activity for wound management (Li *et al.*, 2018).

Most hydrogel scaffolds are nonconductive, necessitating the incorporation of additional compounds to enable intercellular signal transmission, hence constraining their potential in biotechnology (Abdollahiyan *et al.*, 2020). Metal nanocarriers increase the conductivity of hydrogels while simultaneously improving their mechanical properties and substantially increasing their utility in tissue engineering applications. Studies have demonstrated that incorporating AuNPs into CS hydrogels produces constructs with electrical conductivity comparable to cardiac tissue. It has been shown that this composite material increases the ability of cardiac cells to regenerate after a myocardial infarction. This development is crucial for the *in vitro* construction of engineered skin tissues (Peña *et al.*, 2019).

In addition to enhancing mechanical and electrical properties, AuNPs can facilitate wound healing by suppressing bacterial and fungal growth. Studies have revealed that the antibacterial action of AuNPs on *E.coli* entails inhibiting ATPase activity to alter membrane potential while obstructing the interaction between tRNA and ribosomal subunits (Cui *et al.*, 2012). According to Batool *et al.* (2022), a gold nanocarrier hydrogel composite showed increased antibacterial activity, as well as increased amounts of NANOG (transcription factor) and CD34 proteins in mouse wound sites, accelerating wound healing (Batool *et al.*, 2022). Although notable, gold nanocarriers do not possess the same antibacterial efficacy as silver nanocarriers. Consequently, AuNPs can be conjugated with other existing nanoparticles or antimicrobial compounds to augment their effectiveness in eradicating microorganisms. In particular, vancomycin-conjugated AuNPs have been observed to increase the efficacy of vancomycin significantly and to exhibit significant synergistic antibacterial action against *S. aureus* and *E. coli* (Kaur and Kumar, 2021).

Gold nanogels can also be employed for photothermal treatment (PTT) to address bacterial infections. PTT utilizes the adjustable surface plasmon resonance effects of the AuNPs in near-infrared radiation to treat bacterial infections through thermal ablation. Liu and colleagues (2018) have noted the synthesis of a novel hydrogel based on soy proteins integrated with AuNPs and cross-linked with oxidized dextran. This hydrogel displayed strong mechanical properties and photothermal antibacterial efficacy against *E. coli* and *S. aureus* (Liu *et al.*, 2018).

Furthermore, AuNPs may directly affect the advancement of wound healing. Recent topical treatment of AuNPs to cutaneous wounds in rats demonstrated enhanced healing, evidenced by increased re-epithelialization, regrowth of granulation tissue, collagen content, and ECM deposition. The disparities are predominantly observed during the initial healing stages and reduce the overall healing time (Naraginti *et al.*, 2016). Wound healing potential may also be considerably enhanced by cross-linking AuNPs with polymers. The cross-linking of AuNPs with collagen facilitates the integration of various biomolecules, including peptides, polysaccharides, and growth factors, at the surface of AuNPs without modifying the collagen structure. The modified hydrogel displayed features including biodegradability and biocompatibility, rendering them potentially suitable for extensive application in wound healing (Arafa *et al.*, 2018). In addition, a study demonstrating the combination of AuNPs with CS observed a substantially improved free radical scavenging capacity of the AuNPs and enhanced biocompatibility. These positive results were further supported by a rat surgical wound model, which indicated that CS-AuNPs markedly improved hemostasis, epithelial tissue development with an elevated healing rate, and wound closure relative to isolated treatment with conventional CS and Tegaderm bandages (Hsu *et al.*, 2011).

The compelling literature presented has inspired the integration of the beneficial properties of CS and AuNPs to develop a CS hydrogel physically cross-linked with AuNPs *in situ* as an innovative treatment for the predicament of ineffective wound care.

### 3.6 References

Abdollahiyan, P., Baradaran, B., de la Guardia, M., Oroojalian, F., & Mokhtarzadeh, A. (2020). Cutting-edge progress and challenges in stimuli responsive hydrogel microenvironment for success in tissue engineering today. *Journal of Controlled Release*, 328, 514-531.

- Ahmadi, F., Oveisi, Z., Samani, S. M., & Amoozgar, Z. (2015). Chitosan based hydrogels: characteristics and pharmaceutical applications. *Res Pharm Sci*, *10*(1), 1-16.
- Arafa, M. G., El-Kased, R. F., & Elmazar, M. M. (2018). Thermoresponsive gels containing gold nanoparticles as smart antibacterial and wound healing agents. *Scientific Reports*, *8*(1), 13674.
- Aswathy, S. H., Narendrakumar, U., & Manjubala, I. (2020). Commercial hydrogels for biomedical applications. *Heliyon*, *6*(4), e03719. <https://doi.org/10.1016/j.heliyon.2020.e03719>
- Baranoski, S. (2008). Choosing a wound dressing, part 1. *Nursing2023*, *38*(1), 60-61. <https://doi.org/10.1097/01.Nurse.0000305919.47233.61>
- Batool, Z., Muhammad, G., Iqbal, M. M., Aslam, M. S., Raza, M. A., Sajjad, N., Abdullah, M., Akhtar, N., Syed, A., & Elgorban, A. M. (2022). Hydrogel assisted synthesis of gold nanoparticles with enhanced microbicidal and in vivo wound healing potential. *Scientific Reports*, *12*(1), 6575.
- Bilici, C., Can, V., Nöchel, U., Behl, M., Lendlein, A., & Okay, O. (2016). Melt-Processable Shape-Memory Hydrogels with Self-Healing Ability of High Mechanical Strength. *Macromolecules*, *49*(19), 7442-7449. <https://doi.org/10.1021/acs.macromol.6b01539>
- Boateng, J. S., Matthews, K. H., Stevens, H. N., & Eccleston, G. M. (2008). Wound healing dressings and drug delivery systems: a review. *Journal of pharmaceutical sciences*, *97*(8), 2892-2923.
- Catoira, M. C., Fusaro, L., Di Francesco, D., Ramella, M., & Boccafoschi, F. (2019). Overview of natural hydrogels for regenerative medicine applications. *J Mater Sci Mater Med*, *30*(10), 115. <https://doi.org/10.1007/s10856-019-6318-7>
- Chandel, A. K. S., Kannan, D., Nutan, B., Singh, S., & Jewrajka, S. K. (2017). Dually cross-linked injectable hydrogels of poly (ethylene glycol) and poly [(2-dimethylamino) ethyl methacrylate]-b-poly (N-isopropyl acrylamide) as a wound healing promoter. *Journal of Materials Chemistry B*, *5*(25), 4955-4965.
- Chen, S. L., Fu, R. H., Liao, S. F., Liu, S. P., Lin, S. Z., & Wang, Y. C. (2018). A PEG-Based Hydrogel for Effective Wound Care Management. *Cell Transplant*, *27*(2), 275-284. <https://doi.org/10.1177/0963689717749032>

Chen, W.-H., Chen, Q.-W., Chen, Q., Cui, C., Duan, S., Kang, Y., Liu, Y., Liu, Y., Muhammad, W., & Shao, S. (2022). Biomedical polymers: synthesis, properties, and applications. *Science China Chemistry*, *65*(6), 1010-1075.

Chen, Y., Xiang, Y., Zhang, H., Zhu, T., Chen, S., Li, J., Du, J., & Yan, X. (2023). A multifunctional chitosan composite aerogel based on high density amidation for chronic wound healing. *Carbohydrate Polymers*, *321*, 121248. <https://doi.org/https://doi.org/10.1016/j.carbpol.2023.121248>

Cheng, H., Shi, Z., Yue, K., Huang, X., Xu, Y., Gao, C., Yao, Z., Zhang, Y. S., & Wang, J. (2021). Sprayable hydrogel dressing accelerates wound healing with combined reactive oxygen species-scavenging and antibacterial abilities. *Acta Biomaterialia*, *124*, 219-232. <https://doi.org/https://doi.org/10.1016/j.actbio.2021.02.002>

Chouhan, D., Lohe, T. u., Samudrala, P. K., & Mandal, B. B. (2018). In situ forming injectable silk fibroin hydrogel promotes skin regeneration in full thickness burn wounds. *Advanced healthcare materials*, *7*(24), 1801092.

Clayton, K., Vallejo, A. F., Davies, J., Sirvent, S., & Polak, M. E. (2017). Langerhans cells—programmed by the epidermis. *Frontiers in immunology*, *8*, 1676.

Contardi, M., Kossyvaki, D., Picone, P., Summa, M., Guo, X., Heredia-Guerrero, J. A., Giacomazza, D., Carzino, R., Goldoni, L., Scoponi, G., Rancan, F., Bertorelli, R., Di Carlo, M., Athanassiou, A., & Bayer, I. S. (2021). Electrospun polyvinylpyrrolidone (PVP) hydrogels containing hydroxycinnamic acid derivatives as potential wound dressings. *Chemical Engineering Journal*, *409*, 128144. <https://doi.org/https://doi.org/10.1016/j.cej.2020.128144>

Cui, Y., Zhao, Y., Tian, Y., Zhang, W., Lü, X., & Jiang, X. (2012). The molecular mechanism of action of bactericidal gold nanoparticles on Escherichia coli. *Biomaterials*, *33*(7), 2327-2333.

Dabiri, G., Damstetter, E., & Phillips, T. (2016). Choosing a Wound Dressing Based on Common Wound Characteristics. *Adv Wound Care (New Rochelle)*, *5*(1), 32-41. <https://doi.org/10.1089/wound.2014.0586>

Dash, R., Foston, M., & Ragauskas, A. J. (2013). Improving the mechanical and thermal properties of gelatin hydrogels cross-linked by cellulose nanowhiskers. *Carbohydrate Polymers*, *91*(2), 638-645.

- Della Sala, F., Longobardo, G., Fabozzi, A., di Gennaro, M., & Borzacchiello, A. (2022). Hyaluronic Acid-Based Wound Dressing with Antimicrobial Properties for Wound Healing Application. *Applied Sciences*, 12(6), 3091. <https://www.mdpi.com/2076-3417/12/6/3091>
- Derakhshandeh, H., Kashaf, S. S., Aghabaglou, F., Ghanavati, I. O., & Tamayol, A. (2018). Smart bandages: the future of wound care. *Trends in biotechnology*, 36(12), 1259-1274.
- Dhivya, S., Padma, V. V., & Santhini, E. (2015). Wound dressings—a review. *BioMedicine*, 5(4), 22.
- Dong, H., Wang, L., Du, L., Wang, X., Li, Q., Wang, X., Zhang, J., Nie, J., & Ma, G. (2022). Smart Polycationic Hydrogel Dressing for Dynamic Wound Healing. *Small*, 18(25), 2201620. <https://doi.org/https://doi.org/10.1002/sml.202201620>
- Dorgalaleh, A., & Rad, F. (2018). *Congenital bleeding disorders*. Springer.
- Du, X., Liu, Y., Wang, X., Yan, H., Wang, L., Qu, L., Kong, D., Qiao, M., & Wang, L. (2019). Injectable hydrogel composed of hydrophobically modified chitosan/oxidized-dextran for wound healing. *Materials science and engineering: C*, 104, 109930.
- Dzulkharnien, N. S. F., & Rohani, R. (2022). A Review on Current Designation of Metallic Nanocomposite Hydrogel in Biomedical Applications. *Nanomaterials*, 12(10), 1629. <https://www.mdpi.com/2079-4991/12/10/1629>
- Ellis, S., Lin, E. J., & Tartar, D. (2018). Immunology of Wound Healing. *Current Dermatology Reports*, 7(4), 350-358. <https://doi.org/10.1007/s13671-018-0234-9>
- Fallacara, A., Baldini, E., Manfredini, S., & Vertuani, S. (2018). Hyaluronic Acid in the Third Millennium. *Polymers*, 10(7), 701. <https://www.mdpi.com/2073-4360/10/7/701>
- Fan, F., Saha, S., & Hanjaya-Putra, D. (2021). Biomimetic Hydrogels to Promote Wound Healing. *Front Bioeng Biotechnol*, 9, 718377. <https://doi.org/10.3389/fbioe.2021.718377>
- Feng, P., Luo, Y., Ke, C., Qiu, H., Wang, W., Zhu, Y., Hou, R., Xu, L., & Wu, S. (2021). Chitosan-based functional materials for skin wound repair: Mechanisms and applications. *Frontiers in Bioengineering and Biotechnology*, 9, 650598.
- Figuroa-Pizano, M. D., Vélaz, I., & Martínez-Barbosa, M. E. (2020). A freeze-thawing method to prepare chitosan-poly (vinyl alcohol) hydrogels without cross-linking agents and diflunisal release studies. *JoVE (Journal of Visualized Experiments)*(155), e59636.

- Firlar, I., Altunbek, M., McCarthy, C., Ramalingam, M., & Camci-Unal, G. (2022). Functional Hydrogels for Treatment of Chronic Wounds. *Gels*, 8(2). <https://doi.org/10.3390/gels8020127>
- Gantwerker, E. A., & Hom, D. B. (2011). Skin: histology and physiology of wound healing. *Facial Plast Surg Clin North Am*, 19(3), 441-453. <https://doi.org/10.1016/j.fsc.2011.06.009>
- Gonzalez, A. C., Costa, T. F., Andrade, Z. A., & Medrado, A. R. (2016). Wound healing - A literature review. *An Bras Dermatol*, 91(5), 614-620. <https://doi.org/10.1590/abd1806-4841.20164741>
- Grimaudo, M. A., Concheiro, A., & Alvarez-Lorenzo, C. (2019). Nanogels for regenerative medicine. *Journal of Controlled Release*, 313, 148-160. <https://doi.org/https://doi.org/10.1016/j.jconrel.2019.09.015>
- Güiza-Argüello, V. R., Solarte-David, V. A., Pinzón-Mora, A. V., Ávila-Quiroga, J. E., & Becerra-Bayona, S. M. (2022). Current Advances in the Development of Hydrogel-Based Wound Dressings for Diabetic Foot Ulcer Treatment. *Polymers (Basel)*, 14(14). <https://doi.org/10.3390/polym14142764>
- Hao, Y., Zhao, W., Zhang, H., Zheng, W., & Zhou, Q. (2022). Carboxymethyl chitosan-based hydrogels containing fibroblast growth factors for triggering diabetic wound healing. *Carbohydrate Polymers*, 287, 119336.
- Haseeb, M. T., Hussain, M. A., Abbas, K., Youssif, B. G., Bashir, S., Yuk, S. H., & Bukhari, S. N. A. (2017). Linseed hydrogel-mediated green synthesis of silver nanoparticles for antimicrobial and wound-dressing applications. *International journal of nanomedicine*, 2845-2855.
- Highley, C. B., Prestwich, G. D., & Burdick, J. A. (2016). Recent advances in hyaluronic acid hydrogels for biomedical applications. *Current opinion in biotechnology*, 40, 35-40.
- Ho, C., Cheung, A., & Bogie, K. (2020). Chapter 149 - Pressure Ulcers. In W. R. Frontera, J. K. Silver, & T. D. Rizzo (Eds.), *Essentials of Physical Medicine and Rehabilitation (Fourth Edition)* (pp. 849-859). Elsevier. <https://doi.org/https://doi.org/10.1016/B978-0-323-54947-9.00149-8>
- Ho, T. C., Chang, C. C., Chan, H. P., Chung, T. W., Shu, C. W., Chuang, K. P., Duh, T. H., Yang, M. H., & Tyan, Y. C. (2022). Hydrogels: Properties and Applications in Biomedicine. *Molecules*, 27(9). <https://doi.org/10.3390/molecules27092902>

- Holloway, S., & Harding, K. G. (2022). Wound dressings. *Surgery (Oxford)*, 40(1), 25-32.
- Hsu, S.-h., Chang, Y.-B., Tsai, C.-L., Fu, K.-Y., Wang, S.-H., & Tseng, H.-J. (2011). Characterization and biocompatibility of chitosan nanocomposites. *Colloids and Surfaces B: Biointerfaces*, 85(2), 198-206.
- Hurlow, J., & Bowler, P. G. (2022). Acute and chronic wound infections: microbiological, immunological, clinical and therapeutic distinctions. *Journal of Wound Care*, 31(5), 436-445. <https://doi.org/10.12968/jowc.2022.31.5.436>
- Irmukhmetova, G. S., Shaikhutdinov, E. M., Rakhmetullayeva, R. K., Yermukhambetova, B. B., Ishanova, A. K., Temirkhanova, G., & Mun, G. A. (2014). Nanostructured Hydrogel Dressings on Base of Cross-linked Polyvinylpyrrolidone for Biomedical Application. *Advanced Materials Research*, 875-877, 1467-1471. <https://doi.org/10.4028/www.scientific.net/AMR.875-877.1467>
- Jang, J., Seol, Y.-J., Kim, H. J., Kundu, J., Kim, S. W., & Cho, D.-W. (2014). Effects of alginate hydrogel cross-linking density on mechanical and biological behaviors for tissue engineering. *Journal of the Mechanical Behavior of Biomedical Materials*, 37, 69-77. <https://doi.org/https://doi.org/10.1016/j.jmbbm.2014.05.004>
- Kaur, A., & Kumar, R. (2021). Formulation of biocompatible vancomycin conjugated gold nanoparticles for enhanced antibacterial efficacy. *ES Energy & Environment*, 15, 34-44.
- Khan, B., Arbab, A., Khan, S., Fatima, H., Bibi, I., Chowdhry, N. P., Ansari, A. Q., Ursani, A. A., Kumar, S., Hussain, J., & Abdullah, S. (2023). Recent progress in thermosensitive hydrogels and their applications in drug delivery area. *MedComm – Biomaterials and Applications*, 2(3), e55. <https://doi.org/https://doi.org/10.1002/mba2.55>
- Khunmanee, S., Jeong, Y., & Park, H. (2017). Cross-linking method of hyaluronic-based hydrogel for biomedical applications. *Journal of Tissue Engineering*, 8, 2041731417726464. <https://doi.org/10.1177/2041731417726464>
- Koehler, J., Brandl, F. P., & Goepferich, A. M. (2018). Hydrogel wound dressings for bioactive treatment of acute and chronic wounds. *European Polymer Journal*, 100, 1-11. <https://doi.org/https://doi.org/10.1016/j.eurpolymj.2017.12.046>

- Kolarsick, P. A. J., Kolarsick, M. A., & Goodwin, C. (2011). Anatomy and Physiology of the Skin. *Journal of the Dermatology Nurses' Association*, 3(4), 203-213. <https://doi.org/10.1097/JDN.0b013e3182274a98>
- Landén, N. X., Li, D., & Ståhle, M. (2016). Transition from inflammation to proliferation: a critical step during wound healing. *Cellular and Molecular Life Sciences*, 73(20), 3861-3885. <https://doi.org/10.1007/s00018-016-2268-0>
- Lazarus, G. S., Cooper, D. M., Knighton, D. R., Margolis, D. J., Percoraro, R. E., Rodeheaver, G., & Robson, M. C. (1994). Definitions and guidelines for assessment of wounds and evaluation of healing. *Wound Repair and Regeneration*, 2(3), 165-170. <https://doi.org/https://doi.org/10.1046/j.1524-475X.1994.20305.x>
- Lee, K. Y., & Mooney, D. J. (2012). Alginate: Properties and biomedical applications. *Progress in Polymer Science*, 37(1), 106-126. <https://doi.org/https://doi.org/10.1016/j.progpolymsci.2011.06.003>
- Li, M., Liang, Y., Liang, Y., Pan, G., & Guo, B. (2022). Injectable stretchable self-healing dual dynamic network hydrogel as adhesive anti-oxidant wound dressing for photothermal clearance of bacteria and promoting wound healing of MRSA infected motion wounds. *Chemical Engineering Journal*, 427, 132039.
- Li, S., Dong, S., Xu, W., Tu, S., Yan, L., Zhao, C., Ding, J., & Chen, X. (2018). Antibacterial Hydrogels. *Advanced Science*, 5(5), 1700527. <https://doi.org/https://doi.org/10.1002/advs.201700527>
- Li, X., Jiang, Y., Wang, F., Fan, Z., Wang, H., Tao, C., & Wang, Z. (2017). Preparation of polyurethane/polyvinyl alcohol hydrogel and its performance enhancement via compositing with silver particles. *RSC advances*, 7(73), 46480-46485.
- Lindholm, C., & Searle, R. (2016). Wound management for the 21st century: combining effectiveness and efficiency. *Int Wound J*, 13 Suppl 2(Suppl 2), 5-15. <https://doi.org/10.1111/iwj.12623>
- Liu, H., Wang, C., Li, C., Qin, Y., Wang, Z., Yang, F., Li, Z., & Wang, J. (2018). A functional chitosan-based hydrogel as a wound dressing and drug delivery system in the treatment of wound healing. *RSC advances*, 8(14), 7533-7549.

- Liu, J., Li, Z., Lin, Q., Jiang, X., Yao, J., Yang, Y., Shao, Z., & Chen, X. (2018). A robust, resilient, and multi-functional soy protein-based hydrogel. *ACS Sustainable Chemistry & Engineering*, 6(11), 13730-13738.
- Liu, S., Li, D., Wang, Y., Zhou, G., Ge, K., & Jiang, L. (2023). Adhesive, antibacterial and double cross-linked carboxylated polyvinyl alcohol/chitosan hydrogel to enhance dynamic skin wound healing. *International Journal of Biological Macromolecules*, 228, 744-753. <https://doi.org/https://doi.org/10.1016/j.ijbiomac.2022.12.169>
- Maaz Arif, M., Khan, S. M., Gull, N., Tabish, T. A., Zia, S., Ullah Khan, R., Awais, S. M., & Arif Butt, M. (2021). Polymer-based biomaterials for chronic wound management: Promises and challenges. *International Journal of Pharmaceutics*, 598, 120270. <https://doi.org/https://doi.org/10.1016/j.ijpharm.2021.120270>
- Maitra, J., & Shukla, V. K. (2014). Cross-linking in hydrogels-a review. *Am. J. Polym. Sci*, 4(2), 25-31.
- Mir, M., Ali, M. N., Barakullah, A., Gulzar, A., Arshad, M., Fatima, S., & Asad, M. (2018). Synthetic polymeric biomaterials for wound healing: a review. *Prog Biomater*, 7(1), 1-21. <https://doi.org/10.1007/s40204-018-0083-4>
- Mousavi, S., Khoshfetrat, A. B., Khatami, N., Ahmadian, M., & Rahbarghazi, R. (2019). Comparative study of collagen and gelatin in chitosan-based hydrogels for effective wound dressing: Physical properties and fibroblastic cell behavior. *Biochemical and Biophysical Research Communications*, 518(4), 625-631.
- Muchová, M., Münster, L., Capáková, Z., Mikulcová, V., Kuřitka, I., & Vícha, J. (2020). Design of dialdehyde cellulose cross-linked poly (vinyl alcohol) hydrogels for transdermal drug delivery and wound dressings. *Materials science and engineering: C*, 116, 111242.
- Nagle, S. M., Stevens, K. A., & Wilbraham, S. C. (2018). Wound assessment.
- Naraginti, S., Kumari, P. L., Das, R. K., Sivakumar, A., Patil, S. H., & Andhalkar, V. V. (2016). Amelioration of excision wounds by topical application of green synthesized, formulated silver and gold nanoparticles in albino Wistar rats. *Materials science and engineering: C*, 62, 293-300.

Omidian, H., Dey Chowdhury, S., & Babanejad, N. (2023). Cryogels: Advancing Biomaterials for Transformative Biomedical Applications. *Pharmaceutics*, 15(7). <https://doi.org/10.3390/pharmaceutics15071836>

Peña, B., Maldonado, M., Bonham, A. J., Aguado, B. A., Dominguez-Alfaro, A., Laughter, M., Rowland, T. J., Bardill, J., Farnsworth, N. L., Alegret Ramon, N., Taylor, M. R. G., Anseth, K. S., Prato, M., Shandas, R., McKinsey, T. A., Park, D., & Mestroni, L. (2019). Gold Nanoparticle-Functionalized Reverse Thermal Gel for Tissue Engineering Applications. *ACS Appl Mater Interfaces*, 11(20), 18671-18680. <https://doi.org/10.1021/acsami.9b00666>

Percival, N. J. (2002). Classification of wounds and their management. *Surgery (Oxford)*, 20(5), 114-117.

Potekaev, N. N., Borzykh, O. B., Medvedev, G. V., Pushkin, D. V., Petrova, M. M., Petrov, A. V., Dmitrenko, D. V., Karpova, E. I., Demina, O. M., & Shnayder, N. A. (2021). The Role of Extracellular Matrix in Skin Wound Healing. *J Clin Med*, 10(24). <https://doi.org/10.3390/jcm10245947>

Rausch, M. K., Parekh, S. H., Dortdivanlioglu, B., & Rosales, A. M. (2021). Synthetic hydrogels as blood clot mimicking wound healing materials. *Prog Biomed Eng (Bristol)*, 3(4). <https://doi.org/10.1088/2516-1091/ac23a4>

Rezvani Ghomi, E., Khalili, S., Nouri Khorasani, S., Esmaeely Neisiany, R., & Ramakrishna, S. (2019). Wound dressings: Current advances and future directions. *Journal of Applied Polymer Science*, 136(27), 47738. <https://doi.org/https://doi.org/10.1002/app.47738>

Rittié, L. (2016). Cellular mechanisms of skin repair in humans and other mammals. *J Cell Commun Signal*, 10(2), 103-120. <https://doi.org/10.1007/s12079-016-0330-1>

Rodrigues, M., Kosaric, N., Bonham, C. A., & Gurtner, G. C. (2019). Wound Healing: A Cellular Perspective. *Physiological Reviews*, 99(1), 665-706. <https://doi.org/10.1152/physrev.00067.2017>

Rudnicka, E., Napierała, P., Podfigurna, A., Męczekalski, B., Smolarczyk, R., & Grymowicz, M. (2020). The World Health Organization (WHO) approach to healthy ageing. *Maturitas*, 139, 6-11. <https://doi.org/https://doi.org/10.1016/j.maturitas.2020.05.018>

- Sahariah, P., Kontogianni, G.-I., Scoulica, E., Sigurjonsson, O. E., & Chatzinikolaidou, M. (2023). Structure-activity relationship for antibacterial chitosan carrying cationic and hydrophobic moieties. *Carbohydrate Polymers*, *312*, 120796.
- Sanchez, M. F., Guzman, M. L., Apas, A. L., Alovero, F. d. L., & Olivera, M. E. (2021). Sustained dual release of ciprofloxacin and lidocaine from ionic exchange responding film based on alginate and hyaluronate for wound healing. *European Journal of Pharmaceutical Sciences*, *161*, 105789. <https://doi.org/https://doi.org/10.1016/j.ejps.2021.105789>
- Sen, C. K. (2021). Human Wound and Its Burden: Updated 2020 Compendium of Estimates. *Adv Wound Care (New Rochelle)*, *10*(5), 281-292. <https://doi.org/10.1089/wound.2021.0026>
- Shahrousvand, M., Mirmasoudi, S. S., Pourmohammadi-Bejarpasi, Z., Feizkhah, A., Mobayen, M., Hedayati, M., Sadeghi, M., Esmailzadeh, M., Mirkatoul, F. B., & Jamshidi, S. (2023). Polyacrylic acid/ polyvinylpyrrolidone hydrogel wound dressing containing zinc oxide nanoparticles promote wound healing in a rat model of excision injury. *Heliyon*, *9*(8), e19230. <https://doi.org/https://doi.org/10.1016/j.heliyon.2023.e19230>
- Sheng, Z., Liu, Z., Hou, Y., Jiang, H., Li, Y., Li, G., & Zhang, X. (2023). The Rising Aerogel Fibers: Status, Challenges, and Opportunities. *Adv Sci (Weinh)*, *10*(9), e2205762. <https://doi.org/10.1002/advs.202205762>
- Sheokand, B., Vats, M., Kumar, A., Srivastava, C. M., Bahadur, I., & Pathak, S. R. (2023). Natural polymers used in the dressing materials for wound healing: Past, present and future. *Journal of Polymer Science*, *61*(14), 1389-1414. <https://doi.org/https://doi.org/10.1002/pol.20220734>
- Shu, W., Wang, Y., Zhang, X., Li, C., Le, H., & Chang, F. (2021). Functional Hydrogel Dressings for Treatment of Burn Wounds [Review]. *Frontiers in Bioengineering and Biotechnology*, *9*. <https://doi.org/10.3389/fbioe.2021.788461>
- Singh, S., Young, A., & McNaught, C.-E. (2017). The physiology of wound healing. *Surgery (Oxford)*, *35*(9), 473-477.
- Sivaraj, D., Chen, K., Chattopadhyay, A., Henn, D., Wu, W., Noishiki, C., Magbual, N. J., Mittal, S., Mermin-Bunnell, A. M., Bonham, C. A., Trotsyuk, A. A., Barrera, J. A., Padmanabhan, J., Januszyk, M., & Gurtner, G. C. (2021). Hydrogel Scaffolds to Deliver Cell

Therapies for Wound Healing [Review]. *Frontiers in Bioengineering and Biotechnology*, 9. <https://doi.org/10.3389/fbioe.2021.660145>

Skopinska-Wisniewska, J., Tuszynska, M., & Olewnik-Kruszkowska, E. (2021). Comparative Study of Gelatin Hydrogels Modified by Various Cross-Linking Agents. *Materials*, 14(2), 396. <https://www.mdpi.com/1996-1944/14/2/396>

Soni, K. S., Desale, S. S., & Bronich, T. K. (2016). Nanogels: An overview of properties, biomedical applications and obstacles to clinical translation. *Journal of Controlled Release*, 240, 109-126. <https://doi.org/https://doi.org/10.1016/j.jconrel.2015.11.009>

Sood, A., Granick, M. S., & Tomaselli, N. L. (2014). Wound Dressings and Comparative Effectiveness Data. *Adv Wound Care (New Rochelle)*, 3(8), 511-529. <https://doi.org/10.1089/wound.2012.0401>

Surowiecka, A., Strużyna, J., Winiarska, A., & Korzeniowski, T. (2022). Hydrogels in Burn Wound Management—A Review. *Gels*, 8(2), 122. <https://www.mdpi.com/2310-2861/8/2/122>

Tan, Y., Cai, B., Li, X., & Wang, X. (2023). Preparation and Application of Biomass-based Sprayable Hydrogels. *Paper and Biomaterials*, 8(2), 1-19. <https://doi.org/10.26599/PBM.2023.9260006>

Tavakoli, S., Kharaziha, M., Kermanpur, A., & Mokhtari, H. (2019). Sprayable and injectable visible-light Kappa-carrageenan hydrogel for in-situ soft tissue engineering. *Int J Biol Macromol*, 138, 590-601. <https://doi.org/10.1016/j.ijbiomac.2019.07.126>

Tavakoli, S., & Klar, A. S. (2020). Advanced Hydrogels as Wound Dressings. *Biomolecules*, 10(8). <https://doi.org/10.3390/biom10081169>

Tham, K. W., Lim, A. Y. L., & Baur, L. A. (2023). The global agenda on obesity: what does this mean for Singapore? *Singapore Medical Journal*, 64(3), 182-187. <https://doi.org/10.4103/singaporemedj.SMJ-2023-018>

Van Vlierberghe, S., Dubruel, P., & Schacht, E. (2011). Biopolymer-Based Hydrogels As Scaffolds for Tissue Engineering Applications: A Review. *Biomacromolecules*, 12(5), 1387-1408. <https://doi.org/10.1021/bm200083n>

Varaprasad, K., Jayaramudu, T., Kanikireddy, V., Toro, C., & Sadiku, E. R. (2020). Alginate-based composite materials for wound dressing application:A mini review. *Carbohydrate Polymers*, 236, 116025. <https://doi.org/https://doi.org/10.1016/j.carbpol.2020.116025>

- Velnar, T., Bailey, T., & Smrkolj, V. (2009). The wound healing process: an overview of the cellular and molecular mechanisms. *J Int Med Res*, 37(5), 1528-1542. <https://doi.org/10.1177/147323000903700531>
- Wang, T., Yi, W., Zhang, Y., Wu, H., Fan, H., Zhao, J., & Wang, S. (2023). Sodium alginate hydrogel containing platelet-rich plasma for wound healing. *Colloids and Surfaces B: Biointerfaces*, 222, 113096. <https://doi.org/10.1016/j.colsurfb.2022.113096>
- Wang, Y., Lv, Q., Chen, Y., Xu, L., Feng, M., Xiong, Z., Li, J., Ren, J., Liu, J., & Liu, B. (2023). Bilayer hydrogel dressing with lysozyme-enhanced photothermal therapy for biofilm eradication and accelerated chronic wound repair. *Acta Pharmaceutica Sinica B*, 13(1), 284-297.
- Wenhui, L., Changgeng, F., Lei, X., Baozhong, Y., Guobin, L., & Weijing, F. (2021). Hyperbaric oxygen therapy for chronic diabetic foot ulcers: An overview of systematic reviews. *Diabetes Res Clin Pract*, 176, 108862. <https://doi.org/10.1016/j.diabres.2021.108862>
- Wernick, B., Nahirniak, P., & Stawicki, S. P. (2018). Impaired wound healing.
- Wright, E., Tyler, M., Vojnovic, B., Pleat, J., Harris, A., & Furniss, D. (2019). Human model of burn injury that quantifies the benefit of cooling as a first aid measure. *Journal of British Surgery*, 106(11), 1472-1479.
- Xiang, J., Shen, L., & Hong, Y. (2020). Status and future scope of hydrogels in wound healing: Synthesis, materials and evaluation. *European Polymer Journal*, 130, 109609. <https://doi.org/10.1016/j.eurpolymj.2020.109609>
- Xu, X., Zeng, Y., Chen, Z., Yu, Y., Wang, H., Lu, X., Zhao, J., & Wang, S. (2023). Chitosan-based multifunctional hydrogel for sequential wound inflammation elimination, infection inhibition, and wound healing. *International Journal of Biological Macromolecules*, 235, 123847.
- Xu, X., & Zhou, M. (2008). Antimicrobial gelatin nanofibers containing silver nanoparticles. *Fibers and polymers*, 9, 685-690.
- Yahya, E., Alfallous, K., & Abogmaza, A. (2020). Antibacterial cellulose-based aerogels for wound healing application: A review. *Biomedical Research and Therapy*, 7, 4032-4040. <https://doi.org/10.15419/bmrat.v7i10.637>
- Zabaglo, M., & Sharman, T. (2020). Postoperative wound infection.

Zhang, M., & Zhao, X. (2020). Alginate hydrogel dressings for advanced wound management. *Int J Biol Macromol*, *162*, 1414-1428. <https://doi.org/10.1016/j.ijbiomac.2020.07.311>

Zhao, R., Liang, H., Clarke, E., Jackson, C., & Xue, M. (2016). Inflammation in Chronic Wounds. *International Journal of Molecular Sciences*, *17*(12), 2085. <https://www.mdpi.com/1422-0067/17/12/2085>

## **CHAPTER FOUR**

### **MATERIALS AND METHODS**

## 4.1 Materials

Chitosan (CS) (25 kDa, 75% deacetylated), acrylic acid (C<sub>3</sub>H<sub>4</sub>O<sub>2</sub>), 5-fluorouracil (MW = 130.08 g/mol), and lysozyme ( $\geq 90$  % proteins, activity  $\geq 40\ 000$  U/mg) were sourced from Sigma-Aldrich, St. Louis, USA. Gold (III) chloride trihydrate (99%) (HAuCl<sub>4</sub>·3H<sub>2</sub>O), 3-[4,5-dimethylthiazol2-yl]-2,5-diphenyl tetrazolium bromide (MTT), phosphate-buffered saline (PBS), and dimethyl sulfoxide (DMSO) were procured through Merck, Darmstadt, Germany. Human cervical carcinoma (HeLa), breast adenocarcinoma (MCF-7), and embryonic kidney (HEK293) cells were originally supplied by the ATCC, Manassas, VA, USA. Eagle's minimum essential medium (EMEM) with L-glutamine, penicillin/ streptomycin/amphotericin B (100x) antibiotic mixture [amphotericin B (25  $\mu\text{g}\cdot\text{ml}^{-1}$ ), penicillin (10 000 U. $\text{ml}^{-1}$ ), and streptomycin sulfate (10 000  $\mu\text{g}\cdot\text{ml}^{-1}$ )], and trypsin-versene mixture were procured from Lonza Bio Whittaker, Walkersville, USA. Foetal bovine serum (FBS) was sourced from Hyclone, GE Healthcare, Utah, USA. All sterile plasticware was purchased from Corning Inc., Corning, NY, USA. Ultrapure (18 MOhm) water (Milli-Q Academic, Millipore, France) was utilized throughout, and all the reagents were of analytical quality.

## 4.2 Methods

### 4.2.1 Synthesis of Chitosan-gold (CS-Au) Hydrogel

Through continuous stirring overnight at room temperature, a solution was made by dissolving 0.60 g of CS in 0.3 ml of acrylic acid (1.048–1.050 g/ml) and 20 ml of deionized water. Following the complete dissolution of the CS, the solution was heated to 70 °C, followed by the injection of 1 ml of 1% (w/v) HAuCl<sub>4</sub>. A yellowish-brown hydrogel was immediately produced. After stirring for 10 minutes with heating, the colour of the hydrogel changed to a wine red. The resultant CS-Au hydrogel was cooled to room temperature.

### 4.2.2 Characterization

#### 4.2.2.1 UV-visible (UV-vis) Spectroscopy

The absorption spectrum of the CS-Au hydrogel was obtained at 1 nm intervals within a wavelength range of 400-650 nm using a UV-vis spectrophotometer (Jasco V-730 Bio Spectrophotometer, JASCO Corporation, Hachioji, Japan). The maximum absorption peak was referenced against the literature.

#### ***4.2.2.2 Fourier Transform Infrared (FTIR) Spectroscopy***

FTIR was used to confirm the specific functional groups present in the components of the hydrogels. The samples were freeze-dried and analyzed at a temperature of 25°C. The analysis was performed using a Perkin Elmer Spectrum 100 FTIR spectrometer (Waltham, MA, USA), which was fitted with a Universal Attenuated Total Reflectance (ATR) unit. The wavelength range used for the analysis was 400-4000 cm<sup>-1</sup>. The distinctive peaks of the samples were verified by comparing them to those documented in the literature.

#### ***4.2.2.3 Dynamic Light Scattering (DLS)***

The zeta potentials of the hydrogels were determined by employing dynamic light scattering (DLS) using a Malvern Zetasizer Nano-ZS instrument (Malvern Instruments Ltd., Worcestershire, UK). The experiments were performed at ambient temperature using DTS0012 polystyrene cuvettes. The samples were diluted in water using a 1:500 dilution, and the measurements were conducted in triplicate.

#### ***4.2.2.4 Transmission Electron Microscopy (TEM)***

The morphology and size of the AuNPs embedded in the hydrogels were analyzed using transmission electron microscopy (TEM) in their dry state. Approximately, 10 µl of each sample were sonicated for 15 minutes and then placed on a 400-mesh carbon-coated copper grid (Ted Pella Inc., Redding, USA). After air-drying for 1 hour, the samples were examined under a JEOL 1400 TEM (Jeol, Tokyo, Japan). A 3-megapixel digital camera positioned on the side of the iTEM Soft Imaging Systems (SIS) Megaview III was utilized to capture and process the images of the hydrogels.

#### ***4.2.2.5 Scanning Electron Microscopy (SEM)***

The surface morphology of the hydrogels was examined using scanning electron microscopy (SEM). The ZEISS Ultra Plus FEGSE microscope with SmartSEM software V6 (Carl Zeiss, Oberkochen, Baden-Württemberg, Germany) was used to acquire images. The hydrogels were mounted on aluminium stubs with double-sided carbon tape. The samples were gold coated using a gold sputter coater (Quorum Q150 RES, UK) and thereafter viewed and imaged.

#### **4.2.2.6 Thermogravimetric Analysis (TGA)**

The thermal characteristics of the hydrogels were analyzed using the Netzsch DSC-200 PC Phox differential scanning calorimetry (DSC) instrument from Germany. The DSC-TGA assessment of the produced hydrogels was conducted using a closed alumina crucible. The analysis was carried out within a temperature range of 25-650 °C, with a heating rate of 10 °C/min, in an atmosphere of nitrogen.

#### **4.2.2.7 Rheological studies**

The viscosity and thixotropy of the hydrogels were measured using an Anton Paar Modular Compact Rheometer 302 (Anton Paar GmbH, Graz, Austria) at room temperature. Measurements were conducted using a LV spindle 64. The viscosity measurements, expressed in centipoise (cP), were obtained at several shear rates, specifically 10, 20, 50, 60, and 100 rpm, using a torque setting range of 10 to 100%. The viscometry values were determined in triplicate.

#### **4.2.3 Reswelling and pH sensitivity**

The equilibrium swelling ratio of the CS-Au hydrogels at pH 4.5, 7.4, and 10.5 was assessed using a conventional weight measurement technique. Initially, the dehydrated hydrogel was submerged in distilled water at room temperature and left for 24 hours to achieve an equilibrium state of swelling. Subsequently, the hydrogel was removed, and the surface was dried using filter paper to soak up any water that had been absorbed. Equation 4.1 was used to obtain the equilibrium swelling ratio (SR):

$$SR = \frac{W_{\text{wet}}}{W_{\text{dry}}} \times 100\% \quad (4.1)$$

$W_{\text{wet}}$  and  $W_{\text{dry}}$  represent the hydrogel weights obtained after and before the swelling test.

#### **4.2.4 Drug encapsulation**

A vial containing 15 mg of freeze-dried hydrogel was immersed in 5 mL of distilled water. The hydrogel was then soaked in a solution containing 3 mg/ml of 5-FU. The vials were kept at room temperature for 2 days to allow the hydrogel to reach a state of equilibrium. The 5-FU content was determined using UV-vis spectroscopy at a wavelength of 266 nm. The execution

of all procedures was conducted in the absence of light. Equation 4.2 below was used to calculate the encapsulation efficiency of 5-FU:

$$\text{Encapsulation Efficiency (\%)} = \frac{\text{Total (5-FU)} - \text{5-FU (in vial)}}{\text{Total 5-FU}} \times 100\% \quad (4.2)$$

#### 4.2.5 *In vitro* degradation

Gravimetric analysis was used to measure the degree of *in vitro* degradation for both the CS-Au and CS-Au-5-FU hydrogels, which were cured for 2 hours at 37 °C. The brief curing time was chosen to enable the analysis of the hydrogels in settings that closely resemble those in an *in vivo* environment. All samples were maintained in solid form at the start of the testing. The hydrogels, weighing approximately 240 mg, were subjected to 24-hour incubation in PBS at 37 °C until equilibrium was reached. The total weight of the samples was then measured over a period of 28 days in 10 ml of PBS containing lysozyme (1.5 µg/ml) at 37°C. The enzyme concentration employed was comparable to that observed in human serum. The lysozyme was replenished every 2 days to mimic uninterrupted enzyme activity. At predetermined periods, hydrogels were extracted from the solution, dried on filter paper to eliminate surface moisture, and the weight measured. Equation 4.3 was used to express the degree of *in vitro* degradation as a percentage of mass loss.

$$\text{Weight loss \%} = \frac{w_i - w_t}{w_i} \times 100 \% \quad (4.3)$$

Where  $w_i$  and  $w_t$  denote the initial and final weights of the hydrogel. The assay was done in triplicate.

#### 4.2.6 Drug Release

The drug release from the CS-Au-5-FU hydrogel was quantified over a 48-hour timeframe at pH 4.5, 6.5, and 7.4. PBS served as the solvent for release, and the required pH was adjusted using sodium hydroxide (NaOH) or hydrochloride (HCl), allowing for the assessment of the pH-responsive characteristics of the hydrogel. Approximately 15 mg of freeze-dried drug-loaded hydrogel was placed in 5 ml of phosphate-buffered saline (PBS) adjusted to pH 4.5, 6.5, and 7.4, respectively. The experiment was conducted at 37 °C, over 48 hours. At intervals of 4 hours, 10 µl aliquots of dialysates were removed and replaced with the same volume of fresh PBS in order to maintain the sink volume. The quantity of drug in the dialysate was determined

using UV-vis spectroscopy at a wavelength of 266 nm. The measurements were conducted in triplicate for each sample. The quantity of 5-FU released was determined using Equation 4.4.

$$\text{Cumulative drug release (\%)} = \frac{\text{Absorbance of free 5-FU}}{\text{Absorbance of Total 5-FU}} \times 100\% \quad (4.4)$$

#### 4.2.6.1 Drug release kinetics

To examine the drug release mechanism from the CS-Au hydrogel, release results were evaluated using the following models:

$$\text{Zero order: } f_t = K_0 t. \quad (4.5)$$

$$\text{First order: } f_t = 1 - e^{-K_1 t} \quad (4.6)$$

$$\text{Korsmeyer-Peppas model: } f_t = M_t/M_\infty = K t^n \quad (4.7)$$

The symbols  $f_t$  and  $M_t/M_\infty$  represent the drug's fractional release at time  $t$ ,  $K$  denotes the rate constant, and  $n$  signifies the diffusion exponent. Kinetic models were chosen to align with the drug release data, and conclusions were drawn using the coefficient of determination ( $r^2$ ) values.

#### 4.2.7 Cell culture and maintenance

The cell culture assays were performed in a sterile environment using an Airvolution Class II biosafety laminar flow hood (Labotec, South Africa). The cells were grown in 25 cm<sup>2</sup> tissue culture flasks containing 5 ml of EMEM, which was enriched with 10% (v/v) FBS and 1% antibiotics (100 U.ml<sup>-1</sup> penicillin, 100 µg.ml<sup>-1</sup> streptomycin). The cells were maintained at a temperature of 37°C in a HEPA-class 100 Steri-Cult CO<sub>2</sub> incubator (Thermo-Fisher Corporation, Waltham, Massachusetts, USA). The cell growth was observed using a Nikon TMS inverted microscope (Nikon, Tokyo, Japan). The culture medium was regularly replaced, and once confluent, the cells were either subcultured, plated in multi-well plates for experiments, or cryopreserved for future use.

#### 4.2.8 In vitro Cytotoxicity

The HEK293, HeLa, and MCF-7 cells were seeded in 48-well plates at densities of  $2.6 \times 10^4$  cells per well. After an incubation period of 24 hours, the medium (EMEM, 10% FBS, and 1%

antibiotics) was removed from each well and replenished with 200  $\mu$ l of fresh medium. The CS, CS-Au hydrogels, and free 5-FU solutions were subsequently administered to the cells at varying concentrations (10, 20, 30, 40, and 50  $\mu$ g/ml). The assay was conducted in triplicate. Cells were incubated for 48 hours at 37 °C. Thereafter, the used medium was removed and substituted with 200  $\mu$ l of complete medium containing 20  $\mu$ l of MTT solution (5 mg/ml in PBS). The cells were further incubated for 4 hours at 37°C. After the MTT-medium mixtures were removed, 200  $\mu$ l of DMSO was added to dissolve the resulting purple formazan crystals. The optical densities (OD) were measured at a wavelength of 540 nm using a Mindray MR-96A microplate reader (Vacutec, Hamburg, Germany), with DMSO serving as the blank. The cell viability was determined using Equation 4.8.

$$\text{Cell Viability (\%)} = \frac{\text{Absorbance of treated cells}}{\text{Absorbance of control cells}} \times 100\% \quad (4.8)$$

#### 4.2.9 Scratch Assay

A scratch wound assay was used to measure the growth and migration of the HEK293 cells. The cells were seeded in a 48-well plate at a density of  $1.3 \times 10^5$  cells per well and incubated at 37 °C for 24 hours. A linear wound was created in the monolayer with the aid of a sterile pipette tip. The cells were subsequently exposed to concentrations of 15.63, 31.25, 62.5, and 125  $\mu$ g/ml of the CS and CS-Au hydrogels. The width of the scratched region was measured at three distinct sites to observe cell proliferation directly following the scratch and after a period of 24 hours. Images were obtained using a Nikon inverted phase contrast microscope. Wound closure was calculated using Equation 4.9.

$$\text{Wound closure} = \frac{\text{Wound area at day 0} - \text{Wound area at day 1}}{\text{Wound area at day 0}} \times 100\% \quad (4.9)$$

#### 4.2.10 Statistical Analysis

The data has been reported as the mean  $\pm$  standard deviation ( $\pm$  SD, n = 3). The study of FTIR spectra was conducted using the Origin 2019b programme. Statistical analysis of the MTT assay was conducted using one-way ANOVA and Dunnett's post hoc test. The tests were considered statistically significant at  $p < 0.01$  and  $p < 0.05$ . Every experimental value was compared with its corresponding control. The software utilized was Microsoft Excel 2024 and GraphPad Prism 9.

## **CHAPTER FIVE**

### **RESULTS AND DISCUSSION**

## 5.1 Characterization

### 5.1.1 UV-vis Spectroscopy

The CS-Au-hydrogel visually demonstrated the effective reduction of  $\text{HAuCl}_4 \cdot 3\text{H}_2\text{O}$  by transitioning to its characteristic wine-red colour (Figure 5.1). Additionally, the resistance to flow of the hydrogel when inclined indicated mechanical stability and increased viscosity.

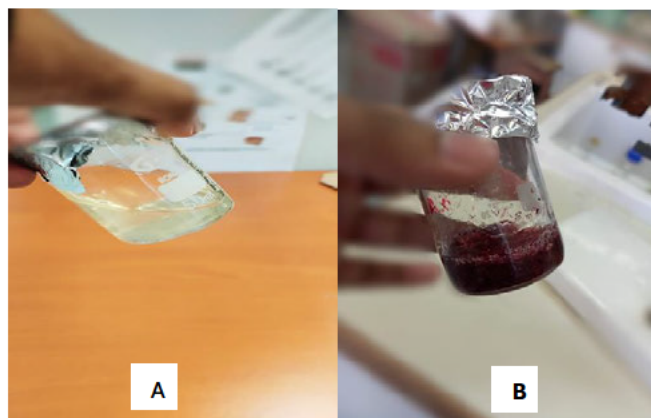


**Figure 5.1:** Images of the formulated (A) CS and (B) CS-Au hydrogels.

Figure 5.2 illustrates the UV-vis spectra for the CS-Au hydrogels after heating for 10 and 20 minutes. The SPR of the AuNPs showed a singular narrow peak at 530 nm, aligning with the predicted  $\lambda_{\text{max}}$  of AuNPs, hence presenting tangible confirmation of the successful synthesis of the AuNPs (Hammami *et al.*, 2021). The peak singularity indicated negligible by-product formation. A significant reduction in absorbance intensity was apparent after a further 10 minutes of heating. As the heating time increased, a greater number of  $\text{AuCl}_4^-$  ions were converted to zerovalent  $\text{Au}^0$  and deposited onto the existing Au domains, leading to the growth and aggregation of these Au domains. NP aggregation diminishes the number of free particles in solution, resulting in a reduction in absorbance intensity as fewer particles transmit to the plasmonic phenomena that facilitate absorbance in UV-vis spectroscopy (Herbani, 2017).

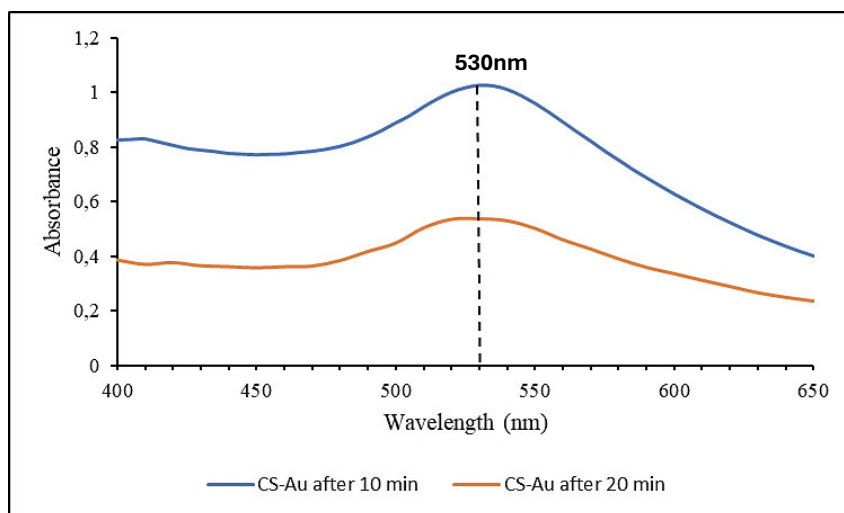


**Figure 5.2:** UV-vis spectroscopy of the CS-Au hydrogel after heating for 10 and 20 minutes.

### 5.1.2 Fourier Transform Infrared (FTIR) Spectroscopy

FTIR is a well-established characterization technique employed to verify the functional groups present in a molecule or, in this case, nanogel or NP. The successful formulation of the CS-Au hydrogel was also corroborated by the FTIR spectra (Figure 5.3) exhibiting corresponding peaks in the AuNPs and CS hydrogel. The emergence of the asymmetrical carboxylate stretching band at  $1557\text{ cm}^{-1}$  confirmed the presence of the AuNPs (Vangari *et al.*, 2024). The pertinent peaks indicated the presence of the foundational CS hydrogel. The peak seen at  $3241\text{ cm}^{-1}$  indicated N-H and O-H stretching, while peaks at  $2916\text{ cm}^{-1}$ ,  $1652\text{ cm}^{-1}$ , and  $1063\text{ cm}^{-1}$  corresponded to C-H symmetric stretching, primary amine N-H bending, and C-O stretching, respectively (Queiroz *et al.*, 2014). In contrast to the standard CS hydrogel, slight peak changes and an enhancement in the strength of the amine peak suggested effective AuNP cross-linking. The characteristic pyrimidine compound peak was visible in the 5-FU spectra at  $1245\text{ cm}^{-1}$ . The vibration of the imide stretch was also observed at  $812\text{ cm}^{-1}$  and  $551\text{ cm}^{-1}$  (Samy *et al.*, 2020). The decrease in strength of the characteristic 5-FU peaks in the CS-Au-5-FU verified the encapsulation of the drug. The peaks indicated a notable alteration in the degree of chemical interactions and corroborated the drug encapsulation.

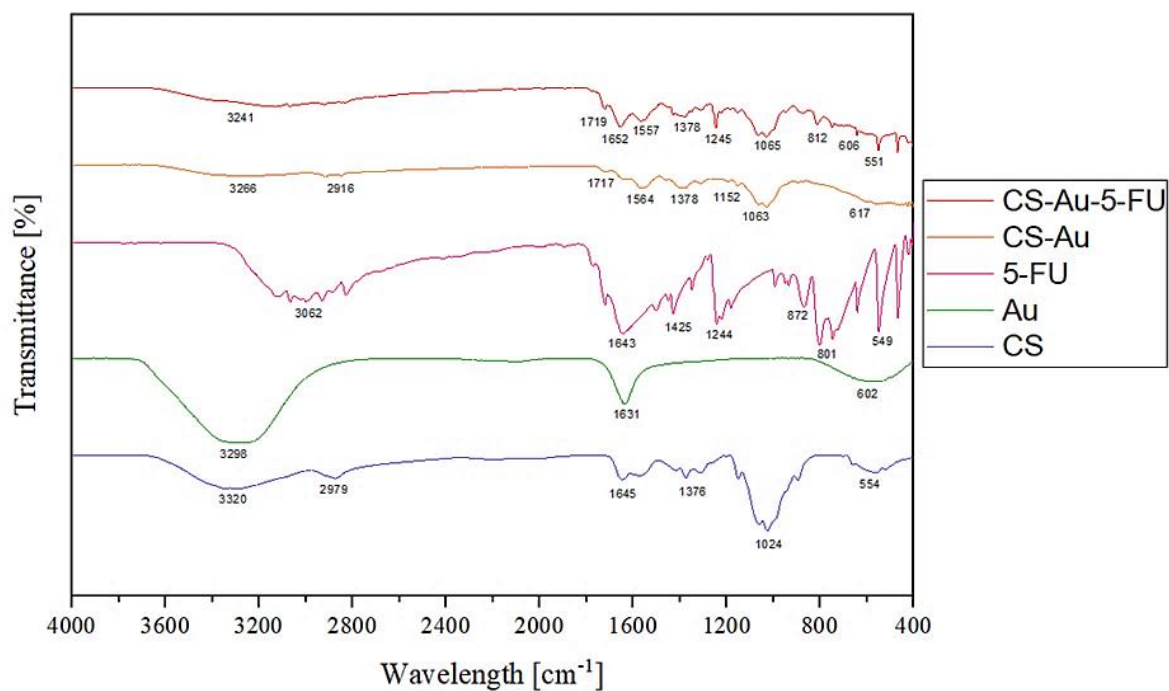


**Figure 5.3:** FTIR spectra of CS, AuNP, 5-FU, CS-Au, and CS-Au-5-FU.

### 5.1.3 Dynamic Light Scattering (DLS)

The zeta potential (ZP) refers to the electrostatic properties of multiagent dispersion systems and assesses the rate of NP agglomeration and aggregation. Consequently, it may indicate the physical stability of the system (Pochapski *et al.*, 2021). The magnitude of the ZP indicates the repulsive interactions between suspended particles and may be employed to predict the affinity of nanogels for cancer cells. NP stability in the context of biological systems poses a significant challenge for the therapeutic application of nanogels due to the high surface area-to-volume ratio (Kamble *et al.*, 2022). Strongly negative or positive ZP values generate significant repulsive forces, thus inhibiting aggregation and facilitating effortless redispersion. A ZP greater than  $\pm 30$  mV is preferred for stability (Souza *et al.*, 2023). The ZPs for the CS-Au and CS-Au-5-FU hydrogels were  $11.1 \pm 0.1$  mV and  $15.87 \pm 1.18$  mV (Table 5.1), respectively, indicating that both hydrogels may offer some short-term stability. CS can act as a high molecular weight stabilizer through steric stabilization. Therefore, values that approximate around  $\pm 20$  mV or lower can provide sufficient stabilization. Large polymers may shift the plane of shear further from the particle surface, thus reducing the ZP. Hence, these particles may, in fact, exhibit a high charge and stability but record a low ZP (Honary and Zahir, 2013). Furthermore, owing to the presence of protonated amino groups, CS yields a positive ZP. The

positive charge may enhance drug delivery due to the electrostatic interaction between negatively charged cancer cells and the positively charged hydrogels.

**Table 5.1:** The zeta potential values of the CS-Au and CS-Au-5-FU hydrogels.

| Nanoparticle hydrogel | Zeta potential (mV) |
|-----------------------|---------------------|
| CS-Au                 | +11.1 ± 0.1         |
| CS-Au-5-FU            | +15.87 ± 1.18       |

#### 5.1.4 Transmission Electron Microscopy (TEM)

TEM utilizes a beam of electrons to examine the homogeneity, ultrastructural morphology, and dispersion of NPs. By virtue of its dense core, the noble metal gold scatters the electron beam from the TEM and appears as black spheres on a bright background. Cellular uptake and drug release directly correspond to the dimensions of the NPs, offering a glimpse at the potential effectiveness of the CS-Au hydrogel. The TEM images of the CS-Au hydrogels (Figure 5.4) exhibited a smooth spherical morphology characterized by a consistent size and shape distribution, with a diameter of approximately 89.31 nm. It has been demonstrated that NPs with a diameter of less than 10 nm are typically expeditiously excreted by the kidneys, but those over 200 nm may trigger the complement system via foreign body clearance mechanisms (Mitchell *et al.*, 2021). The diameters of the NPs observed by TEM (Figure 5.4 A) ranged from 10 to 200 nm, rendering them appropriate for drug delivery as they can penetrate certain biological barriers and avoid clearance. Figure 5.4B illustrates the physical crosslinking matrix of the AuNPs, which underpins enhanced mechanical stability and rigidity. The NPs exhibited a dendrimer-like morphology emanating from the attractive forces among the NPs within the gel matrix that facilitate their movement, agglomeration, and crystal formation (Sámano-Valencia *et al.*, 2014). This was further substantiated by the low ZP values (Table 5.1).

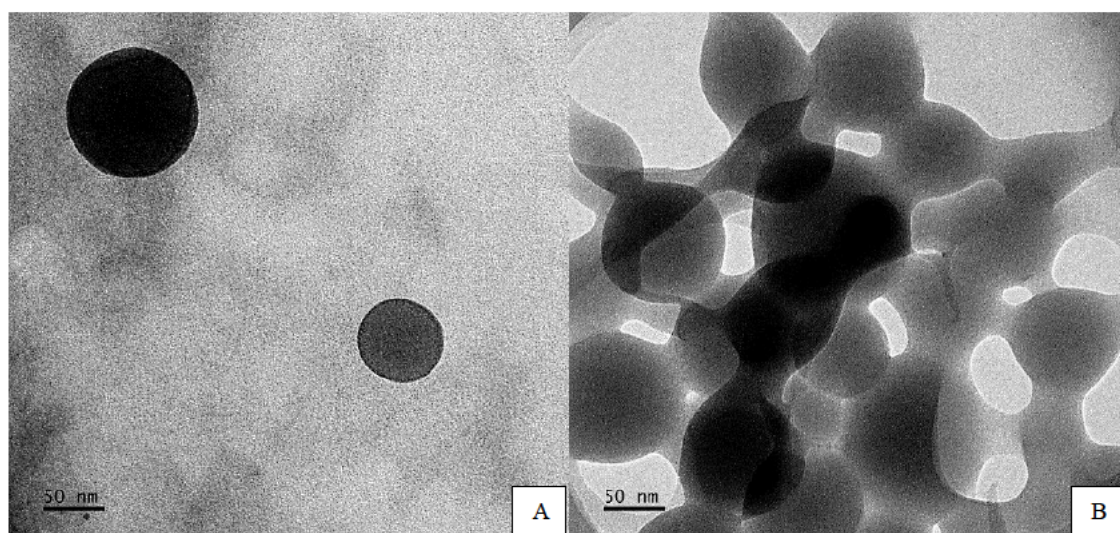


**Figure 5.4:** TEM images of the CS-Au hydrogel exhibiting a (A) spherical morphology and (B) a crosslinking matrix. Scale bar = 50 nm.

The cross-linking matrix affects the capacity for swelling and the viscosity of the hydrogel. Its dense structure may influence the mechanical properties, encapsulation efficiency and applications in drug delivery. In terms of wound healing, the enhanced rigidity resulting from the cross-linking matrix facilitates durability in dynamic wound surface applications. Upholding structural integrity is essential in ensuring the efficacy of the hydrogel throughout the wound-healing process. The observed aggregation indicated by the darker areas, however, may diminish the efficacy of the hydrogel by constraining its accessible surface area for engagement with bacteria, among other components that may compose the wound site.

### 5.1.5 Scanning Electron Microscopy (SEM)

The morphological characteristics of the CS and CS-Au hydrogels were also observed by SEM (Figure 5.5). SEM illustrated the porosity and properties of the hydrogel framework. In addition, the influence of cross-linking on pore size was revealed (Figure 5.5.B). The freeze-dried CS (Figure 5.5A) and CS-Au (Figure 5.5B) hydrogels were analyzed for surface and cross-sectional morphology, revealing a porous matrix with an interconnected channel-like framework. The pore sizes were irregular, ranging from 5 to 20  $\mu\text{m}$  for both hydrogels. However, it is noticeable that the CS-Au hydrogel exhibits smaller yet more structured pore sizes. The cross-linking of the CS-Au hydrogel creates a more tightly packed network, and reduction in pore size. Due to their internalization into the hydrogel matrices, AuNPs are not visible on the hydrogel surfaces in the SEM images. The interconnected pores enabled the

freeze-dried hydrogels to undergo significant swelling, as these channel-like structures facilitate water absorption in the gel matrix by capillary movement, resulting in rapid solvent transport in the matrix.

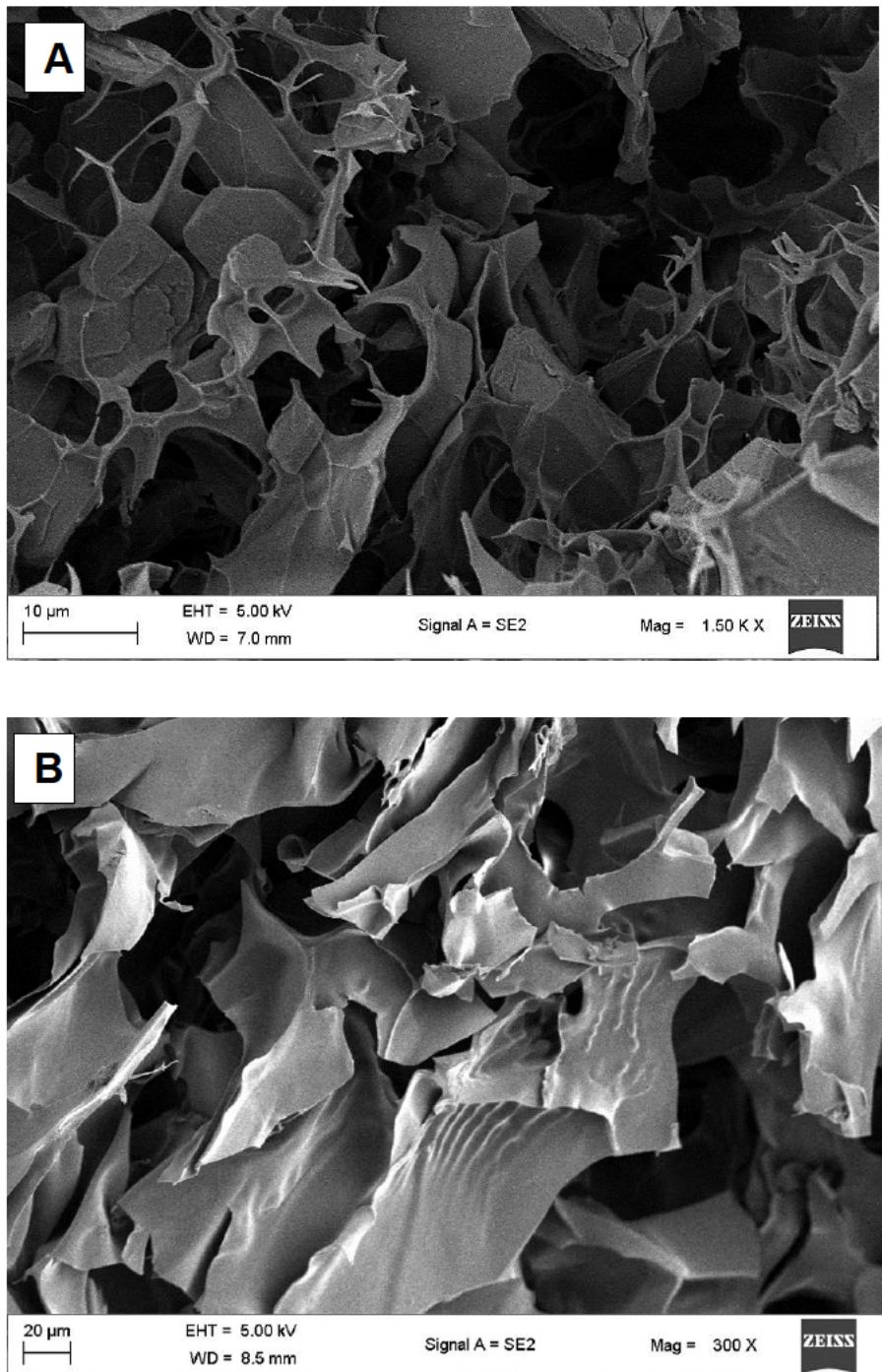


**Figure 5.5:** SEM images depicting the structural morphology of the (A) CS and (B) CS-Au hydrogels. Scale bar =10 µm (A) and 20 µm (B).

Morphological characterization explicates the diverse physical features of hydrogels, including their hydrophilicity, rigidity, and swelling behaviour. The inconsistency in pore size and distribution is a feature of employing a pure CS hydrogel, while uniformity can be addressed in future research through the integration of polymers such as polyacrylamide (Rahman *et al.*, 2019). The porosity of the hydrogels provides the foundational attributes for adequate drug encapsulation and release. The network of interlinked pores also mimics the extracellular matrix, establishing a scaffold for tissue restoration. Furthermore, the porous structure may also facilitate enhanced oxygen exchange and fluid regulation, essential for sustaining the optimal wound environment (Wang *et al.*, 2023).

### 5.1.6 Thermogravimetric Analysis (TGA)

TGA is often used to assess the thermal stability of hydrogels. Sample mass fluctuations are monitored in relation to temperature, rising at a constant rate of 1–10 °C/min. The initial stage of mass loss is identified by a reduction in weight below 100 °C. The weight loss percentages for the CS (Figure 5.6 A) and CS-Au (Figure 5.6 B) hydrogels were 39.95% and 32.94%, respectively. This phase typically entails the evaporation of water and other chemically unstable substances adsorbed on the hydrogel surface. In the CS hydrogels, this refers to the loss of water absorbed from the polysaccharide framework, which comprises hydrophilic hydroxyl and amino groups. The CS-Au hydrogels exhibited a reduced weight loss, attributable to the enhanced stability conferred by their cross-linked structure. Furthermore, the water content in the CS hydrogel is influenced by the quantity and nature of ionic groups within the material (Sámano-Valencia *et al.*, 2014). These ionic sites (hydroxyl and amino) are partially occupied by the AuNPs. Hence, the CS-Au hydrogel exhibited decreased weight loss compared to the CS hydrogel due to fewer ionic functional groups, leading to a reduction in absorbed water.

At 37 °C, the weight percentages were 99.45% for the CS and 99.54% for the CS-Au hydrogel. A sustained and regulated drug release could, therefore, be facilitated by the thermal stability at physiological temperature. With regards to wound healing, the hydrogel can be applied for wound closure as it does not significantly degrade in terms of structure and functionality at body temperature.

The subsequent phase is the decomposition stage (100–600 °C), during which the predominant weight loss results from the degradation of the CS polymer framework. The decomposition of CS entails the disintegration of glycosidic bonds, which significantly contributes to weight

reduction. The electrostatic interactions between the CS and AuNPs were disrupted, resulting in an impairment in thermal stability. Both the CS and CS-Au hydrogels exhibited rapid weight loss, retaining mere residues post-heating.

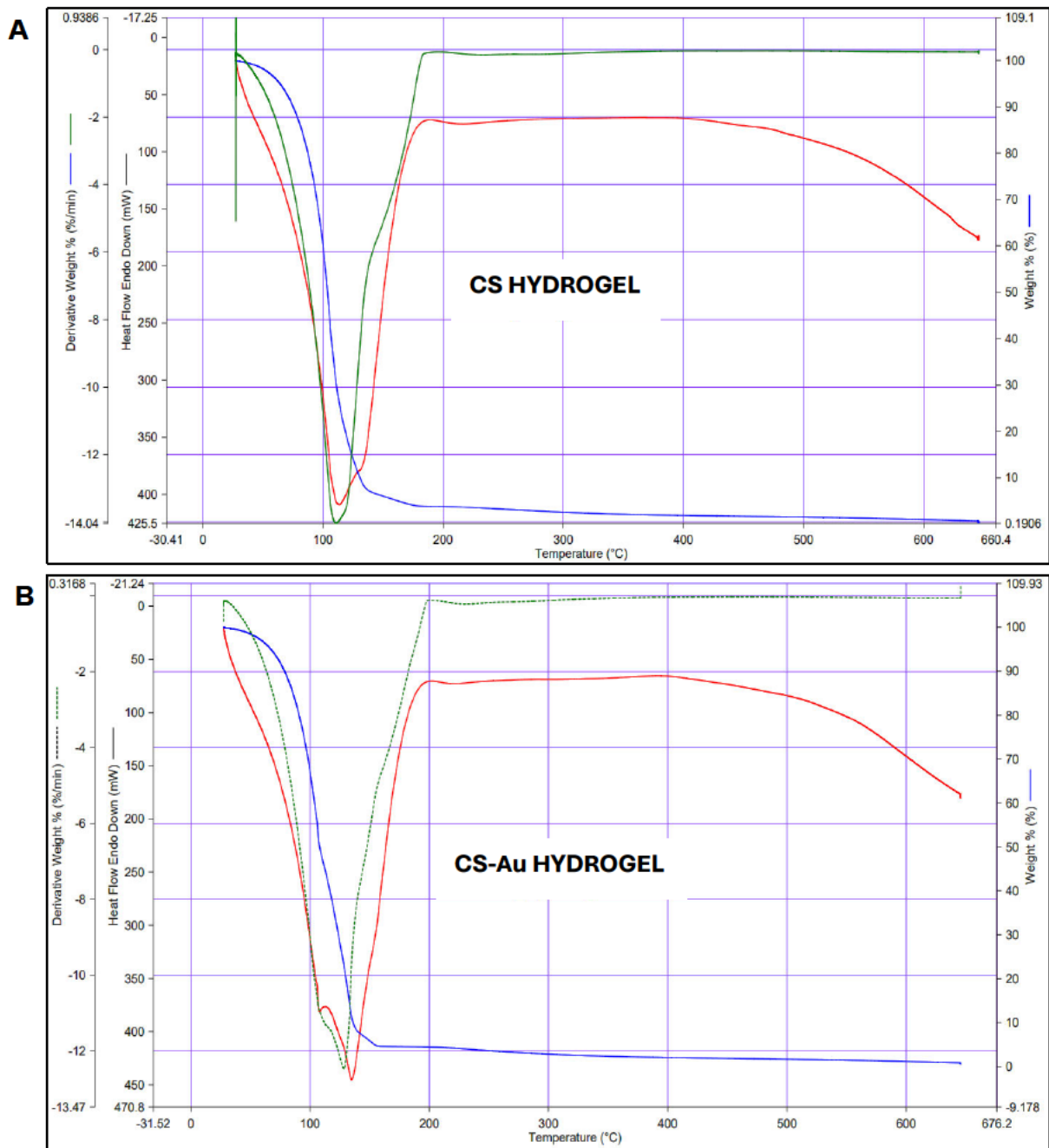


**Figure 5.6:** Thermogravimetric analysis of the (A) CS and (B) CS-Au hydrogels.

Stability is further evidenced by the temperature of the endothermic peak. The CS hydrogel has an endothermic peak at 113.61 °C, whereas the CS-Au demonstrates an endothermic peak

at 134.82 °C. These findings are consistent with a published study for a CS gel incorporating AuNPs (Sámano-Valencia *et al.*, 2014). Therefore, the incorporation of AuNPs into a CS gel enhances thermal stability relative to hydrogels devoid of NPs.

### 5.1.7 Rheological studies

Rheology is the preferred approach for characterizing the dynamic and static viscoelastic behaviour of hydrogels. Flow curves (stationary shear flow) delineate the rheological characteristics of the hydrogel, notably the relationship between viscosity and the applied shear rate. The biomedical application of hydrogels necessitates the ability to exhibit shear-thinning behaviour and rapid self-healing capabilities post-injection. Consequently, the incorporation of physical cross-links through electrostatic interactions between the CS and the AuNPs is essential for transient deformation to facilitate injectability. Shear-thinning (pseudoplastic) hydrogels are regarded as injectable matrices that develop via reversible physical interactions under mild conditions and demonstrate a reduction in viscosity with an increase in shear rate (Jalalvandi and Shavandi, 2019). Both the CS (Figure 5.6 A) and CS-Au (Figure 5.6 B) hydrogels exhibited shear-thinning activity. Over a shear rate of 0.1 to 100 (1/s), the CS and CS-Au hydrogels showed a decrease in viscosity of  $3.124 \times 10^4$  mPa/s to 3498 mPa/s and  $2.097 \times 10^5$  mPa/s to 4030 mPa/s, respectively. As a result, these hydrogels exhibit enhanced deformability through needles and catheters, facilitating the *in vivo* delivery of drugs by injection. The disparity in the initial viscosities of the hydrogels arises from the AuNP crosslinking matrix in the CS-Au hydrogel, which increases the initial viscosity and enhances rigidity. The shear thinning property of the synthesized hydrogels facilitates their flow into fissures and close conformation to the wound bed, thereby enabling full coverage and treatment of the entire surface (Tan *et al.*, 2024). This also reduces mechanical damage to sensitive, regenerating tissues following application or patient movement. By minimizing the possibility of disrupting new tissue, this subtle contact with the wound site helps to promote rapid and less painful healing.

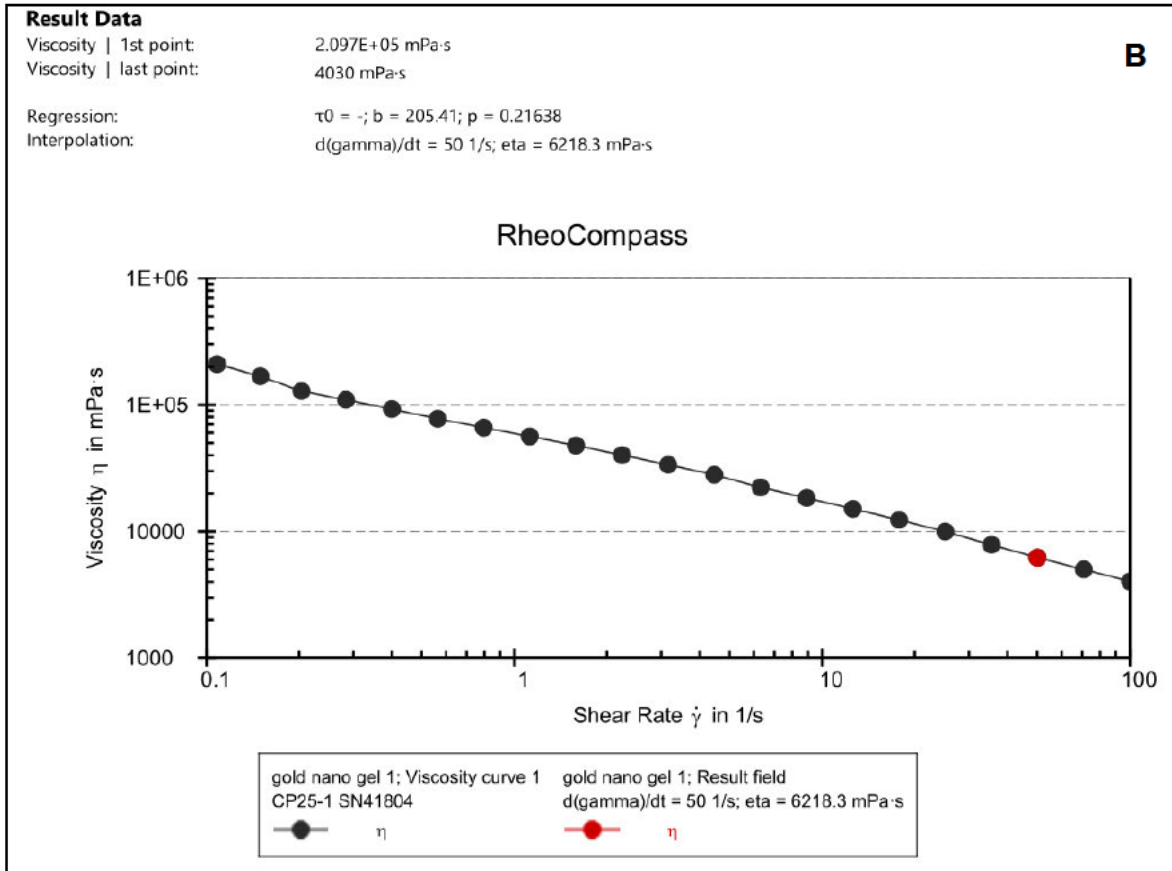
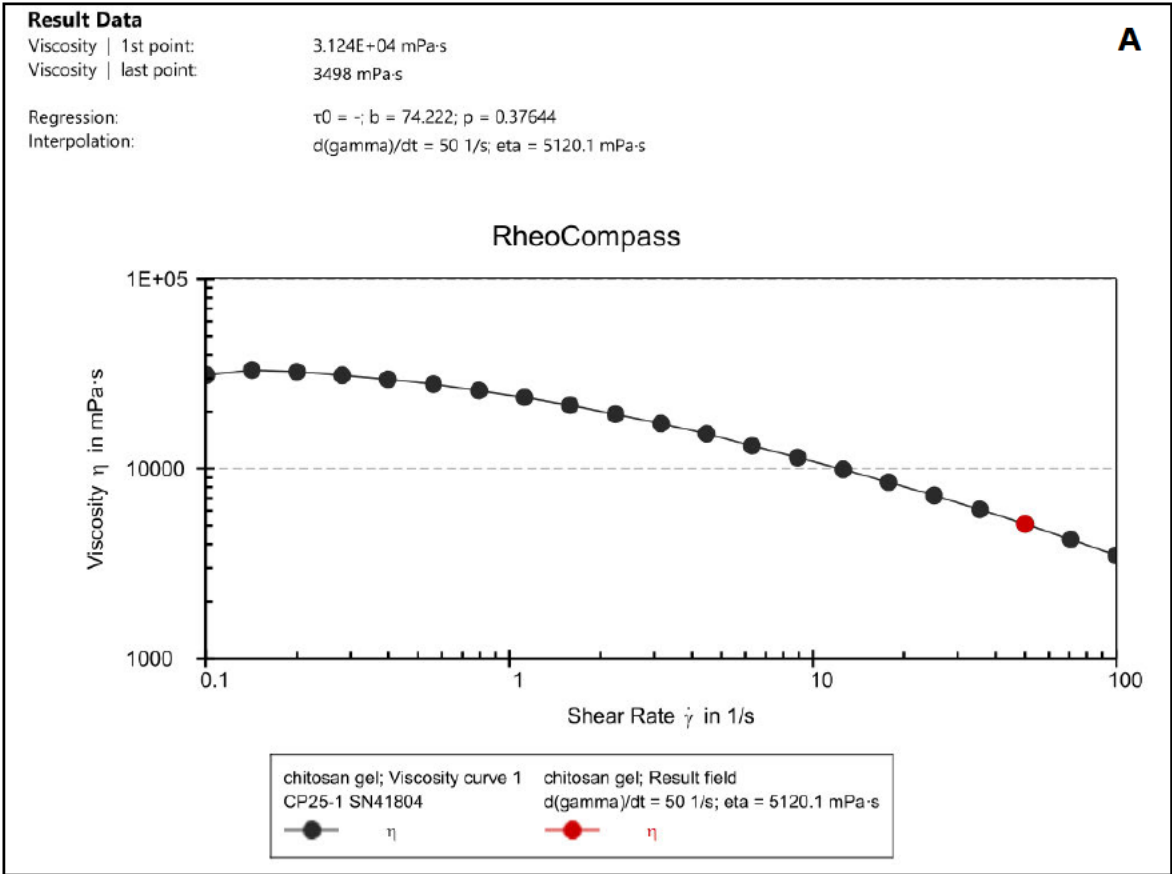


**Figure 5.7:** Flow curves depicting viscosity vs shear rate of the (A) CS and (B) CS-Au hydrogels.

The thixotropic effect on the CS and CS-Au hydrogels is illustrated in Figure 5.8. Thixotropy is the ability of specific fluids and hydrogels to decrease in viscosity when subjected to constant shear and then return to their initial viscosity once the force is removed within an appropriate timeframe (self-healing). Both the CS and CS-Au hydrogels demonstrated self-healing properties. The relative viscosities of the CS and CS-Au hydrogels prior to shear application were  $2.396 \times 10^4$  mPa/s (Figure 5.8 A) and  $5.597 \times 10^4$  mPa/s (Figure 5.8 B), respectively. Shear force was applied between 60 and 65 seconds, resulting in a viscosity reduction measured at 3543 mPa/s for the CS hydrogel and 4898.7 mPa/s for the CS-Au hydrogel. Following shear stress, a viscosity recovery of  $2.358 \times 10^4$  mPa/s and  $5.518 \times 10^4$  mPa/s was observed within 30 seconds for the CS and CS-Au hydrogels, respectively. The recovery in viscosity of the hydrogels indicates a self-healing property following injection. The synthesized CS-Au hydrogel retains its shear-thinning and self-healing characteristics, which can be attributed to its CS hydrogel precursor. This is due to the relatively weak electrostatic interactions between the CS and the AuNPs (Xing *et al.*, 2016). The reversion to a solid gel is clinically essential, as the integrated 5-FU can be administered to the site of injection and remain localized as the hydrogel regenerates. The self-healing capability in wound healing permits reapplication or modification of the hydrogel without undermining its efficacy. It also enhances the long-term durability of the dressing, decreasing the necessity for frequent replacements and thereby minimizing disruption to the wound.

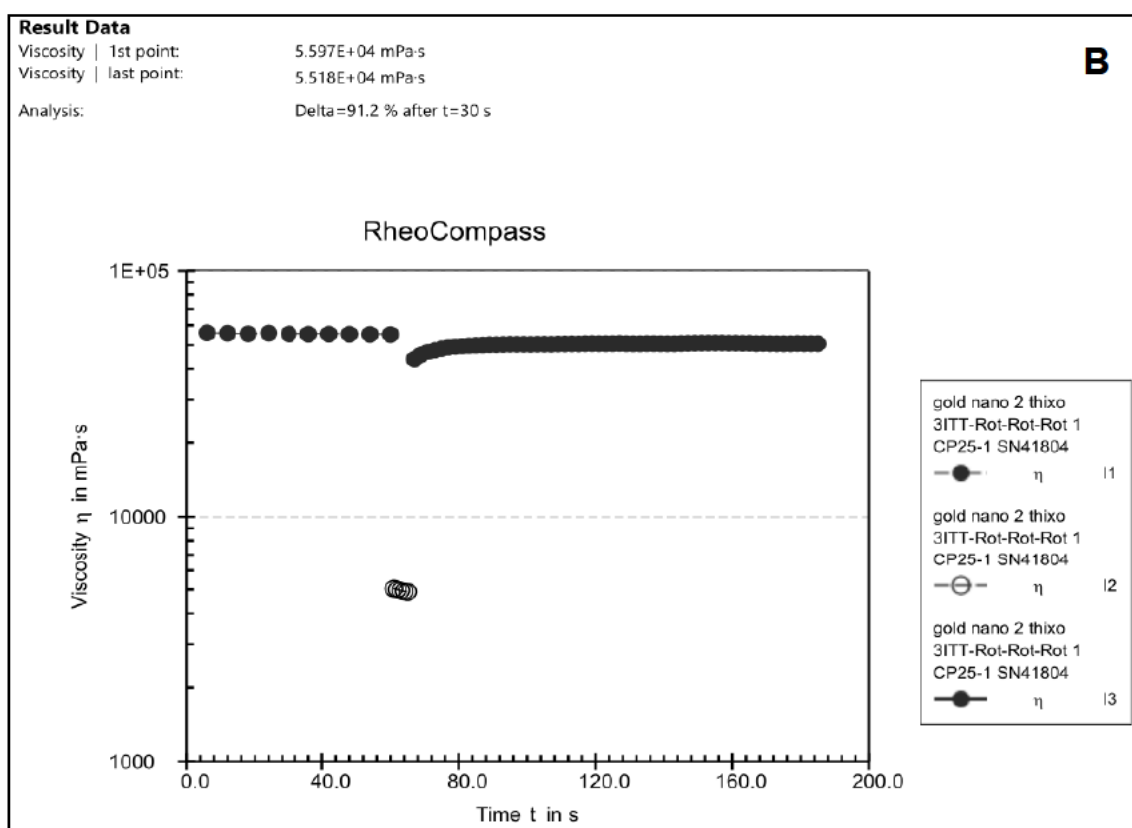
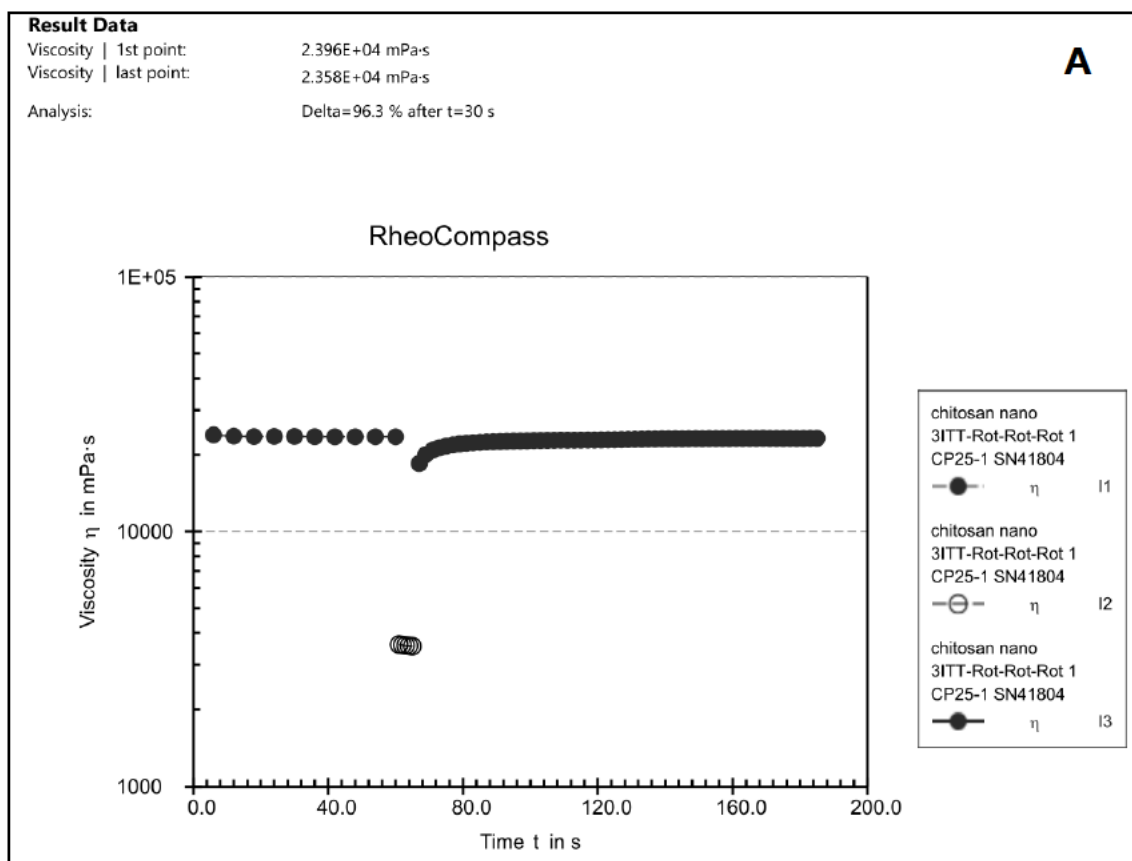


**Figure 5.8:** Thixotropy study demonstrating self-healing for the (A) CS and (B) CS-Au hydrogels.

## 5.2 Re-swelling and pH sensitivity

The swelling capacity of the CS-Au hydrogel was assessed using the equilibrium swelling (SR) ratio in distilled water at room temperature. The study was conducted at pH 4.5, 7.4, and 10.5 to evaluate the pH sensitivity of the hydrogel with respect to its expansion and water absorption when submerged in various pH solutions. During the re-swelling process, water molecules infiltrated the hydrogel, inducing the hydrogel network to expand due to the hydration and unwinding of the CS chains. After 20 min, rapid pH-dependent water uptake was observed for the freeze-dried CS-Au hydrogel in the different pH solutions as the swelling ratios were recorded to be 357.16, 318.57 and 259.1% at pH 4.5, 7.4, and 10.5, respectively (Figure 5.9). Equilibrium was reached after 1 hour, with the swelling ratios recorded as 439.93, 388.23, and 325.87% at pH 4.5, 7.4, and 10.5, respectively. The rapid re-swelling rate of the CS-Au hydrogel can be primarily attributed to its porous interconnecting framework, which offers numerous pathways for the diffusion of water molecules. This extensive swelling further substantiates the morphological analysis. The swelling maxima recorded for the CS-Au hydrogels were 450.77, 409.07, and 340.83% at pH 4.5, 7.4, and 10.5, respectively. The reversible water absorption capacity demonstrated that the CS-Au hydrogel possessed substantial mechanical strength and stability in aqueous solutions. Furthermore, CS exhibited considerable hydrophilicity, which significantly increased the water absorbency of the hydrogel (Michalik and Wandzik, 2020).

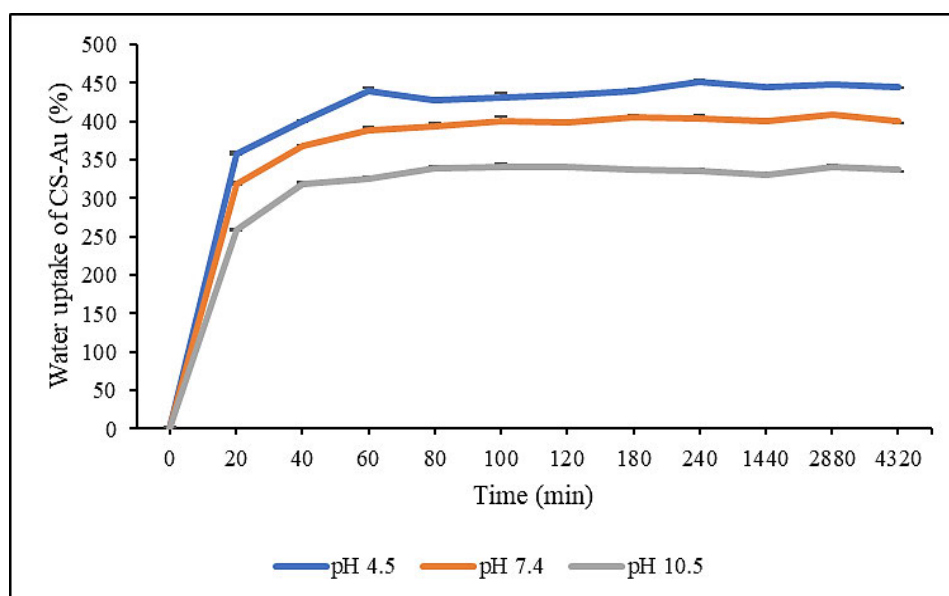


**Figure 5.9:** Re-swelling and pH sensitivity studies of the CS-Au hydrogel at pH 4.5, 7.4, and 10.5. Triplicates of each hydrogel were analyzed (n=3), and each point represents the mean value  $\pm$  standard deviation.

The CS-Au hydrogel displayed notable pH dependence, with markedly enhanced water absorption in acidic solutions relative to basic solutions and at physiological pH (Figure 5.9). This results from the protonation of the amino functional groups in the CS chains, leading to an increase in the mesh size of the cross-linking network. Protonation enhanced the hydrophilic capability of the CS polymer, thus increasing its tendency for interaction with water molecules and resulting in greater swelling. The protonation of amino groups also results in an increase of positive charges along the polymer chains. The repulsion among these positive charges induces the polymer chains to broaden, culminating in the widening of hydrogel pores, which enhances water absorption and results in increased swelling (Shikuku *et al.*, 2024). At neutral or basic pH, amino groups are deprotonated, resulting in reduced swelling.

The pH sensitivity and elevated water absorption are promising for subsequent drug release investigations, as the enhanced water influx and pore expansion at acidic pH may facilitate more efficient diffusion of 5-FU in an acidic cancer microenvironment than at physiological pH (healthy cells) (Shikuku *et al.*, 2024). With regards to wound healing, significant amounts of wound exudate may also be absorbed by the hydrogel due to its high swelling capacity, which also performs a function in the maintenance of moisture. This moisture is critically important for facilitating cell growth and migration, which are crucial for wound healing. A moist wound environment further promotes healing by minimizing tissue dehydration and scab formation, which can obstruct the healing process. Wound exudate management also inhibits bacterial proliferation and infection, which is paramount in preventing the stagnation of the healing process (Ribeiro *et al.*, 2024).

### **5.3 Drug encapsulation**

The concentration of 5-FU in the solvent following immersion of the freeze-dried CS-Au hydrogel was analyzed to determine the encapsulation efficiency of 5-FU. The 5-FU encapsulation efficiency (EE) was evaluated using UV-vis spectroscopy. A favourable EE of 77,71% for the CS-Au hydrogel was achieved. Despite adequacy, augmentation may require an adjustment of the crosslinking density. Reducing density will enhance the porosity and subsequent swelling of the hydrogel, hence increasing drug uptake (Raina *et al.*, 2022). A decrease in the size of AuNPs and aggregation can contribute to a reduction in density and an improvement in drug absorption.

#### 5.4 *In vitro* degradation

The *in vitro* degradation was assessed by measuring the loss of mass of the hydrogels over time in a simulated physiological environment. Lysozyme is present in several tissues and fluids in the human body. Blood serum and wound exudates contain lysozyme at concentrations around 1.5  $\mu\text{g/ml}$ , which breaks down hydrogels used in drug delivery and as wound dressings during the healing process (Moura *et al.*, 2017). Lysozyme was incorporated into a PBS solution to simulate the *in vivo* degradation capabilities. Figure 5.10 showed that both CS hydrogels (cross-linked with AuNPs and encapsulated with 5-FU) exhibited enzymatic breakdown by lysozyme, and comparable weight loss profiles were observed. The standard CS-Au hydrogel showed a slightly slower degradation rate compared to the CS-Au-5-FU hydrogel. The CS-Au-5-FU and CS-Au hydrogel both displayed consistent gradual degradation. However, both hydrogels lost their structural integrity on day 20 and day 24, respectively.

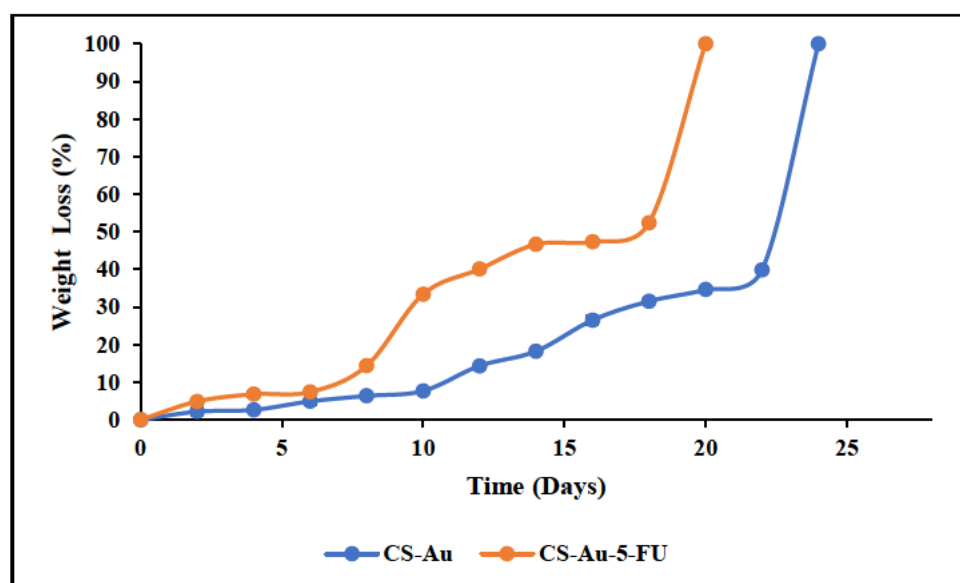


**Figure 5.10:** Comparison of the weight loss of the CS-Au and CS-Au-5-FU hydrogels as a function of incubation time in PBS containing 1.5  $\mu\text{g}$  of lysozyme/ $\text{cm}^3$ , at 37  $^{\circ}\text{C}$ . Triplicates of each hydrogel were analyzed ( $n=3$ ), and each point represents the mean value  $\pm$  standard deviation. Standard deviations were very low and negligible.

According to the morphological analysis, the hydrogels displayed a porous interconnecting network, which is vital for the facilitation of enzyme transport and degradation products that are crucial for tissue repair. The degree of deacetylation of the CS (75%) allows for the action of the lysozyme due to its complexation with the acetyl groups (Lončarević *et al.*, 2017). Lysozyme primarily targets the glycosidic linkages in CS, which are characterized by  $\beta$  (1 $\rightarrow$ 4) links between the glucosamine units. Upon interaction with the hydrogel, lysozyme catalyzes

the hydrolysis of these bonds, resulting in the degradation of CS into glucosamine units, which are then more readily metabolized or expelled by the body (Lončarević *et al.*, 2017). Among the essential requirements of hydrogels such as biocompatibility and high porosity, biodegradation at the rate of new tissue formation is essential. Lysozyme-facilitated degradation is advantageous as the resultant byproducts (glucosamine) may enhance the regeneration and repair of tissues (Anushree *et al.*, 2023). Biodegradation also guarantees that the hydrogel does not require surgical removal following drug delivery, as it will disintegrate naturally over time. The disparity in degradation rates is not significant; nevertheless, the accelerated breakdown of the CS-Au-5-FU hydrogel may be attributed to the encapsulation of 5-FU. 5-FU has been noted for its ionic complexation with CS chains (Ullah *et al.*, 2022). This binding may potentially lower the stability of the cross-linking network that is stabilized by ionic bonding, thereby compromising its internal structure. However, further studies are required to fully understand this mechanism.

### 5.5 Drug Release

The pH-responsive behaviour of the CS-Au-5-FU hydrogel in simulated *in vivo* conditions was evaluated by generating a drug release profile at pH 4.5, 6.5, and 7.4 (Figure 5.11). Cancer tissue presents with a mildly acidic microenvironment (pH 4.0–5.5); thus, these parameters were chosen to simulate the acidic cancer and near-neutral physiological environment. As seen in Figure 5.11, CS-Au-5-FU exhibited an initial release of 5-FU over 4 hours across all incubation media, ranging from 19% to 25%. The initial quick-release, termed the "burst effect," occurred due to quantities of 5-FU being localized on the hydrogel surface via adsorption, allowing for rapid release through diffusion (Peers *et al.*, 2020). Subsequent to this initial burst, a sustained and controlled release transpired at all pH values during the incubation period. The release of 5-FU at pH 4.5 exhibited a biphasic pattern, with a secondary burst occurring after 44 hours. Throughout the 48-hour period, 60.21% of 5-FU was released at pH 4.5, 39.04% at pH 6.5, and 33.41% at pH 7.4, respectively (Figure 5.11).

The diffusion of proteins, NPs, or drugs within hydrogels is contingent upon the pores formed by the crosslinking of polymer chains (Raghuwanshi and Garnier, 2019). Morphological studies demonstrated that the interconnected porous network facilitates the dispersion of 5-FU. The hydrogel mesh size (local cross-linked structure) is significantly influenced by pH and ionic strength due to the protonation or deprotonation of CS, as evidenced in the reswelling and pH sensitivity assay. Consequently, at acidic pH, the relaxation and protonation of the CS

polymer chains result in an enlargement of the pore size within the cross-linking matrix, subsequently enhancing swelling and accelerating diffusion (Raghuwanshi and Garnier, 2019).

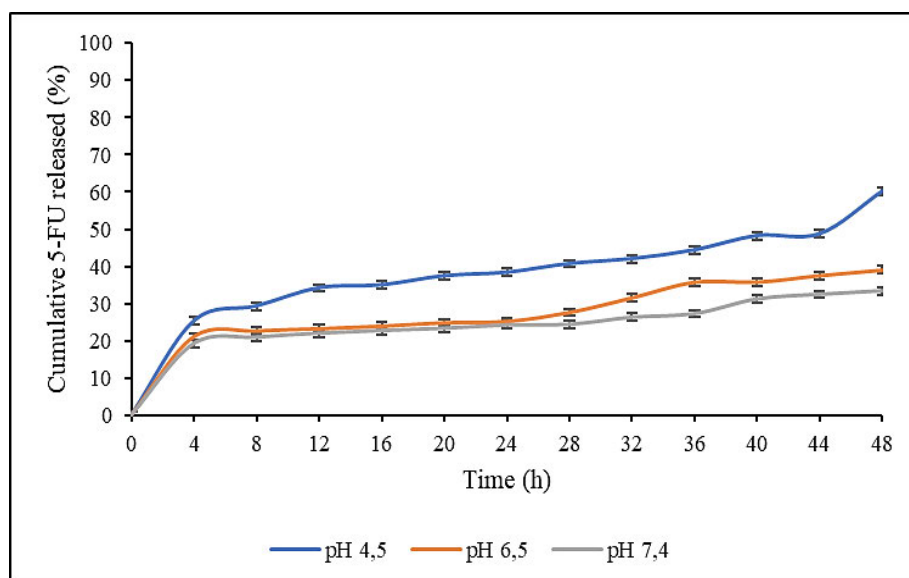


**Figure 5.11:** *In vitro* drug release profile of 5-FU from the CS-Au-5-FU hydrogel at pH 4.5, 6.5, and 7.4, at 37 °C. Triplicates of each hydrogel were analyzed, and each point represents the mean value  $\pm$  standard deviation (n=3).

From Figure 5.12 it can be seen that the hydrogels at acidic pH have significantly swelled; however, at pH 7.4, diminished expansion was noted. The drug release patterns of the hydrogel at the various pH levels displayed labile behaviour, establishing that the release of 5-FU from the porous matrix was mostly regulated by the pH. This pH sensitivity would enable the drug to be released more effectively at the acidic tumour target sites. As a reduced amount of drug (33.41%) was released at physiological pH, the hydrogel, therefore, offers promise for therapy by reducing cytotoxicity in healthy cells

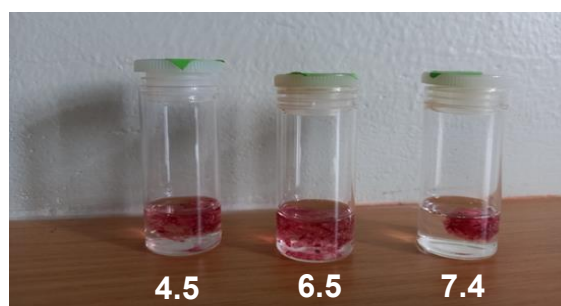


**Figure 5.12:** Image illustrating the expansion of the CS-Au-5-FU at pH 4.5, 6.5, and 7.4.

This study demonstrates a sustained drug release pattern, which allows for the continuous exposure of anticancer agents to the cancer tissue. Continuous release is essential for minimizing large dosage regimens, which represent a significant disadvantage in drug administration (Pillai *et al.*, 2023). A diminished release at a neutral pH is advantageous for minimizing damage to healthy tissue and its associated negative effects. Furthermore, the prolonged release profile holds promise for future wound healing strategies that involve the delivery of antibacterial or anti-inflammatory drugs, as it can reduce the need for reapplication and improve the durability of each individual therapy.

### 5.5.1 Drug Release Kinetics

The objective of a drug release system is to sustain the quantity of the therapeutic in the bloodstream or target tissues at the desired level for an extended period, regulating the rate and duration of its release. A controlled-release device can initially discharge a portion of the dose to swiftly achieve the effective therapeutic dosage of the drug (burst release). Well-defined drug release kinetics can help to ensure the maintenance of an efficient drug concentration level (Mehrotra and Pathak, 2024). Hence, the CS-Au-5-FU hydrogel may be deemed a suitable drug delivery system in accordance with the release profile demonstrated in Figure 5.11. The drug release rate of a polymer-based delivery system is affected by variables, including diffusion, swelling, erosion, and the surrounding environment (Akinyelu and Singh, 2019). The *in vitro* drug release data were analyzed using three kinetic models (zero order, first order, and Korsmeyer-Peppas) to clarify the drug release process. The kinetic assessment of drug release (Table 5.2) suggested that the predominant release mechanism across all pH levels was via the Korsmeyer-Peppas model. This model was designed primarily for the release of drugs from a mesh of polymer chains such as a hydrogel (Fu and Kao, 2010). The Korsmeyer-Peppas model generalizes the drug delivery mechanism via the release exponent "n," where  $n \leq 0.5$  indicates Fickian diffusion,  $n > 1$  signifies non-Fickian diffusion, and  $0.5 < n < 1$  represents anomalous diffusion (Salome Amarachi *et al.*, 2023). According to Table 5.2, all values of "n" are below 0.5, suggesting that the release mechanism adhered to the principle of Fickian diffusion. In the Fickian model, the rate of solvent transport or diffusion considerably exceeds the rate of the relaxation of polymer chains. In the swollen state, polymer chains exhibit significant mobility, facilitating solvent penetration. The equilibrium of absorption on the exposed surface of the polymeric system occurs swiftly, resulting in linear time-dependent release conditions (Talevi and Ruiz, 2021). The kinetics are defined by diffusivity, facilitating more predictable and

regulated drug distribution. This allows for the design of systems that provide a consistent release of drugs over time.

**Table 5.2:** Kinetic parameters at pH 4.5, 6.5, and 7.4, where  $(r)^2$  is the coefficient and  $n^{(a)}$  is the Korsmeier-Peppas release exponent.

| pH  | Zero $(r)^2$ | First $(r)^2$ | Korsmeier-Peppas $(r)^2$ | $n^{(a)}$ |
|-----|--------------|---------------|--------------------------|-----------|
| 4.5 | 0,9314       | 0,8854        | 0,9959                   | 0,2797    |
| 6.5 | 0,9384       | 0,9308        | 0,9671                   | 0,3168    |
| 7.4 | 0,9428       | 0,9329        | 0,9759                   | 0,2442    |

### 5.6 *In vitro* cytotoxicity

The cytotoxic effects of the CS, CS-Au, CS-Au-5-FU hydrogels, and free 5-FU on two cancer (HeLa and MCF-7) and one non-cancer (HEK293) cell line were examined using the quantitative, colorimetric MTT assay. The fundamental principle posits that only metabolically active cells can sustain their mitochondrial enzyme function and convert the water-soluble, yellow tetrazolium salt into insoluble, purple formazan products by its dehydrogenase enzymes (Riss *et al.*, 2016). The cytotoxicity profiles of the CS, CS-Au, CS-Au-5-FU hydrogels, and free 5-FU determined at various concentrations can be seen in Figures 5.13–5.15.

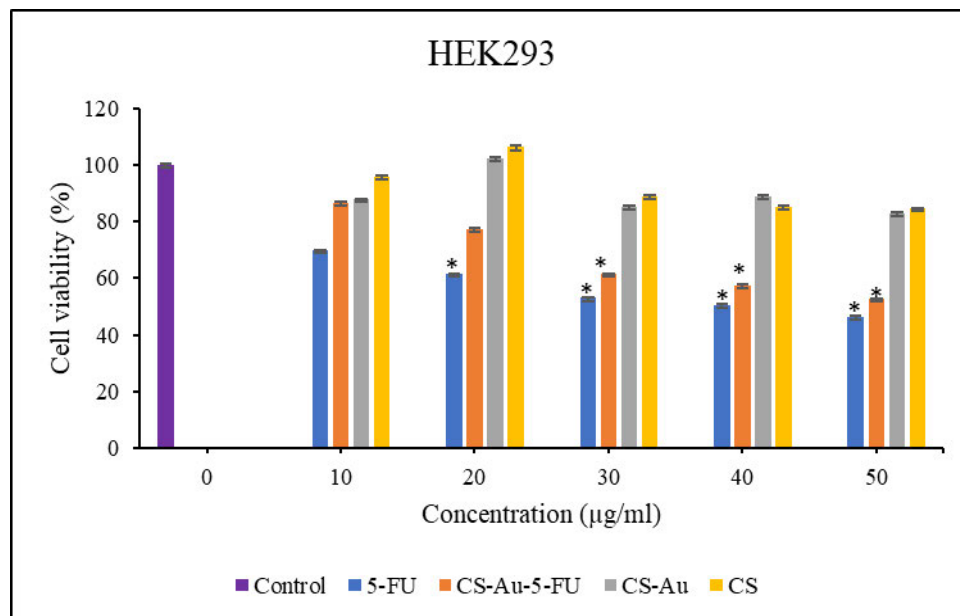


**Figure 5.13:** MTT cytotoxicity of the free 5-FU, CS-Au-5-FU, CS-Au, and CS hydrogels in HEK293 cells. Data are represented as means  $\pm$  SD ( $n=3$ ). \*  $p < 0.05$ , \*\*  $p < 0.01$  were considered statistically significant.

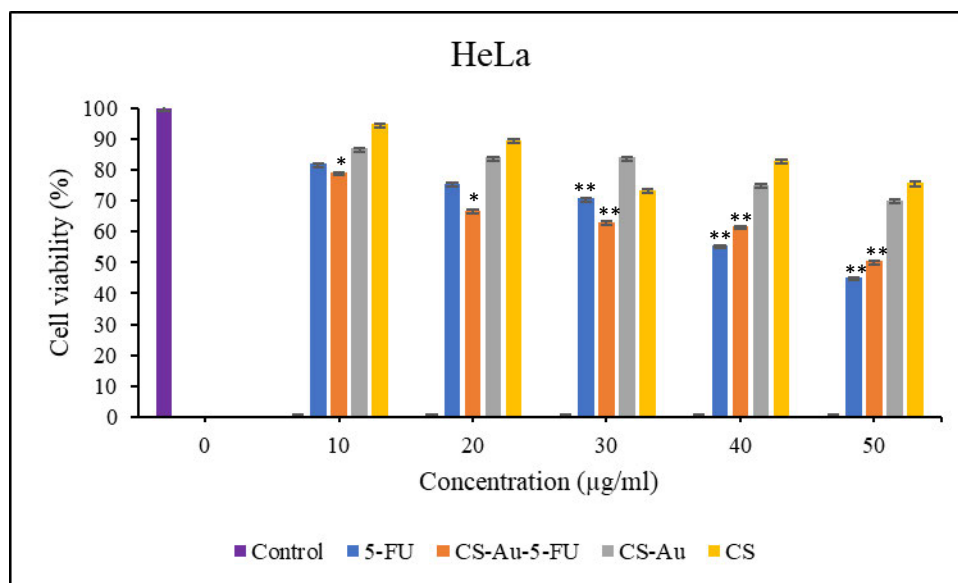


**Figure 5.14:** MTT cytotoxicity of the free 5-FU, CS-Au-5-FU, CS-Au, and CS hydrogels in the HeLa cells. Data are represented as means  $\pm$  SD (n=3). \*  $p < 0.05$ , \*\*  $p < 0.01$  were considered statistically significant.

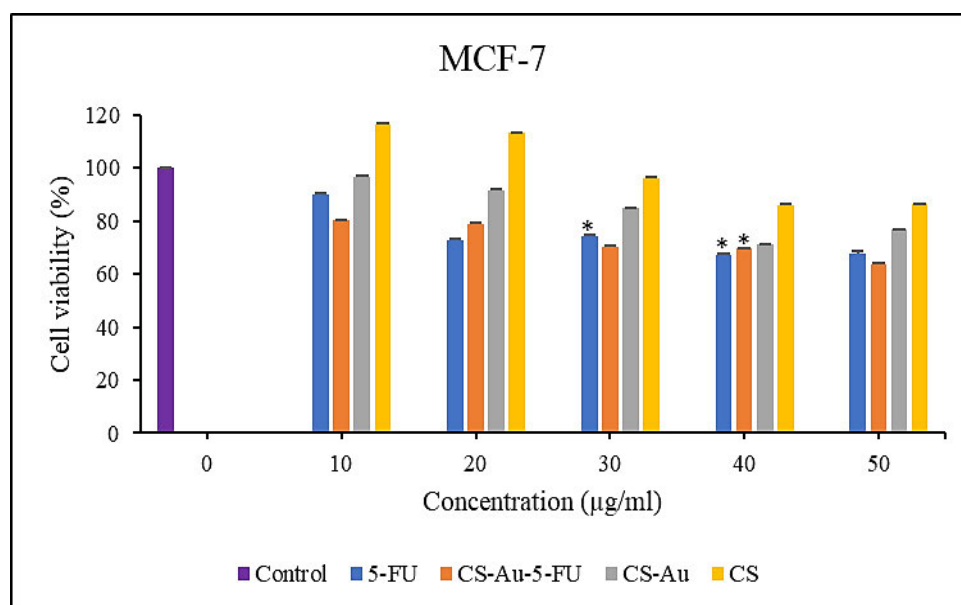


**Figure 5.15:** MTT cytotoxicity of the free 5-FU, CS-Au-5-FU, CS-Au, and CS hydrogels in the MCF-7 cells. Data are represented as means  $\pm$  SD (n=3). \*  $p < 0.05$ , \*\*  $p < 0.01$  were considered statistically significant.

The HEK293 cells were utilized as a control to assess the cytotoxic effects on non-cancer cells. Both CS and CS-Au hydrogels exhibited remarkably low cytotoxicity in the HEK293 cells (Figure 5.13). The cytotoxicity of CS and CS-Au are comparable at all concentrations, with the lowest being 82.76% for CS-Au at 50  $\mu\text{g/ml}$ . The analogous results reflect the relative non-

toxic nature of the AuNP cross-linkers owing to its chemically inert core, which is further enhanced by CS functioning as a protective barrier in the CS-Au hydrogel. Cell proliferation is observed at a concentration of 20  $\mu\text{g}/\text{ml}$  for both the CS and CS-Au hydrogels, with increased viabilities of 106.27% and 102.13%, respectively. This concentration may be optimal for the hydrated state of the hydrogels, which mimics the ECM and facilitates nutrient and oxygen transport through the pores. The minimal cytotoxicity demonstrates the effectiveness of the hydrogels in wound healing, which was further clarified through scratch test experiments. The CS-Au-5-FU hydrogel exhibited cytotoxicity in HEK293 cells, as anticipated from the drug release profile (Figure 5.13). At the physiological pH of 7.4, associated with healthy cells such as HEK293, 33.41% of 5-FU was released from the hydrogel after 48 hours, leading to reduced cell viability. The treatment of HEK293 with the CS-Au-5-FU hydrogel achieved greater cell viability compared to free 5-FU, indicating its superiority over the free drug in cancer therapy. Research suggests that non-cancer cells, with their neutral or slightly positive charge from buffer systems and ion channels, contribute to increased cell viability by reducing their attraction to positively charged hydrogels (Chen *et al.*, 2016). From the zeta potential studies the CS-Au-5-FU hydrogel possessed a positive charge ( $+15.87 \pm 1.18$ ) (Table 5.1), which may have added to the reduced cytotoxicity.

The CS-Au-5-FU hydrogel exhibited concentration-dependent anticancer efficacy against the HeLa and MCF-7 cells (Figures 5.14 and 5.15). The CS and CS-Au demonstrated minor anticancer effectiveness, showing moderate reductions in cell viability in a concentration-dependent manner, with a minimum cell viability of 70.24% observed. As a result, it may be concluded that the anticancer capabilities of the AuNPs further render them suitable as cross-linkers by enhancing the potential of the hydrogel in cancer therapy. The CS-Au-5-FU hydrogel exhibited cytotoxicity that resembled that of free 5-FU, with negligible variation observed in the MCF-7 cells. In the HeLa cells (Figure 5.14), a significant reduction in cell viability when treated with the CS-Au-5-FU hydrogel was observed at lower doses in comparison to the free 5-FU. However, at higher concentrations (40 and 50  $\mu\text{g}$ ), free 5-FU demonstrated greater cytotoxicity. Treatment with lower quantities of the CS-Au-5-FU hydrogel is, therefore, an advantageous alternative to free 5-FU, as it offers elevated cytotoxicity towards cancer cells while reducing cytotoxicity in non-cancer cells, limiting adverse side effects. These results can be attributed to the strong affinity of the CS-Au-5-FU hydrogel for the negatively charged cancer cell membranes in conjunction with the controlled release and retention of 5-FU due to the cationic CS, which augments the swelling and drug diffusion into the acidic cancer

microenvironment. CS has also been noted to protect drugs from harsh *in vivo* conditions and inhibit degradation, in contrast to free drugs that are susceptible to breakdown (Desai *et al.*, 2023). The introduction of cross-linked AuNPs in the cationic CS hydrogel positively impacted the cytotoxicity in the cancer cells, as they penetrated the cell membranes due to their diminutive size and synergistically acted with the drug payload. Thus, the CS-Au-5-FU hydrogel may provide a decrease in dosage regimens and further mitigate the adverse effects associated with prolonged anticancer drug treatment.

### 5.7 Scratch assay

Throughout the course of wound healing, cells from the edges of the wound begin to proliferate and migrate into the centre of the site of injury, facilitating re-epithelialization of the surface and restoring the barrier function of the skin. The promotion of migration is a key criterion for an optimal wound dressing material. Scratch assays are frequently employed to examine the *in vitro* movement of cells in reaction to diverse stimuli. This study examined the migration of HEK293 cells (normal cell model) following treatment with the CS and CS-Au hydrogels over a duration of 3 days.

Figures 5.16-5.19 illustrated that the migratory distance of cells treated with the extraction solutions of the CS and CS-Au hydrogels exceeded that of the control group, exhibiting a dose-dependent pattern. All concentrations of both hydrogel treatments demonstrated wound closure properties and may be considered appropriate for wound healing (Table 5.3 and 5.4). Confirmation is established through the gradual migration of cells towards the centre of the scratched surface (Figure 5.16-5.19). This arises from the hydrogels mimicking the ECM, which supplies cells with a microenvironment that more precisely reflects the dynamic interdependence between cells and their surroundings. The ECM influences cell migration in terms of both the temporal and tension scales of cell-ECM interactions, as cells detect their environment via their membrane and adapt by reorganizing cytoskeletal components (Solbu *et al.*, 2023). The ECM functions as a substrate for cellular adhesion, enabling cell attachment, spreading, and migration (Chen *et al.*, 2024). The mechanical properties of hydrogels can also influence the capacity of cells to exert traction forces, thereby impacting migration velocity and/or mode (Doyle *et al.*, 2015). Nonetheless, the treatment efficacy was predominantly observed at the lower dosages of 15.63 ( $\mu\text{g/ml}$ ) and 31.25 ( $\mu\text{g/ml}$ ). At a concentration of 15.63  $\mu\text{g/ml}$ , both the CS and CS-Au hydrogels achieved full wound closure on day 1. This parallels the MTT experiment, where cell proliferation was observed at a concentration of 20  $\mu\text{g/ml}$ . At

a dosage of 31.25 ( $\mu\text{g/ml}$ ), both treatments achieved complete wound closure, albeit at a diminished rate, as completion was noted only after day 3. At higher doses (62.5  $\mu\text{g/ml}$  and 125  $\mu\text{g/ml}$ ), a decrease in the effectiveness of the CS-Au hydrogel is apparent (Table 5.4). The CS hydrogel showed complete wound closure by day 3 at a dose of 62.5  $\mu\text{g/ml}$ , exhibiting a similar response to that observed at 31.25  $\mu\text{g/ml}$ . At a concentration of 125 ( $\mu\text{g/ml}$ ), efficacy declined significantly, with wound closure reaching just 30.23% on day 3 (Table 5.3). CS displayed a comparable wound closure to the control, which had a closure rate of 32.09% after day 3. Therefore, treatment at 125  $\mu\text{g/ml}$  with the CS hydrogel may not hinder the wound healing process but rather prove ineffectual. Conversely, the CS-Au hydrogel may be considered disruptive to the wound healing process at higher doses (62.5  $\mu\text{g/ml}$  and 125  $\mu\text{g/ml}$ ), as it demonstrated wound closure percentages of 21.89% and 20% following day 3. The wound closure percentages are inferior to the control (32.09%) and may be considered detrimental to the wound healing process owing to possible AuNP toxicity through instability and possible aggregation (Blaškovičová *et al.*, 2023).

The disparities in cell migration between the CS and CS-Au hydrogels arise from the mechanical matrix features. The interplay between the intrinsic contractility of the cell and the ECM stiffness influences cell adhesion characteristics (Solbu *et al.*, 2023). Cell migration is observed to be hastened in softer gels and impeded in stiffer ones, substantiating the results achieved (Doyle *et al.*, 2015). Nevertheless, the integration of AuNPs as cross-linkers is crucial to ensure the stability and water retention required for cellular control and application *in vivo*. During treatment for wound healing under adverse conditions, such as bacterial presence, the AuNPs may prove more suitable, as gold nanocarriers can adhere to bacterial membranes, causing the release of bacterial components and eventually resulting in bacterial cell death (Wang *et al.*, 2024). The findings of the scratch assay suggest that both hydrogels at reduced concentrations facilitated the migration of cells to the injury site and triggered the proliferative phase of wound healing, as evidenced by the complete closure of the HEK293 cell monolayer.

**DAY 0**

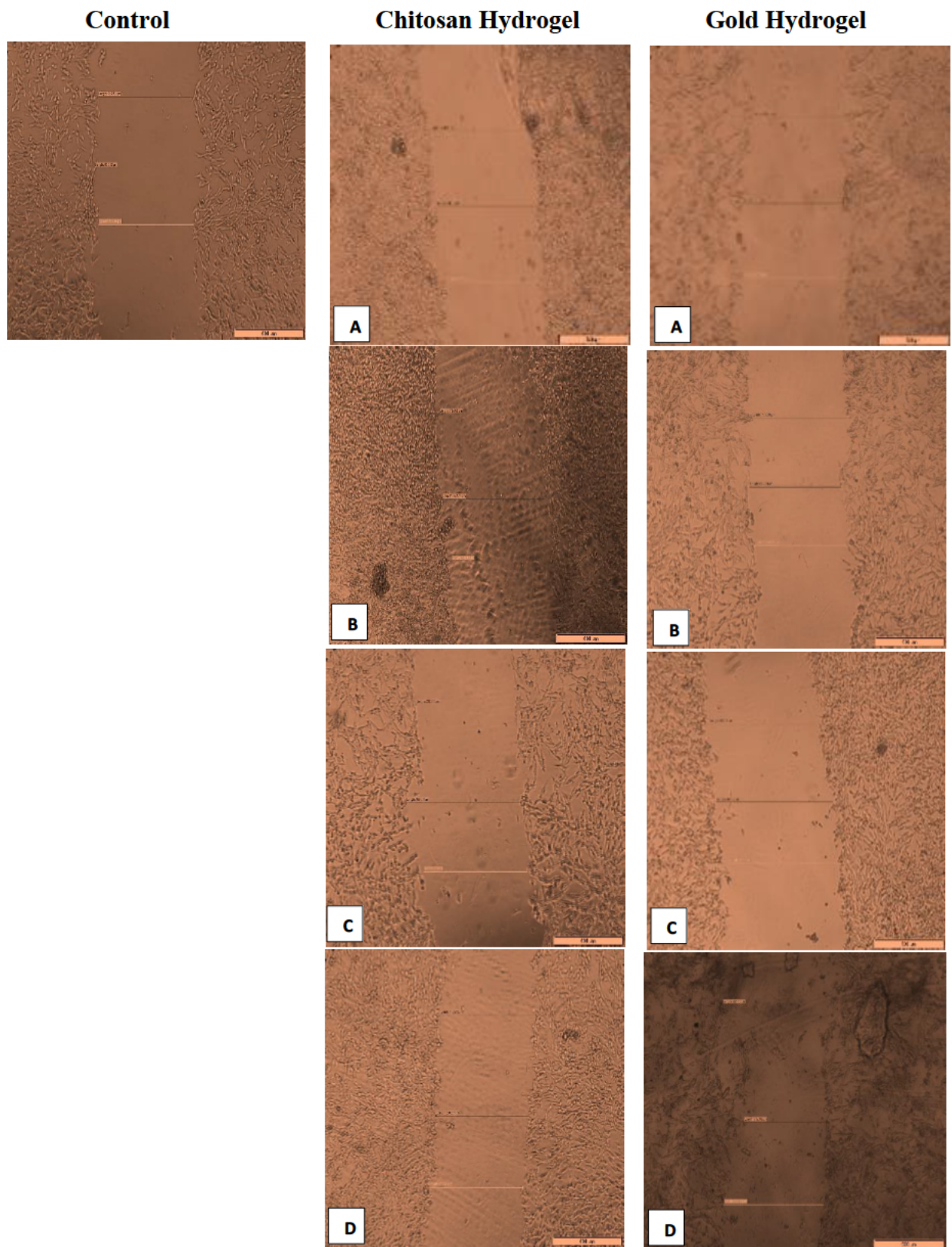


**Figure 5.16:** Images displaying the migration of HEK293 cells for wound closure when treated with A (15.63  $\mu\text{g/ml}$ ), B (31.25  $\mu\text{g/ml}$ ), C (62.5  $\mu\text{g/ml}$ ), D (125  $\mu\text{g/ml}$ ) of the CS and CS-Au hydrogels on day 0.

**DAY 1**

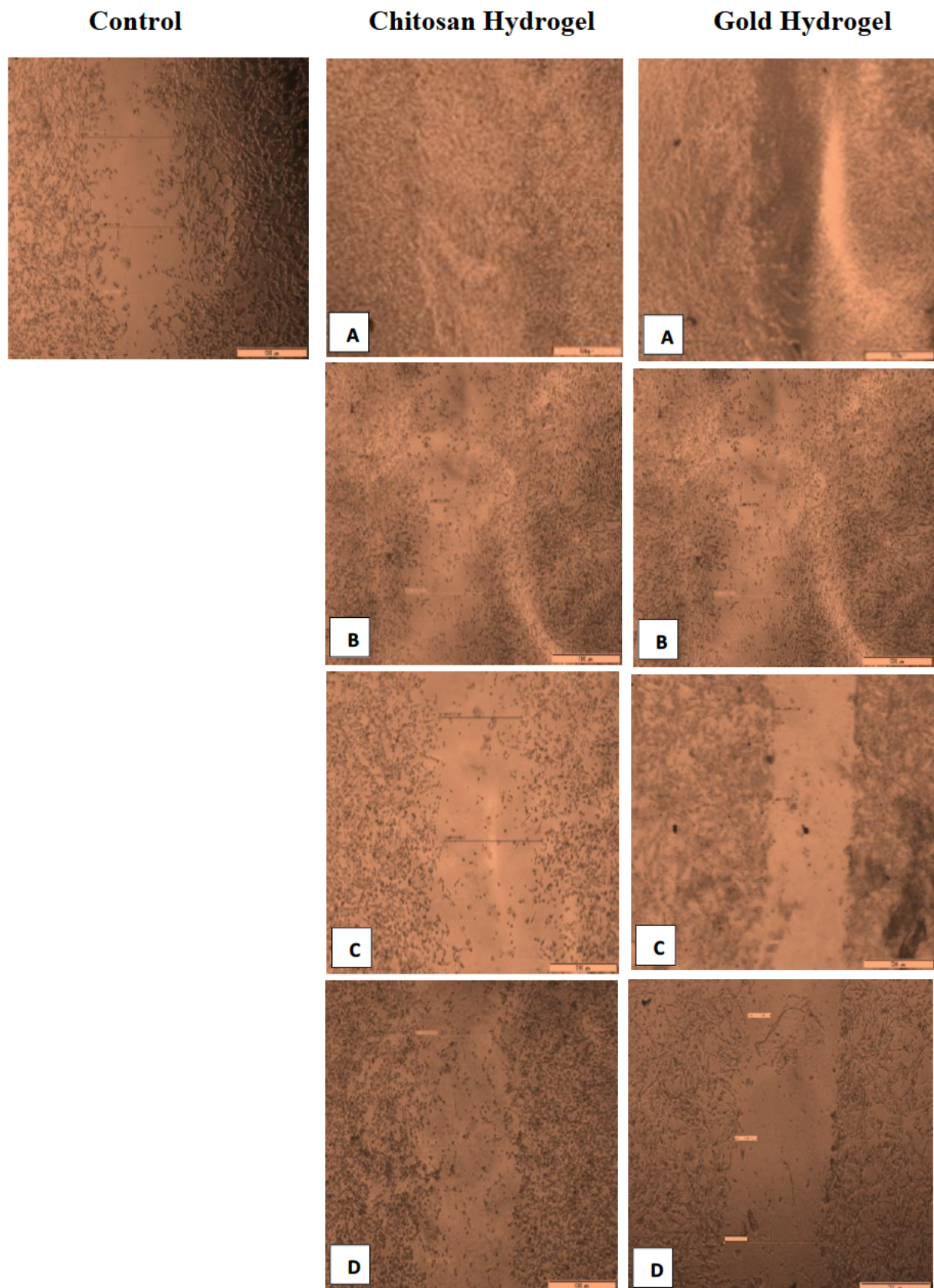


**Figure 5.17:** Images displaying the migration of cells for wound closure when treated with A (15.63  $\mu\text{g/ml}$ ), B (31.25  $\mu\text{g/ml}$ ), C (62.5  $\mu\text{g/ml}$ ), D (125  $\mu\text{g/ml}$ ) of the CS and CS-Au hydrogels on day 1.

DAY 2

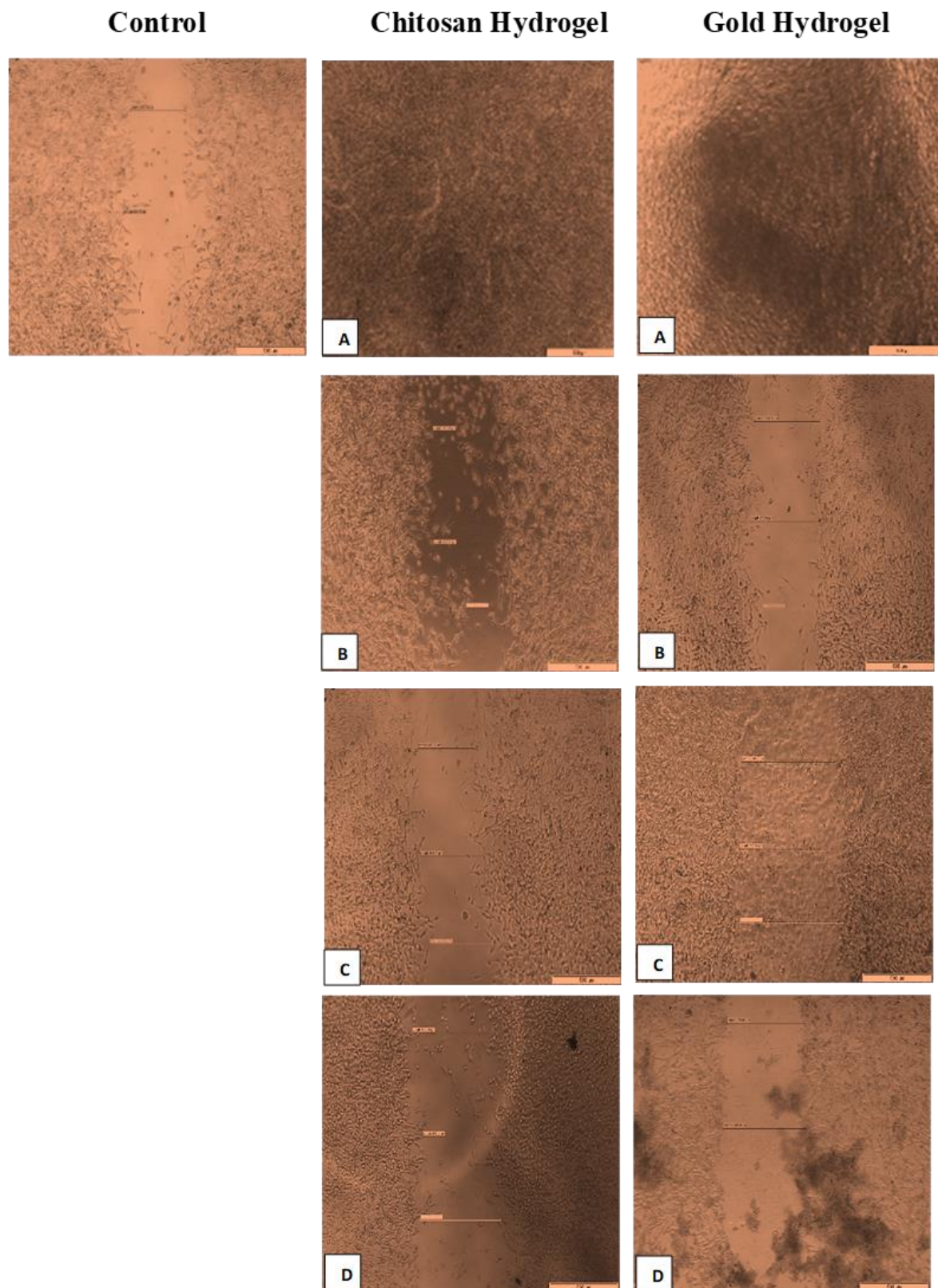


**Figure 5.18:** Images displaying the migration of cells for wound closure when treated with A (15.63  $\mu\text{g/ml}$ ), B (31.25  $\mu\text{g/ml}$ ), C (62.5  $\mu\text{g/ml}$ ), D (125  $\mu\text{g/ml}$ ) of the CS and CS-Au hydrogels on day 2.

**DAY 3**

**Control**

**Chitosan Hydrogel**

**Gold Hydrogel**

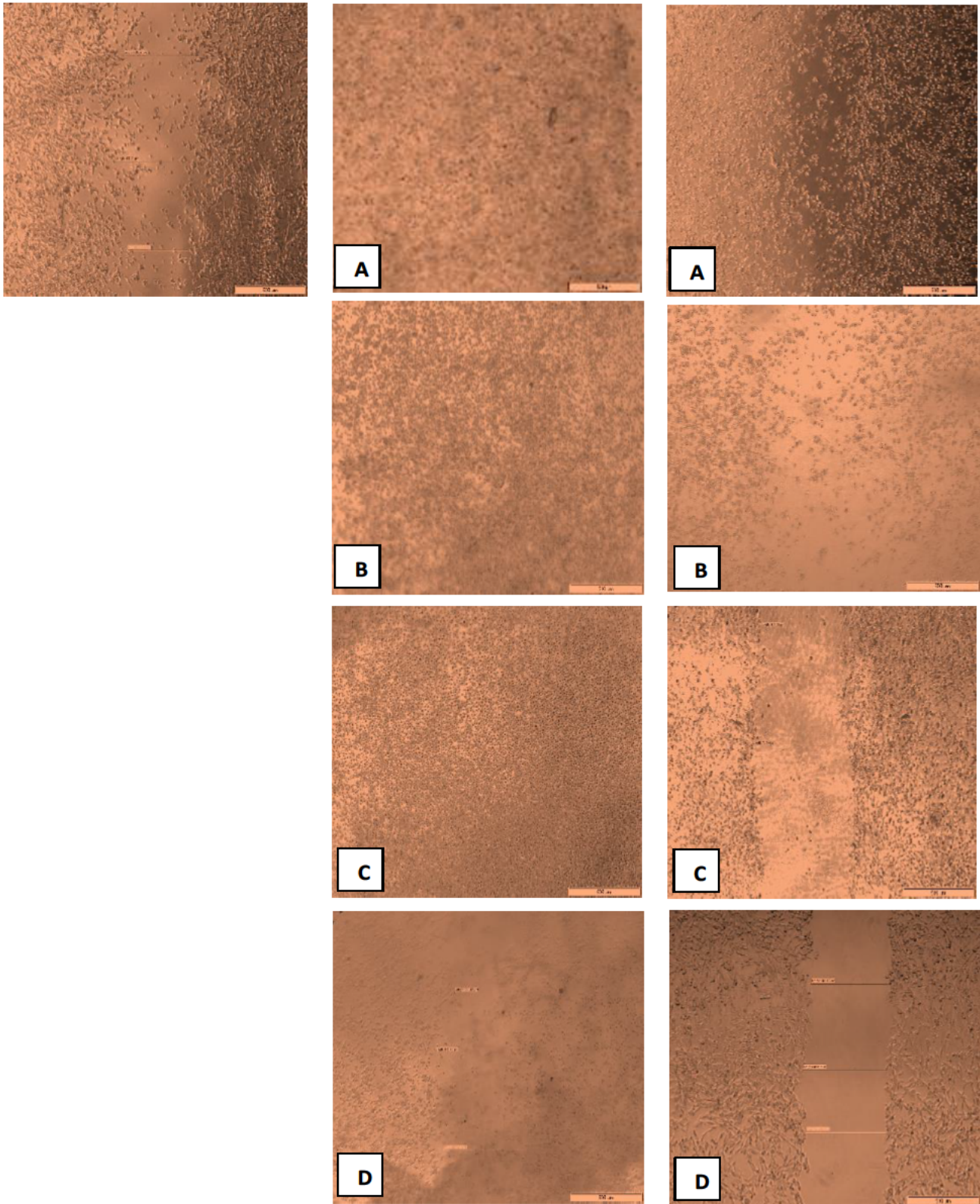


**Figure 5.19:** Images displaying the migration of cells for wound closure when treated with A (15.63  $\mu\text{g/ml}$ ), B (31.25  $\mu\text{g/ml}$ ), C (62.5  $\mu\text{g/ml}$ ), D (125  $\mu\text{g/ml}$ ) of the CS and CS-Au hydrogels on day 3.

**Table 5.3:** Wound closure (%) after treatment with various concentrations of the CS hydrogel over a 3-day period.

| Days  | % Wound closure at different CS Hydrogel concentrations |               |              |             |
|-------|---|---------------|--------------|-------------|
|       | 15.63 (µg/ml)   | 31.25 (µg/ml) | 62.5 (µg/ml) | 125 (µg/ml) |
| Day 1 | 100%  | 25.97%        | 9.95%        | 2.97%       |
| Day 2 | 100%  | 46.25%        | 40.90%       | 13.74%      |
| Day 3 | 100%  | 100%          | 100%         | 30.23%      |

**Table 5.4:** Wound closure (%) after treatment with various concentrations of the CS-Au hydrogel over a 3-day period

| Days  | % Wound closure at different CS-Au Hydrogel concentrations |               |              |             |
|-------|--|---------------|--------------|-------------|
|       | 15.63 (µg/ml)  | 31.25 (µg/ml) | 62.5 (µg/ml) | 125 (µg/ml) |
| Day 1 | 100%   | 21.87%        | 7.79%        | 4.75%       |
| Day 2 | 100%   | 32.62%        | 9.46%        | 14.82%      |
| Day 3 | 100%   | 100%          | 21.89%       | 20%         |

## 5.8 References

- Aibani, N., Rai, R., Patel, P., Cuddihy, G., & Wasan, E. K. (2021). Chitosan Nanoparticles at the Biological Interface: Implications for Drug Delivery. *Pharmaceutics*, 13(10). <https://doi.org/10.3390/pharmaceutics13101686>
- Akinyelu, J., & Singh, M. (2018). Folate-tagged chitosan-functionalized gold nanoparticles for enhanced delivery of 5-fluorouracil to cancer cells. *Applied Nanoscience*, 9, 7-17.
- Anushree, U., Punj, P., Vasumathi, & Bharati, S. (2023). Phosphorylated chitosan accelerates dermal wound healing in diabetic wistar rats. *Glycoconjugate Journal*, 40(1), 19-31.
- Blašková, J., Vyskočil, V., Augustín, M., & Purdešová, A. (2023). Ethanol and NaCl-Induced Gold Nanoparticle Aggregation Toxicity toward DNA Investigated with a DNA/GCE Biosensor. *Sensors*, 23(7), 3425. <https://www.mdpi.com/1424-8220/23/7/3425>
- Chen, B., Le, W., Wang, Y., Li, Z., Wang, D., Ren, L., Lin, L., Cui, S., Hu, J. J., & Hu, Y. (2016). Targeting negative surface charges of cancer cells by multifunctional nanoprobe. *Theranostics*, 6(11), 1887.

- Chen, Z., Du, C., Liu, S., Liu, J., Yang, Y., Dong, L., Zhao, W., Huang, W., & Lei, Y. (2024). Progress in biomaterials inspired by the extracellular matrix. *Giant*, *19*, 100323. <https://doi.org/https://doi.org/10.1016/j.giant.2024.100323>
- Desai, N., Rana, D., Salave, S., Gupta, R., Patel, P., Karunakaran, B., Sharma, A., Giri, J., Benival, D., & Kommineni, N. (2023). Chitosan: A Potential Biopolymer in Drug Delivery and Biomedical Applications. *Pharmaceutics*, *15*(4). <https://doi.org/10.3390/pharmaceutics15041313>
- Doyle, A. D., Carvajal, N., Jin, A., Matsumoto, K., & Yamada, K. M. (2015). Local 3D matrix microenvironment regulates cell migration through spatiotemporal dynamics of contractility-dependent adhesions. *Nature communications*, *6*(1), 8720.
- Fu, Y., & Kao, W. J. (2010). Drug release kinetics and transport mechanisms of non-degradable and degradable polymeric delivery systems. *Expert Opin Drug Deliv*, *7*(4), 429-444. <https://doi.org/10.1517/17425241003602259>
- Hammami, I., Alabdallah, N. M., jomaa, A. A., & kamoun, M. (2021). Gold nanoparticles: Synthesis properties and applications. *Journal of King Saud University - Science*, *33*(7), 101560. <https://doi.org/https://doi.org/10.1016/j.jksus.2021.101560>
- Herbani, Y. (2017). Aggregation effect on absorbance spectrum of laser ablated gold nanoparticles. *Journal of Physics: Conference Series*,
- Honary, S., & Zahir, F. (2013). Effect of zeta potential on the properties of nano-drug delivery systems-a review (Part 2). *Tropical journal of pharmaceutical research*, *12*(2), 265-273.
- Jalalvandi, E., & Shavandi, A. (2019). Shear thinning/self-healing hydrogel based on natural polymers with secondary photocrosslinking for biomedical applications. *Journal of the Mechanical Behavior of Biomedical Materials*, *90*, 191-201. <https://doi.org/https://doi.org/10.1016/j.jmbbm.2018.10.009>
- Kamble, S., Agrawal, S., Cherumukkil, S., Sharma, V., Jasra, R. V., & Munshi, P. (2022). Revisiting Zeta Potential, the Key Feature of Interfacial Phenomena, with Applications and Recent Advancements. *ChemistrySelect*, *7*(1), e202103084. <https://doi.org/https://doi.org/10.1002/slct.202103084>

Lončarević, A., Ivanković, M., & Rogina, A. (2017). Lysozyme-induced degradation of chitosan: the characterisation of degraded chitosan scaffolds. *Journal of Tissue Repair and Regeneration*, 1(1), 12-22.

Mehrotra, S., & Pathak, K. (2024). Chapter 1 - Controlled release drug delivery systems: principles and design. In A. K. Nayak & K. K. Sen (Eds.), *Novel Formulations and Future Trends* (pp. 3-30). Academic Press. [https://doi.org/https://doi.org/10.1016/B978-0-323-91816-9.00014-X](https://doi.org/10.1016/B978-0-323-91816-9.00014-X)

Michalik, R., & Wandzik, I. (2020). A Mini-Review on Chitosan-Based Hydrogels with Potential for Sustainable Agricultural Applications. *Polymers (Basel)*, 12(10). <https://doi.org/10.3390/polym12102425>

Mitchell, M. J., Billingsley, M. M., Haley, R. M., Wechsler, M. E., Peppas, N. A., & Langer, R. (2021). Engineering precision nanoparticles for drug delivery. *Nature Reviews Drug Discovery*, 20(2), 101-124. <https://doi.org/10.1038/s41573-020-0090-8>

Moura, M. J., Brochado, J., Gil, M. H., & Figueiredo, M. M. (2017). In situ forming chitosan hydrogels: Preliminary evaluation of the in vivo inflammatory response. *Materials Science and Engineering: C*, 75, 279-285.

Peers, S., Montembault, A., & Ladavière, C. (2020). Chitosan hydrogels for sustained drug delivery. *Journal of Controlled Release*, 326, 150-163. [https://doi.org/https://doi.org/10.1016/j.jconrel.2020.06.012](https://doi.org/10.1016/j.jconrel.2020.06.012)

Pillai, A., Bhande, D., & Pardhi, V. (2023). Controlled Drug Delivery System. In T. S. Santra & A. U. S. Shinde (Eds.), *Advanced Drug Delivery: Methods and Applications* (pp. 267-289). Springer Nature Singapore. [https://doi.org/10.1007/978-981-99-6564-9\\_11](https://doi.org/10.1007/978-981-99-6564-9_11)

Pochapski, D. J., Carvalho dos Santos, C., Leite, G. W., Pulcinelli, S. H., & Santilli, C. V. (2021). Zeta Potential and Colloidal Stability Predictions for Inorganic Nanoparticle Dispersions: Effects of Experimental Conditions and Electrokinetic Models on the Interpretation of Results. *Langmuir*, 37(45), 13379-13389. <https://doi.org/10.1021/acs.langmuir.1c02056>

Queiroz, M. F., Teodosio Melo, K. R., Sabry, D. A., Sasaki, G. L., & Rocha, H. A. O. (2014). Does the use of chitosan contribute to oxalate kidney stone formation? *Marine drugs*, 13(1), 141-158.

Raghuwanshi, V. S., & Garnier, G. (2019). Characterisation of hydrogels: Linking the nano to the microscale. *Advances in Colloid and Interface Science*, 274, 102044. <https://doi.org/https://doi.org/10.1016/j.cis.2019.102044>

Rahman, M. S., Islam, M. M., Islam, M. S., Zaman, A., Ahmed, T., Biswas, S., Sharmeen, S., Rashid, T. U., & Rahman, M. M. (2019). Morphological Characterization of Hydrogels. In M. I. H. Mondal (Ed.), *Cellulose-Based Superabsorbent Hydrogels* (pp. 819-863). Springer International Publishing. [https://doi.org/10.1007/978-3-319-77830-3\\_28](https://doi.org/10.1007/978-3-319-77830-3_28)

Raina, N., Pahwa, R., Bhattacharya, J., Paul, A. K., Nissapatorn, V., de Lourdes Pereira, M., Oliveira, S. M. R., Dolma, K. G., Rahmatullah, M., Wilairatana, P., & Gupta, M. (2022). Drug Delivery Strategies and Biomedical Significance of Hydrogels: Translational Considerations. *Pharmaceutics*, 14(3). <https://doi.org/10.3390/pharmaceutics14030574>

Ribeiro, M., Simões, M., Vitorino, C., & Mascarenhas-Melo, F. (2024). Hydrogels in Cutaneous Wound Healing: Insights into Characterization, Properties, Formulation and Therapeutic Potential. *Gels*, 10(3). <https://doi.org/10.3390/gels10030188>

Riss, T. L., Moravec, R. A., Niles, A. L., Duellman, S., Benink, H. A., Worzella, T. J., & Minor, L. (2016). Cell viability assays. *Assay guidance manual [Internet]*.

Salome Amarachi, C., Onunkwo, G., & Onyishi, I. (2013). Kinetics and mechanisms of drug release from swellable and non swellable matrices: A review. *Research Journal of Pharmaceutical, Biological and Chemical Sciences*, 4, 97-103.

Sámamo-Valencia, C., Martínez-Castañón, G. A., Martínez-Gutiérrez, F., Ruiz, F., Toro-Vázquez, J. F., Morales-Rueda, J. A., Espinosa-Cristóbal, L. F., Zavala Alonso, N. V., & Niño Martínez, N. (2014). Characterization and Biocompatibility of Chitosan Gels with Silver and Gold Nanoparticles. *Journal of Nanomaterials*, 2014(1), 543419. <https://doi.org/https://doi.org/10.1155/2014/543419>

Samy, M., Abd El-Alim, S. H., Rabia, A. E. G., Amin, A., & Ayoub, M. M. H. (2020). Formulation, characterization and in vitro release study of 5-fluorouracil loaded chitosan nanoparticles. *International Journal of Biological Macromolecules*, 156, 783-791. <https://doi.org/https://doi.org/10.1016/j.ijbiomac.2020.04.112>

Shikuku, R., Hasnat, M. A., Mashrur, S. B. A., Haque, P., Rahman, M. M., & Khan, M. N. (2024). Chitosan-based pH-sensitive semi-interpenetrating network nanoparticles as a

sustained release matrix for anticancer drug delivery. *Carbohydrate Polymer Technologies and Applications*, 7, 100515. <https://doi.org/https://doi.org/10.1016/j.carpta.2024.100515>

Solbu, A. A., Caballero, D., Damigos, S., Kundu, S. C., Reis, R. L., Halaas, Ø., Chahal, A. S., & Strand, B. L. (2023). Assessing cell migration in hydrogels: An overview of relevant materials and methods. *Materials Today Bio*, 18, 100537. <https://doi.org/https://doi.org/10.1016/j.mtbio.2022.100537>

Souza, I. D. L., Saez, V., & Mansur, C. R. E. (2023). Lipid nanoparticles containing coenzyme Q10 for topical applications: An overview of their characterization. *Colloids and Surfaces B: Biointerfaces*, 230, 113491. <https://doi.org/https://doi.org/10.1016/j.colsurfb.2023.113491>

Talevi, A., & Ruiz, M. E. (2021). Korsmeyer-Peppas, Peppas-Sahlin, and Brazel-Peppas: Models of Drug Release. In *The ADME Encyclopedia: A Comprehensive Guide on Biopharmacy and Pharmacokinetics* (pp. 1-9). Springer International Publishing. [https://doi.org/10.1007/978-3-030-51519-5\\_35-1](https://doi.org/10.1007/978-3-030-51519-5_35-1)

Tan, Y., Xu, C., Liu, Y., Bai, Y., Li, X., & Wang, X. (2024). Sprayable and self-healing chitosan-based hydrogels for promoting healing of infected wound via anti-bacteria, anti-inflammation and angiogenesis. *Carbohydrate Polymers*, 337, 122147. <https://doi.org/https://doi.org/10.1016/j.carbpol.2024.122147>

Tan, Y., Xu, C., Liu, Y., Bai, Y., Li, X., & Wang, X. (2024). Sprayable and self-healing chitosan-based hydrogels for promoting healing of infected wound via anti-bacteria, anti-inflammation and angiogenesis. *Carbohydrate Polymers*, 337, 122147. <https://doi.org/https://doi.org/10.1016/j.carbpol.2024.122147>

Ullah, S., Azad, A. K., Nawaz, A., Shah, K. U., Iqbal, M., Albadrani, G. M., Al-Joufi, F. A., Sayed, A. A., & Abdel-Daim, M. M. (2022). 5-fluorouracil-loaded folic-acid-fabricated chitosan nanoparticles for site-targeted drug delivery cargo. *Polymers*, 14(10), 2010.

Vangari, V., Reddy, P. R., Rao, L. N., Mohammed, A., & Reddy, A. P. (2024). Microwave-assisted synthesis of Au nanoparticles using fruit peel waste: antioxidant activity and catalytic reduction of malachite green. *Reaction Kinetics, Mechanisms and Catalysis*. <https://doi.org/10.1007/s11144-024-02726-7>

Wang, W., Dai, J., Huang, Y., Li, X., Yang, J., Zheng, Y., & Shi, X. (2023). Extracellular matrix mimicking dynamic interpenetrating network hydrogel for skin tissue engineering. *Chemical Engineering Journal*, 457, 141362. <https://doi.org/10.1016/j.cej.2023.141362>

Wang, Y., Zhang, M., Yan, Z., Ji, S., Xiao, S., & Gao, J. (2024). Metal nanoparticle hybrid hydrogels: the state-of-the-art of combining hard and soft materials to promote wound healing. *Theranostics*, 14(4), 1534-1560. <https://doi.org/10.7150/thno.91829>

Xing, R., Liu, K., Jiao, T., Zhang, N., Ma, K., Zhang, R., Zou, Q., Ma, G., & Yan, X. (2016). An Injectable Self-Assembling Collagen-Gold Hybrid Hydrogel for Combinatorial Antitumor Photothermal/Photodynamic Therapy. *Adv Mater*, 28(19), 3669-3676. <https://doi.org/10.1002/adma.201600284>

## **CHAPTER SIX**

### **CONCLUSION AND FUTURE PERSPECTIVES**

## 6.1 Conclusion

To address deficiencies in drug delivery and wound healing, an innovative hybrid CS-Au hydrogel was synthesized by the reduction of  $\text{HAuCl}_4$  in the acidic CS-acrylic acid hydrogel, as verified by UV-vis spectroscopy, FTIR, and TEM analysis. The hydrogel exhibited an irregular porous structure and an elevated pH-dependent water absorption capacity, as demonstrated by the SEM and reswelling assays, facilitating the diffusion of 5-FU in cancer microenvironments and emulating the ECM for wound healing. The CS-Au hydrogel exhibited good drug encapsulation (77.71%) of 5-FU, enabling effective cellular uptake for enhanced *in vitro* cytotoxicity. Comprehensively, this study offers substantial evidence supporting the approach that prolonged pH-dependent drug release from the CS-Au-5-FU hydrogel results in localized cytotoxicity in cancer cells. This was further supported by the cytotoxicity assay, which indicated that the CS-Au-5-FU hydrogel displayed augmented and more selective anticancer efficacy in the HeLa and MCF-7 cells compared to the free drug, suggesting the feasibility of using lower dosage regimens and reduced drug concentrations. The wound healing properties of the CS and CS-Au hydrogels were demonstrated in the scratch assay, which illustrated complete wound closure at low concentrations, indicating the effective simulation of the ECM. Overall, the synthesized hydrogels have demonstrated the potential for use as future drug delivery systems in cancer therapy and scaffolds for wound healing applications. This opens up new avenues to investigate and necessitates further enhancements and optimizations.

## 6.2 Future studies

Future research may focus on improving the stability of the AuNPs by integrating CS with polyethylene glycol. The incorporation of this polymer may also yield a more uniform porosity and enhance the therapeutic efficacy. In addition, a targeting moiety may be incorporated into the NP for cellular selectivity. This would include focusing the research on a particular type of cancer, such as using a galactose-containing ligand to target asialoorosomucoid receptors that are excessively expressed on the surface of hepatocellular carcinoma cells. The incorporation of a thermosensitive polymer such as N-isopropylacrylamide (NIPAM) may offer an alternate therapeutic approach by leveraging the surface plasmon resonance effect of cross-linked AuNPs. Near-infrared light can excite the surface plasmon resonance of AuNPs, and the heat generated by this excitation can trigger a drug-impregnated hydrogel to collapse, facilitating a dual-responsive drug delivery system. This excitation can also be employed in photothermal

treatment (PTT) for wound healing applications via thermal ablation. Furthermore, the sustained release pattern demonstrated by the CS-Au hydrogel may facilitate the incorporation of antibacterial drugs, including Ciprofloxacin and Gentamicin, to enhance the antibacterial effectiveness of the hydrogel in wound healing.

Review

## Hydrogels and Wound Healing: Current and Future Prospects

Varshan Gounden and Moganavelli Singh \* 

Nano-Gene and Drug Delivery Laboratory, Discipline of Biochemistry, University of KwaZulu-Natal, Private Bag X54001, Durban 4000, South Africa; 219006317@stu.ukzn.ac.za  
\* Correspondence: singhm1@ukzn.ac.za; Tel.: +27-31-2607170

**Abstract:** The care and rehabilitation of acute and chronic wounds have a significant social and economic impact on patients and global health. This burden is primarily due to the adverse effects of infections, prolonged recovery, and the associated treatment costs. Chronic wounds can be treated with a variety of approaches, which include surgery, negative pressure wound therapy, wound dressings, and hyperbaric oxygen therapy. However, each of these strategies has an array of limitations. The existing dry wound dressings lack functionality in promoting wound healing and exacerbating pain by adhering to the wound. Hydrogels, which are commonly polymer-based and swell in water, have been proposed as potential remedies due to their ability to provide a moist environment that facilitates wound healing. Their unique composition enables them to absorb wound exudates, exhibit shape adaptability, and be modified to incorporate active compounds such as growth factors and antibacterial compounds. This review provides an updated discussion of the leading natural and synthetic hydrogels utilized in wound healing, details the latest advancements in hydrogel technology, and explores alternate approaches in this field. Search engines Scopus, PubMed, Science Direct, and Web of Science were utilized to review the advances in hydrogel applications over the last fifteen years.

**Keywords:** chronic wounds; wound dressings; hydrogels; wound healing; polymers



Citation: Gounden, V.; Singh, M. Hydrogels and Wound Healing: Current and Future Prospects. *Gels* **2024**, *10*, 43. <https://doi.org/10.3390/gels10010043>

Academic Editor: Xin Zhao

Received: 17 November 2023

Revised: 11 December 2023

Accepted: 3 January 2024

Published: 5 January 2024



Copyright: © 2024 by the authors. Licensee MDPI, Basel, Switzerland. This article is an open access article distributed under the terms and conditions of the Creative Commons Attribution (CC BY) license (<https://creativecommons.org/licenses/by/4.0/>).

### 1. Introduction

Wounds have plagued patients for millennia, imposing a substantial burden on their carers, thus earning its designation as the ‘silent epidemic’ [1]. Approximately 4 million cutaneous wounds have been documented to occur annually in affluent countries, with the number in developing nations in ascendance [2]. Skin injury compromises the integrity of the skin’s framework, leading to a wound healing process that is characterized by a well-coordinated series of cellular and molecular reactions that aim to recuperate or replace the injured tissue [3]. Wounds distinguished by synergistic and ordered processes, which lead to uninterrupted wound regeneration, are commonly referred to as ‘acute wounds’. Although minor cutaneous injuries can recuperate, several variables frequently impact wound rehabilitation. These include severe oxidative stress, infection, and underlying medical conditions that result in the development of “chronic or inert wounds” [4]. Chronic wounds exhibit distinctive attributes, which include recurrent infections, a heightened inflammatory phase, and impaired responsiveness of epidermal cells to reparative signals [5].

In addition to the impact on psychological, social, and physical health, diminished productivity and high treatment costs impose a financial strain on the healthcare sector, emphasizing the need for efficient wound treatment. The current industry-standard therapies include skin grafts and flaps, dermal substitutes, and skin growth procedures. However, these procedures encounter significant challenges, such as a scarcity of sites for donors and the development of hypertrophied scars, resulting in physiological complications [6]. Hence, there is a dire need for an efficient alternative to overcome the present limitations.

Hydrogels can be described as intricate three-dimensional structures composed of hydrophilic polymer chains and exhibit a quick swelling response upon contact with water,

## Appendix B – Turnitin Report

### Varshan Gounden Masters thesis

---

#### ORIGINALITY REPORT

---

**14%**

SIMILARITY INDEX

**8%**

INTERNET SOURCES

**9%**

PUBLICATIONS

**7%**

STUDENT PAPERS

---

#### PRIMARY SOURCES

---

**1**

**Submitted to University of KwaZulu-Natal**

Student Paper

**4%**

---

**2**

**www.mdpi.com**

Internet Source

**1%**

---

**3**

**Rui Chen, Qi Chen, Da Huo, Yin Ding, Yong Hu, Xiqun Jiang. "In situ formation of chitosan-gold hybrid hydrogel and its application for drug delivery", Colloids and Surfaces B: Biointerfaces, 2012**

Publication

**1%**

---

**4**

**Maria José Moura, João Brochado, Maria Helena Gil, Maria Margarida Figueiredo. "In**

**1%**